

Exploring Relationships Between Chemical Structure and Molecular Conductance: From α,ω -Functionalised Oligoynes to Molecular Circuits

Elena Gorenskaia,^{a†} Jarred Potter,^{a†} Marcus Korb,^a Colin Lambert,^{b*} Paul J. Low^{a*}

^a *School of Molecular Sciences, University of Western Australia, 35 Stirling Highway,
Crawley, Western Australia, 6026, Australia*

^b *Department of Physics, University of Lancaster, Lancaster LA1 4YB, England*

paul.low@uwa.edu.au; c.lambert@lancaster.ac.uk

[†] These authors contributed equally

Supporting Information

1. Conductance measurements
 - 1.1 STM-BJ
 - 1.2 Data analysis
 - 1.3 Experimental results

2. Molecular Synthesis and Characterization
 - 2.1 General Conditions
 - 2.2 Synthetic Methods
 - 2.2.1 Synthesis of Series 1
 - 2.2.2 Synthesis of Series 2
 - 2.2.3 Synthesis of Series 3
 - 2.2.4 Synthesis of Series 4
 - 2.2.5 Synthesis of Additional Compounds
 - 2.3 Molecular and Crystal Structures
 - 2.4 Crystallographic Data
 - 2.5 NMR Data
 - 2.6 MS Data

1. Conductance measurements

1.1 STM-BJ

For the STM-BJ experiment, the gold-on-glass substrates (Arrandee™) were cleaned by immersion in a freshly prepared piranha solution (1 part H₂O₂ (33%) in 3 parts H₂SO₄ (98%)), then removed, rinsed with deionised water and dried under a nitrogen stream. A freshly cut gold wire (99.99% purity, 0.25 mm diameter) was used as the STM tip. Analyte solutions of each compounds (1 mM) were prepared in 1,3,5-trimethylbenzene (TMB). The substrate surface was examined by STM imaging in the analyte solution before commencing conductance–distance measurements. The set-point is chosen such that the gold STM tip is driven into the gold substrate to create a fused metallic contact. As the tip retracts, a metallic filament is drawn from the surface which progressively thins, as evinced by the decrease in junction conductance in steps corresponding to the quantum of conductance $G_0 = 2e^2/h = 77.5 \mu\text{S}$. Upon cleavage of the last Au-Au contact, the current undergoes a rapid decay and decreases exponentially as the tip is further retracted. When a molecule bridge between two separated electrodes, a plateau in the conductance-distance trace is observed. The measurements have been carried out at -100 mV bias voltage. All traces have been recorded at a rate of 5 nm/sec containing 1000 points per trace.

1.2 Data analysis

2000 traces for each compound have been used for data analysis and used without further selection. The 1D histograms were constructed by taking the logarithm of conductance and binning the data (bin width $\Delta\log(G/G_0) = 0.01$) and normalised to the number of traces as counts per trace. In our instrument set up the noise level appears at the region around $\log(G/G_0) = -6$. The conductance peaks revealed in these plots were fitted with Gaussian-shaped curves to estimate the most probable single-molecule conductance.

2D histograms were constructed against the relative stretching distances. To align the data, in each traces the data point corresponding to the breaking the final Au–Au nanocontact was set to $\Delta z = 0$ and all current-distance traces overlaid and plotted to give a 2D conductance versus relative displacement density map.

1.3 Experimental results

Plots of the 1D and 2D histograms, and conductance ($\log(G/G_0)$) vs electrode displacement curves from compounds **1b-d**, **2b-d**, **3b-d**, **4b-d**, **5-8** recorded from the STM-BJ experiments are plotted below.

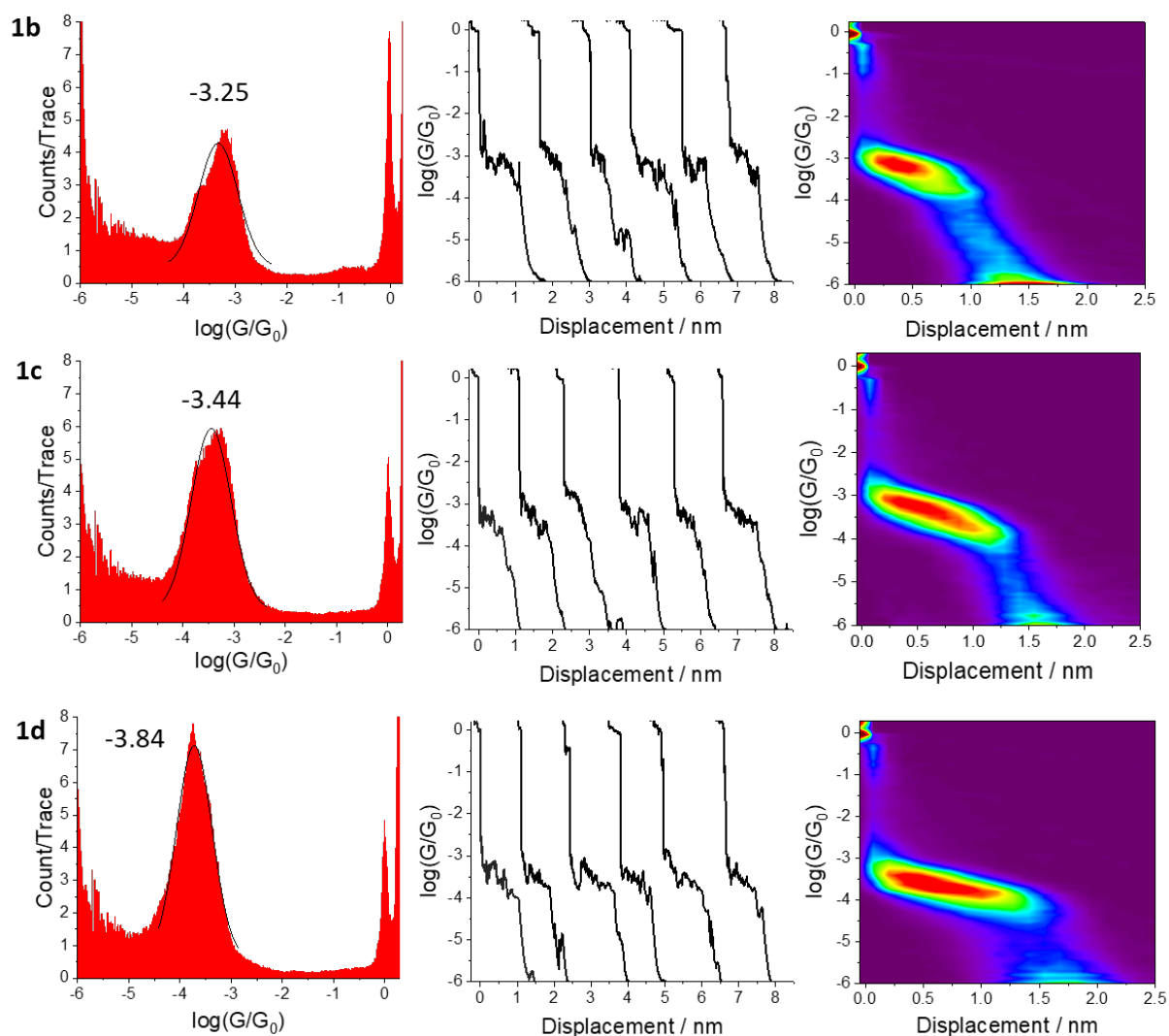


Figure S1. 1D conductance histograms, conductance ($\log(G/G_0)$) vs electrode displacement curves, and 2D conductance–relative displacement histograms of compounds **1b–d**.

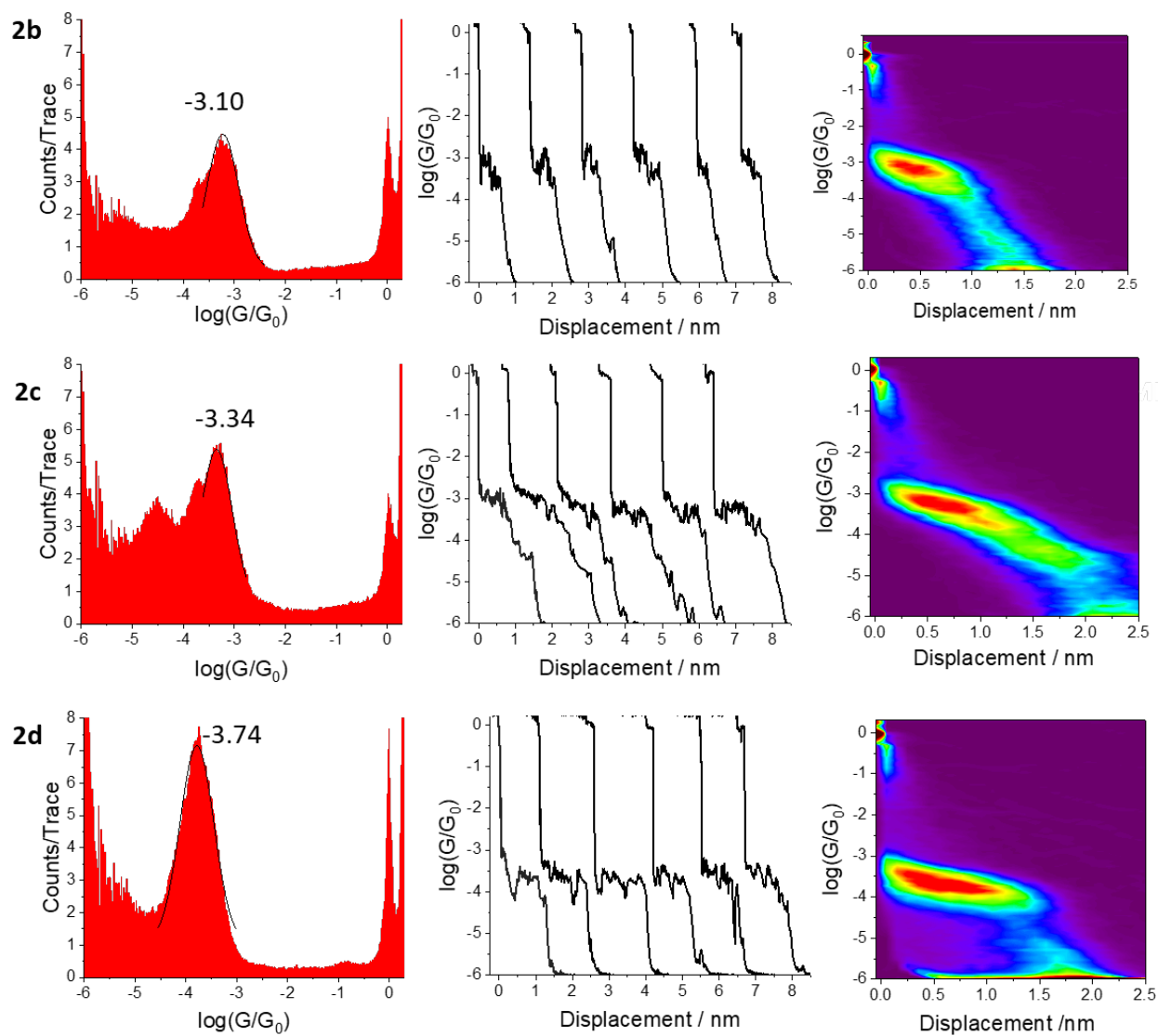


Figure S2. 1D conductance histograms, conductance ($\log(G/G_0)$) vs electrode displacement curves, and 2D conductance-relative displacement histograms of compounds **2b–d**.

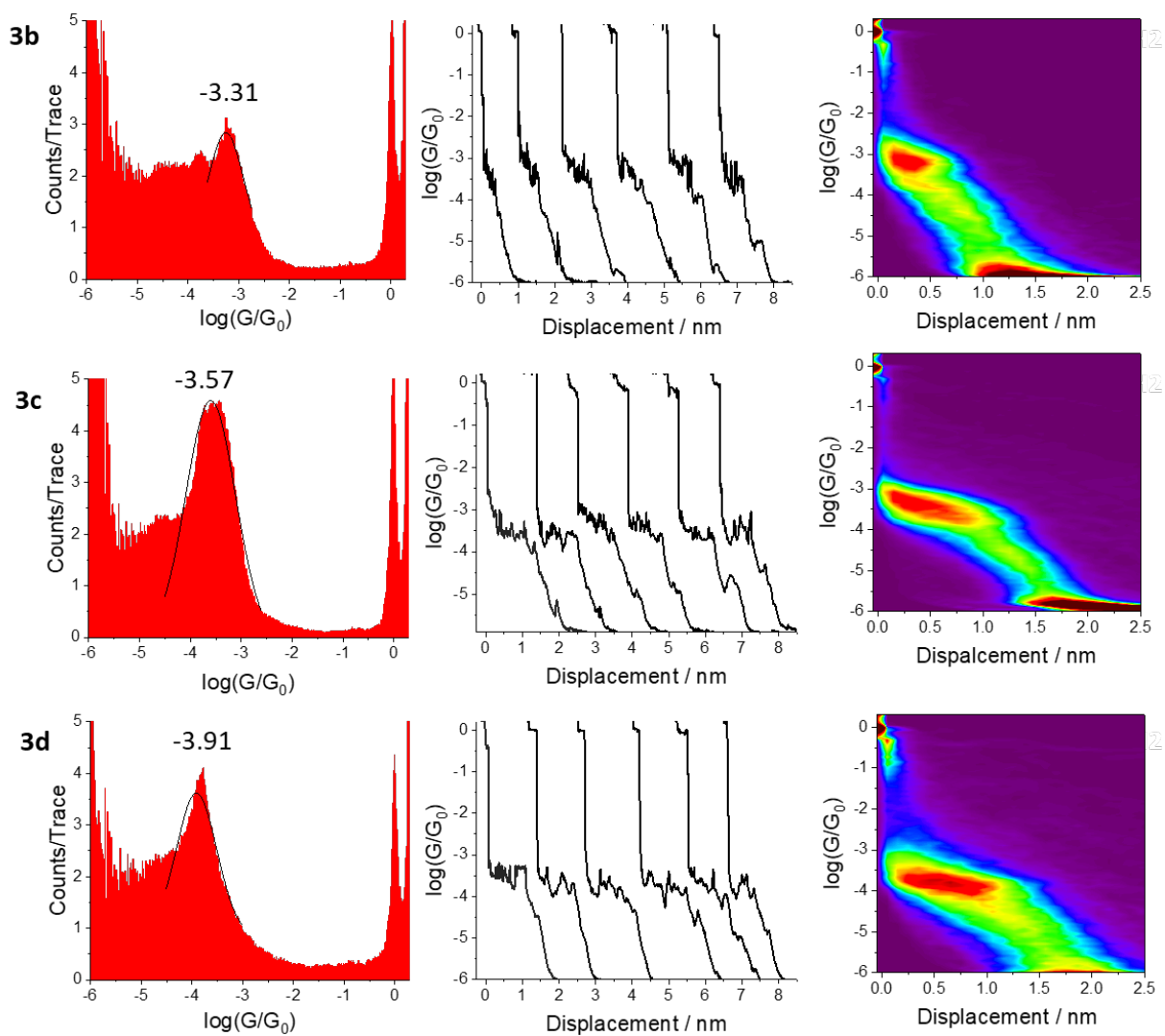


Figure S3. 1D conductance histograms, conductance ($\log(G/G_0)$) vs electrode displacement curves, and 2D conductance-relative displacement histograms of compounds **3b–d**.

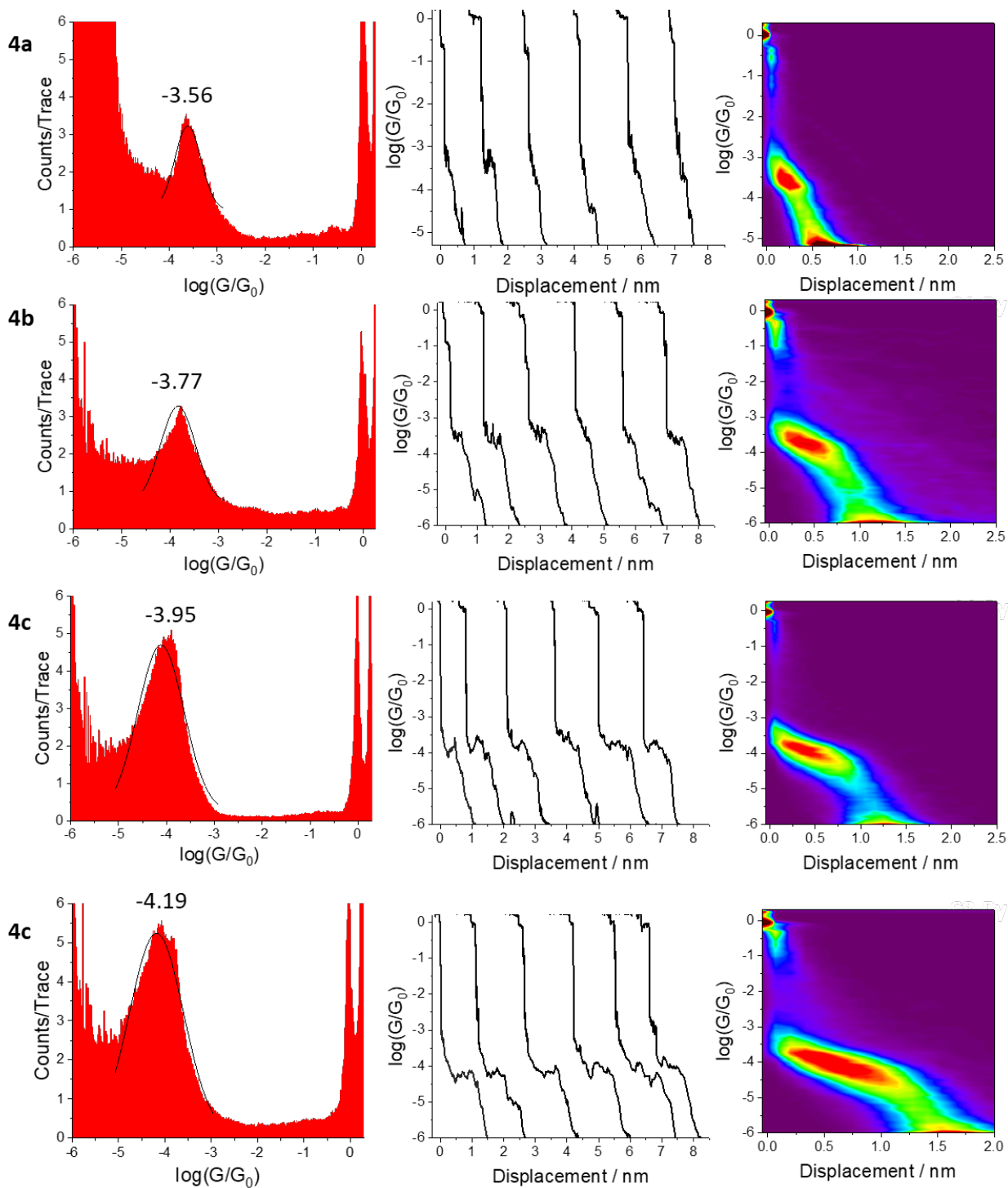


Figure S4. 1D conductance histograms, conductance ($\log(G/G_0)$) vs electrode displacement curves, and 2D conductance-relative displacement histograms of compounds **4b-d**.

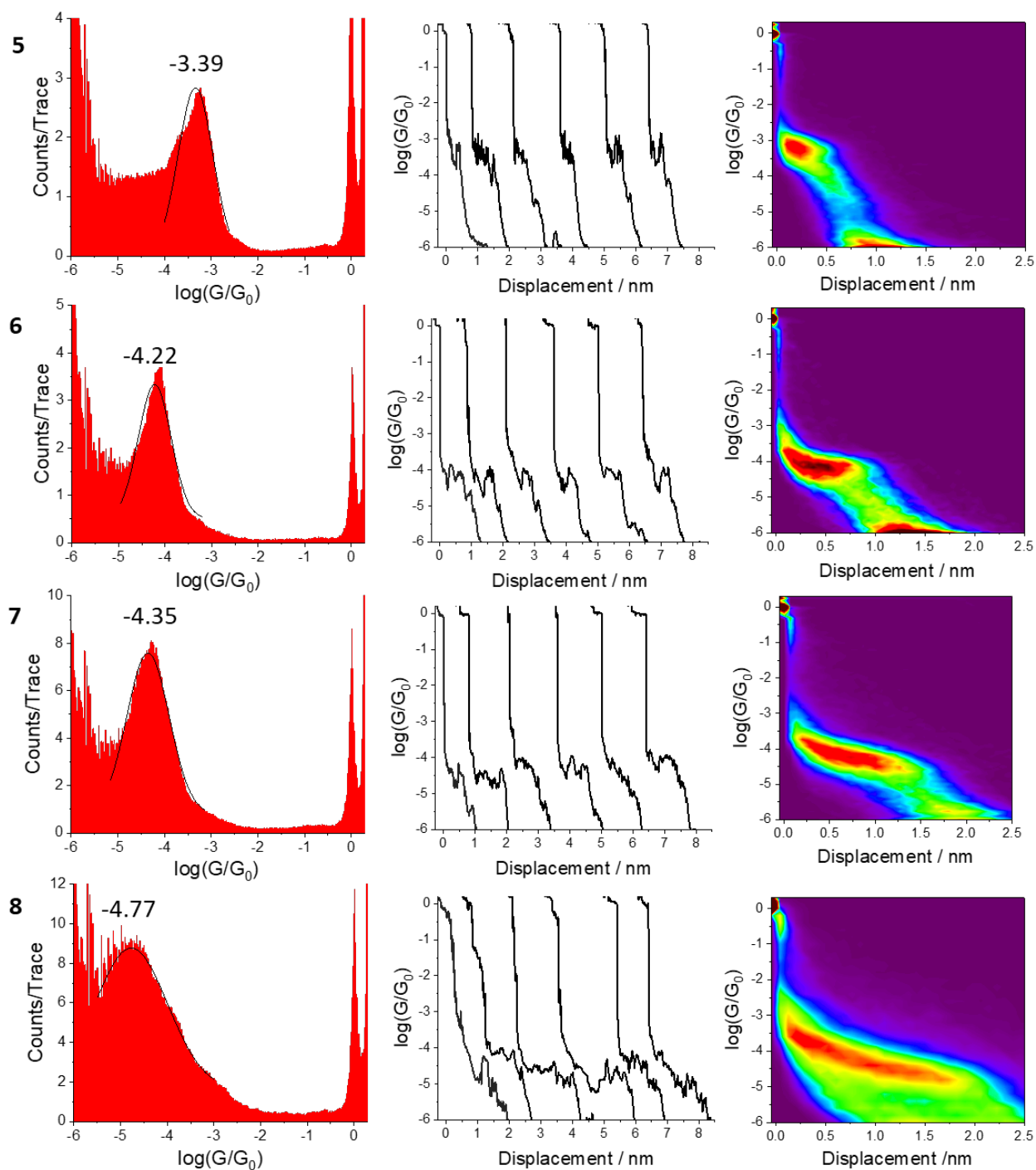


Figure S5. 1D conductance histograms, conductance ($\log(G/G_0)$) vs electrode displacement curves, and 2D conductance-relative displacement histograms of compounds **5** – **8**.

Table S1. Summary of experimental conductance values determined for compounds **1a–d**, **2a–d**, **3a–d**, **4a–d**, **5 – 8** from STM-BJ measurements in mesitylene.

Compound	$\log(G^{\text{exp}}/G_0)$	$\ln(G)$	G (nS)
1a ¹	–3.10	4.11	61.54
1b	–3.25	3.77	43.57
1c	–3.44	3.34	28.13
1d	–3.84	2.42	11.20
2a ¹	–2.70	5.04	154.59
2b	–3.10	4.12	61.54
2c	–3.34	3.57	35.42
2d	–3.74	2.65	14.10
3a ¹	–3.20	3.89	48.89
3b	–3.31	3.64	37.95
3c	–3.57	3.04	20.85
3d	–3.91	2.25	9.53
4a	–3.56	3.06	21.32
4b	–3.77	2.58	13.16
4c	–3.95	2.16	8.69
4d	–4.19	1.61	5.00
5	–3.39	3.45	31.56
6	–4.22	1.54	4.67
7	–4.35	1.24	3.46
8	–4.77	0.27	1.32

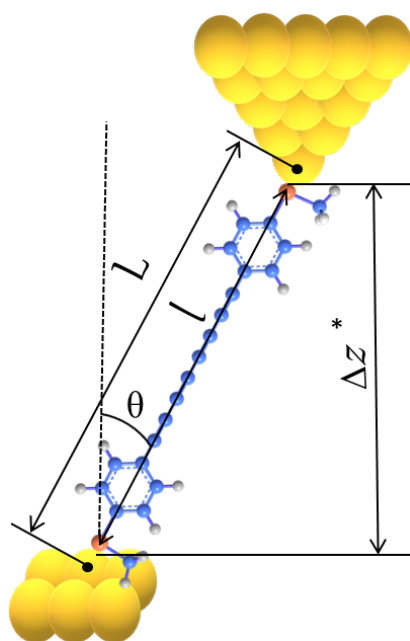


Figure S6. Schematic illustration of the molecular length l (crystallographically determined S···S or N···N separation or S···S or N···N separation determined by geometry optimisation using the Gaussian software package), L (the maximum possible length of the corresponding junction ($L = l + 2d$, where d is the distance between the anchor atom and the centre of the contacting gold atom of an idealised pyramidal-shaped electrode), and Δz^* (experimentally determined break-off distance), tilt angle θ calculated from $\cos^{-1}((\Delta z^* + z_{\text{corr}}) / L)$ where z_{corr} (0.5 nm) is the estimated snap-back distance of the gold electrodes upon cleavage of the last Au-Au contact.²

Table S2. Summary table of experimental conductivity $\log(G^{\text{exp}}/G_0)$ of all compounds and $\log(G^{\text{th}}/G_0)$ calculated from **Equation 1** using parameters from Table 3; **Equation 3** using parameters from Table 1 and Table 2 (or Table S4); **Equation 7** using parameters from Table 3 and Table 5.

Compound	$\log(G^{\text{exp}}/G_0)$	$\log(G/G_0)$ Eq 1 $\log(G_{XBY}/G_0) = a_X + b_B + a_Y$	$\log(G/G_0)$ Eq 3 $G = G_{2c}^N e^{-\beta^N N}$	$\log(G/G_0)$ Eq 7 $\log(G/G_0) = \sum a_i + \sum b_i$
1a¹	-3.1	-3.13	-3.08	-3.17
1b	-3.25	-3.35	-3.32	-3.39
1c	-3.44	-3.57	-3.56	-3.61
1d	-3.84	-3.92	-3.80	-3.96
2a¹	-2.70	-2.73	-2.77	-2.73
2b	-3.10	-2.95	-3.07	-2.95
2c	-3.34	-3.17	-3.37	-3.17
2d	-3.74	-3.52	-3.68	-3.52
3a¹	-3.2	-3.19	-3.14	-3.21
3b	-3.31	-3.41	-3.39	-3.43
3c	-3.57	-3.63	-3.63	-3.65
3d	-3.91	-3.98	-3.88	-4.00
4a	-3.56	-3.47	-3.52	-3.47
4b	-3.77	-3.69	-3.75	-3.69
4c	-3.95	-3.91	-3.98	-3.91
4d	-4.19	-4.26	-4.21	-4.26
5	-3.39	-	-	-3.41
6	-4.22	-	-	-4.25
7	-4.35	-	-	-4.56
8	-4.77	-	-	-4.96
RSS^a	-	0.16	0.04	0.24

^a The residual sum of squares has been used to evaluate the amount of variance in the data (experimental molecular conductivity obtained from STM-BJ experiment vs estimated molecular conductivity obtained from QCR).

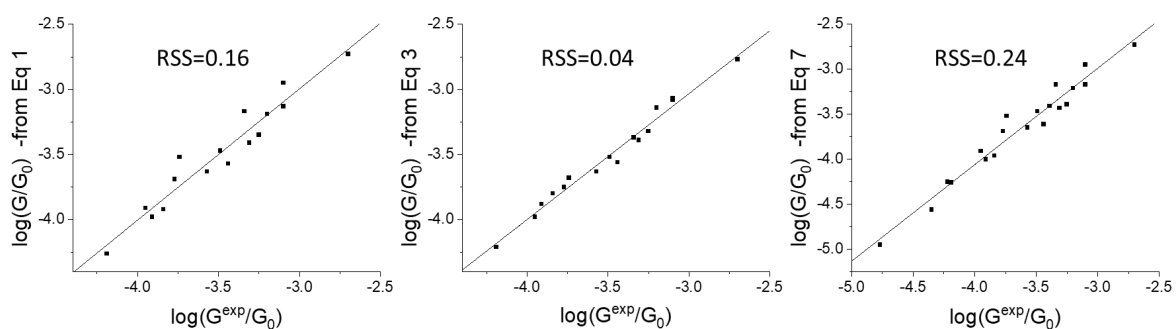


Figure S7. Scatter graph showing the correlation between the experimental measured conductance (x axis) and estimated conductance values obtained using **Eq 1**, **Eq 3**, and **Eq 7** (y axis).

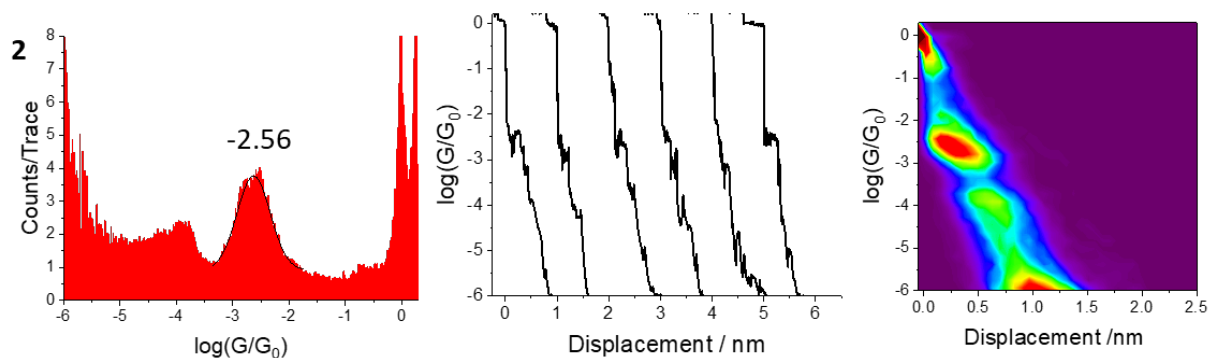


Figure S8. 1D conductance histograms, conductance ($\log(G/G_0)$) vs electrode displacement curves, and 2D conductance-relative displacement histograms of compound **2**.

Table S3. Conductivity values of compounds characteristic lengths, tilt angle θ , Junction Formation Probability (JFP) of compound **2**.

Compound	$\log(G/G_0)^a$	σ^b	$\log(G/G_0)^c$	l (Å) ^d	L (Å) ^e	Δz^* (Å) ^f	$\Delta z^* + z_{\text{corr}}$ (Å) ^g	Tilt angle θ , (°) ^h	JFP (%) ⁱ
2	-2.56 ± 0.01	0.29	-2.42	9.80	14.6	5.0	10.0	46.8	100

^a Experimentally determined most probable molecular conductance from STM-BJ measurements in mesitylene; the error bars are based on the standard deviation in the Gaussian fitting of the 1D conductance histograms.

^b Standard deviation from the statistical spread of the points forming the conductance histogram peak.

^c Molecular conductance calculated from Equation 1.

^d S...S separation determined by Gaussian software.

^e The maximum possible length of the corresponding junction ($L = l + 2d$, where d is the distance between the anchor atom and the centre of the contacting gold atom of an idealised pyramidal-shaped electrode: for DMBT Au-S, $d = 0.24$ nm).

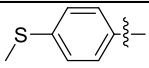
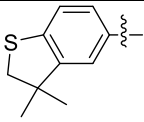
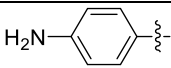
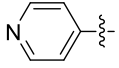
^f Experimentally determined break-off distance.

^g Break-off distance allowing for snap-back of the gold electrodes (0.5 nm).²

^h Calculated from $\cos^{-1}((\Delta z^* + z_{\text{corr}}) / L)$.

ⁱ Proportion of current-distance curves containing the featured molecular plateau.

Table S4. Conductance of contact groups G_{2C}^N obtained from the intersection at $N=0$ per two sites.

Contact group or anchor group	$\ln (G_{2C}^N)$	$\log (G_{2C}^N/G_0)$	G_{2C}^N (nS)
	4.71	-2.84	111.49
	5.59	-2.46	267.74
	4.60	-2.89	99.78
	3.68	-3.29	39.72

2. Molecular Synthesis and Characterisation

2.1 General Conditions

All reactions were carried out undertaken under ambient atmosphere unless otherwise indicated. Tetrahydrofuran, toluene, and dichloromethane were purified and dried on an Inert PureSolv Micro Solvent Purification System, whilst NEt_3 was dried by distillation over CaH_2 . All other solvents were obtained from commercial suppliers and used as received. The 4-ethynylthioanisole,³ 4-ethynylaniline,⁴ 5-ethynyl-3,3-dimethyl-2,3-dihydrobenzo[*b*]thiophene,³ 5-bromo-3,3-dimethyl-2,3-dihydrobenzo[*b*]thiophene,³ 1,6-bis(triphenylphosphinegold(I))-hexa-1,3,5-triyne,⁵ and 4-bromo-1-(trimethylsilylethynyl)benzene⁶ were synthesised according to literature methods. All other materials were obtained from commercial suppliers and used as received.

NMR spectra were recorded from solutions of samples in deuterated chloroform on Varian 400 MHz, Bruker Avance 400 MHz (^1H : 399.86 MHz, ^{13}C : 100.6 MHz) or 500 MHz (^1H : 500.10 MHz, ^{13}C : 125.8 MHz) spectrometers and referenced against residual protio-solvent resonances (CHCl_3 : ^1H 7.26 ppm, $^{13}\text{C}\{^1\text{H}\}$ 77.16 ppm). Infrared (IR) spectra were recorded on an Agilent Technologies Cary 630 spectrometer using ATR sampling methods. High-resolution mass spectra (HR-MS) were recorded using a Waters LCT Premier XE or Thermo Scientific Orbitrap Exploris 120 mass spectrometer using positive mode electrospray ionization (ESI+) or atmospheric pressure chemical ionization (APCI+).

Cautionary Notes!

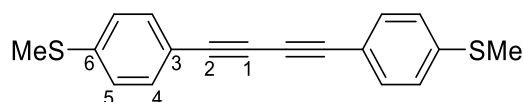
Although no problems were experienced in this work, solid-state terminal buta-1,3-diyne analogues have been reported as explosive.⁷ Care should be taken during the handling of these compounds. Aryl octa-1,3,5,7-tetraynes have been reported as explosive at high temperatures (>245 °C).⁸ High temperature characterisation of octa-1,3,5,7-tetrayne should be avoided.

2.2 Synthetic Methods

2.2.1 Synthesis of Series 1 compounds

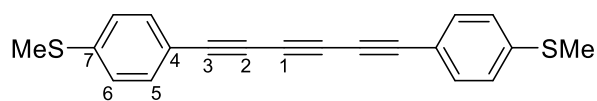
Compound **1a**¹ was synthesised according to literature procedure.

Synthesis of 1,4-bis(4-(methylthio)phenyl)buta-1,3-diyne (**1b**)



A solution of 4-ethynylthioanisole (200 mg, 1.4 mmol), 4-(dimethylamino)pyridine (20 mg, 0.2 mmol) and CuI (10 mg, 0.07 mmol) in acetonitrile (15 mL) was stirred open to air for 20 h at room temperature. The solvent was removed in vacuo and the resulting residue was purified by column chromatography (silica, hexanes followed by 6:1, hexanes:dichloromethane). Evaporation of the eluent afforded the product as a yellow solid (150 mg, 73 %). IR (ATR, $\tilde{\nu}$): $\nu(\text{C-H})$ 2917; $\nu(\text{C}\equiv\text{C})$ 2116 cm^{-1} . ^1H NMR (CDCl_3 , 400 MHz): δ 2.42 (s, 6H, SMe); 7.11 (d, $J = 8.6$ Hz, 4H, H5); 7.48 (d, $J = 8.6$ Hz, 4H, H4) ppm. $^{13}\text{C}\{^1\text{H}\}$ NMR (CDCl_3 , 101 MHz): δ 15.3 (SMe); 74.2 (C1); 81.8 (C2); 118.0 (C3); 125.8 (C5); 132.8 (C4); 141.0 (C6) ppm. HR-MS (APCI(+)) m/z : calcd for $\text{C}_{18}\text{H}_{14}\text{S}_2$ 294.0537; found 294.0539 $[\text{M}]^+$. Spectroscopic data are in agreement with literature values.³

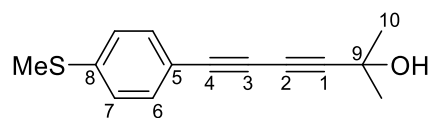
Synthesis of 1,6-bis(4-(methylthio)phenyl)hexa-1,3,5-triyne (**1c**)



To a degassed solution of 4-iodothioanisole (150 mg, 0.62 mmol), $\text{PdCl}_2(\text{PPh}_3)_2$ (11 mg, 0.02 mmol) and CuI (3 mg, 0.02 mmol) in dry dichloromethane (25 mL) under N_2 atmosphere was added 1,6-bis(triphenylphosphinegold(I))-hexa-1,3,5-triyne (310 mg, 0.31 mmol) and the mixture heated to 50 $^\circ\text{C}$ for 5 h. After completion of the reaction, the solvent was evaporated and the residue purified by column chromatography (silica, 1:1 dichloromethane/hexanes). Evaporation of the eluent gave the product as a pale-yellow solid (64 mg, 65 %). IR (ATR, $\tilde{\nu}$): $\nu(\text{C-H})$ 2921; $\nu(\text{Ar-C}\equiv\text{C})$ 2183 cm^{-1} . ^1H NMR (CDCl_3 , 400 MHz): δ 2.49 (s, 6H, SMe); 7.17 (d, $J = 8.6$, 4H, H6); 7.43 (d, $J = 8.6$, 4H, H5) ppm. $^{13}\text{C}\{^1\text{H}\}$ NMR (CDCl_3 , 101 MHz): δ 15.2 (SMe); 66.9 (C1); 74.8 (C2); 78.8 (C3); 117.0 (C4); 125.7 (C6); 133.3 (C5); 141.8 (C7) ppm.

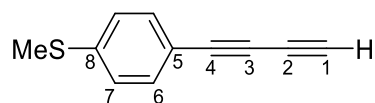
HR-MS (ESI(+)) m/z : calcd for $C_{20}H_{14}S_2+H$ 319.0615; found 319.0617 $[M+H]^+$. Spectroscopic data are in agreement with literature values.⁹

Synthesis of 2-methyl-6-(4-(methylthio)phenyl)hexa-3,5-diyne-2-ol (1d-1)



To a solution of chloroform (2.1 mL) and dioxane (0.7 mL) was added 4-ethynylthioanisole (200 mg, 1.3 mmol), 2-methyl-3-butyn-2-ol (0.16 mL, 1.6 mmol), copper powder (4 mg, 0.07 mmol) and TMEDA (0.03 mL, 0.3 mmol). The reaction vessel was fitted with a condenser and the solution was stirred open to air at 50 °C for 24 h. The solvent was removed in vacuo and the residue purified by column chromatography (silica, 1:1 dichloromethane/hexanes). After evaporation of the eluent the product was obtained as a pale-yellow solid (200 mg, 64 %). IR (ATR, $\tilde{\nu}$): $\nu(O-H)$ 3304; $\nu(C-H)$ 2924-2984; $\nu(Ar-C\equiv C)$ 2229 cm^{-1} . 1H NMR ($CDCl_3$, 400 MHz): δ 1.58 (s, 6H, H10); 1.98 (s, 1H, OH); 2.48 (s, 3H, SMe); 7.16 (d, $J = 8.6$ Hz, 2H, H7); 7.38 (d, $J = 8.6$ Hz, 2H, H6) ppm. $^{13}C\{^1H\}$ NMR ($CDCl_3$, 101 MHz): δ 15.3 (SMe); 31.3 (C10); 65.9 (C9); 67.3 (C1); 73.3 (C2); 78.9 (C3); 86.9 (C4); 117.6 (C5); 125.7 (C7); 132.9 (C6); 141.1 (C8) ppm. HR-MS (ESI(+)) m/z : calcd for $C_{14}H_{14}OS$ 230.0765; found 230.0765 $[M+H]^+$.

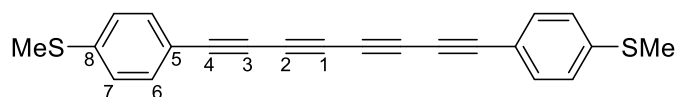
Synthesis of 4-(buta-1,3-diyne)thioanisole (1d-2)



To a degassed solution of **1d-1** (300 mg, 1.3 mmol) in dry toluene (25 mL), under N_2 atmosphere, was added KOH (150 mg, 2.7 mmol) and the mixture heated to 135 °C for 5 min. After completion of the reaction as determined by TLC, the mixture was cooled to room temperature, and the solvent evaporated in vacuo. The residue was purified by flash column chromatography (silica, 4:1 dichloromethane/hexanes). Evaporation of the eluent gave the product as a brown solid that was immediately transferred to the subsequent reaction flask. IR (ATR, $\tilde{\nu}$): $\nu(C\equiv C-H)$ 3280; $\nu(C-H)$ 2854-2961; $\nu(C\equiv C)$ 2201; $\nu(Ar-C\equiv C)$ 2116 cm^{-1} . 1H NMR ($CDCl_3$, 400 MHz): δ 2.49 (s, 3H, SMe); 2.49 (s, 1H, H1); 7.17 (d, $J = 8.6$ Hz, 2H, H7);

7.41 (d, $J = 8.6$ Hz, 2H, H6) ppm. $^{13}\text{C}\{^1\text{H}\}$ NMR (CDCl_3 , 101 MHz): δ 15.2 (SMe); 68.4 (C3); 71.5 (C1); 73.7 (C2); 75.4 (C4); 117.1 (C5); 125.7 (C7); 133.1 (C6); 141.5 (C8) ppm.

Synthesis of 1,8-bis(4-(methylthio)phenyl)octa-1,3,5,7-tetrayne (**1d**)

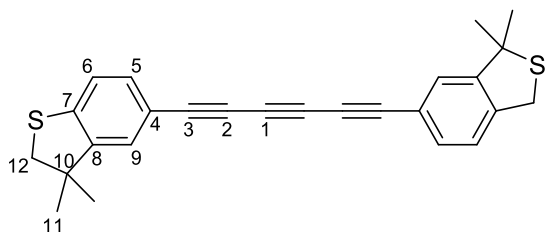


To a solution of chloroform (9 mL) and dioxane (3 mL) was added **1d-2** (220 mg, 1.3 mmol), CuCl (6 mg, 0.06 mmol), and TMEDA (0.04 mL, 0.3 mmol), and the resulting solution was stirred open to air at 50 °C for 48 h. The solvent was evaporated and the residue purified by column chromatography (silica, 1:1 dichloromethane/hexanes). After evaporation of the eluent the product was obtained as a yellow-green solid (200 mg, 90%). IR (ATR, $\tilde{\nu}$): $\nu(\text{C-H})$ 2853-2957; $\nu(\text{Ar-C}\equiv\text{C})$ 2193 cm^{-1} . ^1H NMR (CDCl_3 , 400 MHz): δ 2.49 (s, 6H, SMe); 7.17 (d, $J = 8.6$ Hz, 4H, H7); 7.43 (d, $J = 8.6$ Hz, 4H, H6) ppm. $^{13}\text{C}\{^1\text{H}\}$ NMR (CDCl_3 , 101 MHz): δ 15.1 (Sme); 64.1 (C1); 67.6 (C2); 74.8 (C3); 78.0 (C4); 116.4 (C5); 125.6 (C7); 133.5 (C6); 142.4 (C8) ppm. HR-MS (APCI(+)) m/z : calcd for $\text{C}_{22}\text{H}_{14}\text{S}_2+\text{H}$ 342.0537; found 342.0540 $[\text{M}]^+$. Spectroscopic data are in agreement with literature values.⁹

2.2.2 Synthesis of Series 2 compounds

Compounds **2a**¹ and **2b**³ were synthesised according to literature procedures.

Synthesis of 1,6-bis(3,3-dimethyl-2,3-dihydrobenzo[*b*]thiophen-5-yl)hexa-1,3,5-triyne (**2c**)

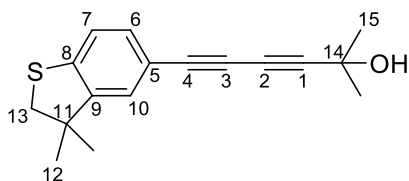


To a degassed solution of 5-bromo-3,3-dimethyl-2,3-dihydrobenzo[*b*]thiophene (61 mg, 0.25 mmol), $\text{Pd}_2(\text{dba})_3$ (3 mg, 0.003 mmol), JohnPhos¹ (0.5 mg, 0.003 mmol), and CuI (0.5 mg, 0.002 mmol) in dry toluene (25 mL) under N_2 atmosphere was added 1,6-

¹ JohnPhos = (2-Biphenyl)di-*tert*-butylphosphine

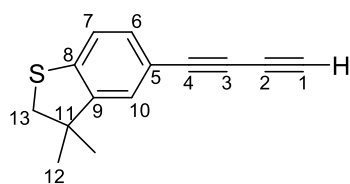
bis(triphenylphosphinegold(I))-hexa-1,3,5-triyn-2-yl (130 mg, 0.13 mmol) and the mixture heated to 90 °C for 21 h. After completion of the reaction, the solvent was evaporated and the residue purified by column chromatography (silica, hexanes followed by 1:1 dichloromethane/hexanes). Evaporation of the eluent and washing with pentane gave the product as an orange solid (8 mg, 6 %). IR (ATR, $\tilde{\nu}$): $\nu(\text{C-H})$ 2867-2962; $\nu(\text{Ar-C}\equiv\text{C})$ 2197 cm^{-1} . ^1H NMR (CDCl_3 , 400 MHz): δ 1.37 (s, 12H, H11); 3.19 (s, 4H, H12); 7.13 (d, $J = 8.0$ Hz, 2H, H6); 7.18 (d, $J = 1.5$ Hz, 2H, H9); 7.29 (dd, $J = 1.5, 8.0$ Hz, 2H, H5) ppm. $^{13}\text{C}\{^1\text{H}\}$ NMR (CDCl_3 , 101 MHz): δ 27.5 (C11); 47.4 (C10); 47.4 (C12); 66.9 (C1); 74.4 (C2); 79.4 (C3); 116.8 (C4); 122.6 (C6); 127.2 (C9); 132.4 (C5); 144.0 (C7); 148.6 (C8) ppm. HR-MS (APCI(+)) m/z : calcd for $\text{C}_{26}\text{H}_{22}\text{S}_2+\text{H}$ 398.1163; found 398.1164 $[\text{M}]^+$.

*Synthesis of 6-(3,3-dimethyl-2,3-dihydrobenzo[*b*]thiophen-5-yl)-2-methylhexa-3,5-diyne-2-ol (2d-1)*



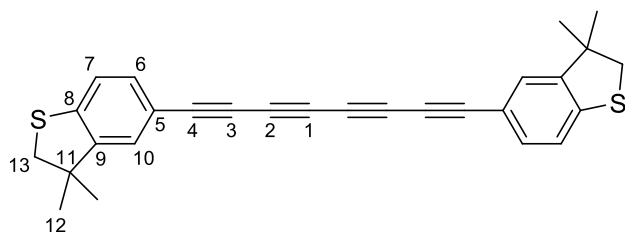
To a solution of chloroform (1.5 mL) and dioxane (0.5 mL) was added copper powder (2 mg, 0.03 mmol), TMEDA (0.02 mL, 0.1 mmol), 5-ethynyl-3,3-dimethyl-2,3-dihydrobenzo[*b*]thiophene (100 mg, 0.53 mmol), 2-methyl-3-butyn-2-ol (0.08 mL, 0.8 mmol) and the resulting mixture was stirred open to air at 50 °C for 16 h. The solvent was evaporated in vacuo and the residue purified by column chromatography (silica, 3:1 dichloromethane/hexanes). After evaporation of the eluent the product was obtained as a colourless solid (83 mg, 58 %). IR (ATR, $\tilde{\nu}$): $\nu(\text{O-H})$ 3325; $\nu(\text{C-H})$ 2867-2960; $\nu(\text{Ar-C}\equiv\text{C})$ 2231 cm^{-1} . ^1H NMR (CDCl_3 , 400 MHz): δ 1.36 (s, 6H, H12); 1.57 (s, 6H, H15); 1.97 (br s, 1H, OH); 3.18 (s, 2H, H13); 7.12 (d, $J = 8.0$ Hz, 1H, H7); 7.14 (d, $J = 1.5$ Hz, 1H, H10); 7.24 (dd, $J = 1.5, 8.0$ Hz, 1H, H6) ppm. $^{13}\text{C}\{^1\text{H}\}$ NMR (CDCl_3 , 101 MHz): δ 27.5 (C12); 31.3 (C15); 47.4 (C11); 47.4 (C13); 65.9 (C14); 67.4 (C1); 72.7 (C2); 79.5 (C3); 86.7 (C4); 117.3 (C5); 122.5 (C7); 126.8 (C10); 131.9 (C6); 143.3 (C8); 148.5 (C9) ppm. HR-MS (APCI(+)) m/z : calcd for $\text{C}_{17}\text{H}_{18}\text{OS}+\text{H}$ 271.1157; found 271.1156 $[\text{M}+\text{H}]^+$.

Synthesis of 5-(buta-1,3-diynyl)-3,3-dimethyl-2,3-dihydrobenzo[*b*]thiophene (**2d-2**)



To a degassed solution of **2d-1** (160 mg, 0.59 mmol) in dry toluene (20 mL), under N₂ atmosphere, was added NaOH (80 mg, 2.0 mmol) and the mixture heated to 135 °C for 3 h. After completion of the reaction as determined by TLC, the mixture was cooled to room temperature, and the solvent evaporated in vacuo. The residue was purified by flash column chromatography (silica, 1:1 dichloromethane/hexanes). Evaporation of the eluent gave the product as a yellow oil that was immediately transferred to the subsequent reaction vessel. IR (ATR, $\tilde{\nu}$): $\nu(\text{C}\equiv\text{C}-\text{H})$ 3287; $\nu(\text{C}-\text{H})$ 2850-2960; $\nu(\text{Ar}-\text{C}\equiv\text{C})$ 2203; cm^{-1} . ¹H NMR (CDCl₃, 400 MHz): δ 1.36 (s, 6H, H12); 2.47 (s, 1H, H1); 3.19 (s, H2, H13); 7.12 (d, $J = 8.0$ Hz, 1H, H7); 7.17 (d, $J = 1.5$ Hz, 1H, H10); 7.27 (dd, $J = 1.5, 8.0$ Hz, 1H, H6) ppm. ¹³C{¹H} NMR (CDCl₃, 101 MHz): δ 27.5 (C12); 47.4 (C11); 47.4 (C13); 68.5 (C3); 71.3 (C1); 73.2 (C2); 76.1 (C4); 116.8 (C5); 122.5 (C7); 127.1 (C10); 132.2 (C6); 143.8 (C8); 148.6 (C9) ppm.

Synthesis of 1,8-bis(3,3-dimethyl-2,3-dihydrobenzo[*b*]thiophen-5-yl)octa-1,3,5,7-tetrayne (**2d**)



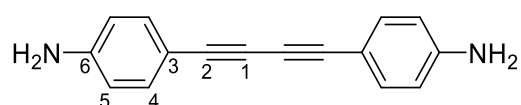
To a solution of chloroform (6 mL) and dioxane (2 mL) was added **2d-2** (130 mg, 0.59 mmol), CuCl (3 mg, 0.03 mmol), and TMEDA (0.02 mL, 0.1 mmol), and the resulting solution was stirred open to air at 50 °C for 16 h. The solvent was evaporated and the residue purified by column chromatography (silica, 1:1 dichloromethane/hexanes). After evaporation of the eluent the product was obtained as a yellow solid (100 mg, 83%). IR (ATR, $\tilde{\nu}$): $\nu(\text{C}-\text{H})$ 2323-2958; $\nu(\text{Ar}-\text{C}\equiv\text{C})$ 2195 cm^{-1} . ¹H NMR (CDCl₃, 400 MHz): δ 1.36 (s, 12H, H12); 3.20 (s, 4H, H13); 7.13 (d, $J = 8.0$ Hz, 2H, H7); 7.18 (d, $J = 1.6$ Hz, 2H, H10); 7.29 (dd, $J = 1.6, 8.0$ Hz, 2H H6) ppm. ¹³C{¹H} NMR (CDCl₃, 101 MHz): δ 27.5 (C12); 47.4 (C11); 47.5 (C13); 64.2 (C1); 67.6 (C2); 74.4 (C3); 78.6 (C4); 116.3 (C5); 122.6 (C7); 127.4 (C10);

132.7 (C6); 144.6 (C8); 148.7 (C9) ppm. HR-MS (ESI(+)) m/z : calcd for $C_{28}H_{22}S_2$ 422.1163; found 422.1162 $[M]^+$.

2.2.3 Synthesis of Series 3 compounds

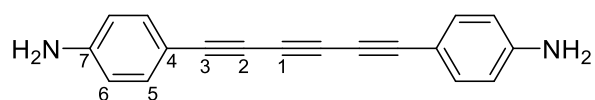
Compound **3a**¹ was synthesised according to literature procedure.

Synthesis of 4,4'-(buta-1,3-diyne-1,4-diyl)dianiline (**3b**)



Copper acetate (780 mg, 4.3 mmol) and 4-ethynylaniline (200 mg, 1.7 mmol) were added to a solution of methanol (10 mL) and pyridine (10 mL). The resulting mixture was stirred for 3 days at room temperature. The solvent was removed in vacuo and the resulting solid purified by column chromatography (silica, 9:1 dichloromethane/hexanes with 1% NEt_3). After evaporation of the eluent the product was obtained as an orange solid (110 mg, 57 %). IR (ATR, $\tilde{\nu}$): $\nu(N-H)$ 3443, 3406, 3322; $\nu(C\equiv C)$ 2209 cm^{-1} . 1H NMR ($CDCl_3$, 400 MHz): δ 3.86 (s, 4H, NH_2); 6.59 (d, $J = 8.6$ Hz, 4H, H5); 7.31 (d, $J = 8.6$ Hz, 4H, H4) ppm. $^{13}C\{^1H\}$ NMR ($CDCl_3$, 101 MHz): δ 72.4 (C1); 81.8 (C2); 111.2 (C3); 114.6 (C5); 133.9 (C4); 147.2 (C6) ppm. HR-MS (ESI(+)) m/z : calcd for $C_{16}H_{12}N_2+H$ 233.1079; found 233.1080 $[M+H]^+$. Spectroscopic data are in agreement with literature values.¹⁰

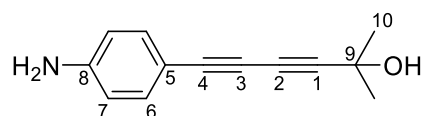
Synthesis of 4,4'-(hexa-1,3,5-triyne-1,6-diyl)dianiline (**3c**)



To a degassed solution of 4-iodoaniline (170 mg, 0.78 mmol), $PdCl_2(PPh_3)_2$ (14 mg, 0.02 mmol) and CuI (4 mg, 0.02 mmol) in dry dichloromethane (25 mL), under N_2 atmosphere, was added 1,6-bis(triphenylphosphinegold(I))-hexa-1,3,5-triyne (390 mg, 0.39 mmol) and the mixture heated to 50 °C for 19 h. After completion of the reaction, the solvent was evaporated and the residue purified by column chromatography (silica, 9:1 dichloromethane/hexanes). Evaporation of the eluent gave the product as an orange solid (74 mg, 74 %). IR (ATR, $\tilde{\nu}$):

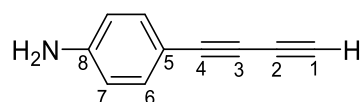
$\nu(\text{N-H})$ 3420, 3299, 3192; $\nu(\text{Ar-C}\equiv\text{C})$ 2170 cm^{-1} . $^1\text{H NMR}$ (CDCl_3 , 400 MHz): δ 3.92 (br s, 4H, NH_2); 6.58 (d, $J = 8.7$ Hz, 4H, H5); 7.33 (d, $J = 8.7$ Hz, 4H, H6) ppm. $^{13}\text{C}\{^1\text{H}\}$ NMR (CDCl_3 , 101 MHz): δ 66.6 (C1); 73.2 (C2); 79.7 (C3); 110.2 (C4); 114.7 (C6); 134.7 (C5); 147.9 (C7) ppm. HR-MS (ESI(+)) m/z : calcd for $\text{C}_{18}\text{H}_{12}\text{N}_2+\text{H}$ 257.1079; found 257.1079 $[\text{M}+\text{H}]^+$.

Synthesis of 6-(4-aminophenyl)-2-methylhexa-3,5-diyne-2-ol (**3d-1**)



To a solution of chloroform (9 mL) and dioxane (3 mL) was added 4-ethynylaniline (200 mg, 1.7 mmol), 2-methyl-3-butyn-2-ol (0.21 mL, 2.2 mmol), CuCl (9 mg, 0.09 mmol) and TMEDA (0.05 mL, 0.3 mmol). The resulting mixture was stirred open to air at 50 °C for 48 h. The solvent was evaporated in vacuo and the residue purified by column chromatography (silica, 3:1 hexanes/ethyl acetate). Evaporation of the eluent gave the product as an orange solid (200 mg, 59 %). IR (ATR, $\tilde{\nu}$): $\nu(\text{N-H})$ 3460, 3524; $\nu(\text{O-H})$ 3356; $\nu(\text{C-H})$ 2854-2974; $\nu(\text{Ar-C}\equiv\text{C})$ 2231 cm^{-1} . $^1\text{H NMR}$ (CDCl_3 , 400 MHz): δ 1.57 (s, 6H, H10); 1.96 (br s, 1H, OH); 3.88 (br s, 2H, NH_2); 6.58 (d, $J = 8.6$ Hz, 2H, H7); 7.29 (d, $J = 8.6$ Hz, 2H, H6) ppm. $^{13}\text{C}\{^1\text{H}\}$ NMR (CDCl_3 , 101 MHz): δ 31.4 (C10); 65.9 (C9); 67.7 (C1); 71.3 (C2); 80.1 (C3); 85.9 (C4); 110.6 (C5); 114.7 (C7); 134.2 (C6); 147.7 (C8) ppm. HR-MS (ESI(+)) m/z : calcd for $\text{C}_{13}\text{H}_{13}\text{NO}+\text{H}$ 200.1075; found 200.1076 $[\text{M}+\text{H}]^+$. Spectroscopic data are in agreement with literature values.¹¹

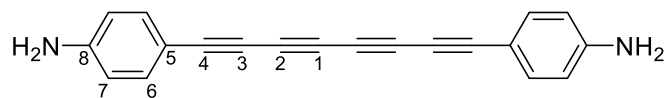
Synthesis of 4-(buta-1,3-diyne)aniline (**3d-2**)



To a degassed solution of **3d-1** (300 mg, 1.5 mmol) in dry toluene (25 mL), under N_2 atmosphere, was added NaOH (150 mg, 3.9 mmol) and the mixture heated to 135 °C for 90 min. After completion of the reaction as determined by TLC, the mixture was cooled to room temperature, and the solvent evaporated in vacuo. The residue was purified by flash column chromatography (silica, 1:1 hexanes/ethyl acetate with 1 % NEt_3). Evaporation of the eluent

gave the product as an orange oil that rapidly began to turn brown/black and was immediately transferred to the subsequent reaction vessel. IR (ATR, $\tilde{\nu}$): $\nu(\text{N-H})$ 3389, 3479; $\nu(\text{C}\equiv\text{C-H})$ 3285; $\nu(\text{Ar-C}\equiv\text{C})$ 2201 cm^{-1} . ^1H NMR (CDCl_3 , 400 MHz): δ 2.45 (s, 1H, H1); 3.91 (br s, 2H, NH_2); 6.58 (d, $J = 8.6$ Hz, 2H, H7); 7.32 (d, $J = 8.6$ Hz, 2H, H6) ppm. $^{13}\text{C}\{^1\text{H}\}$ NMR (CDCl_3 , 101 MHz): δ 68.8 (C3); 70.6 (C1); 71.8 (C2); 76.6 (C4); 109.9 (C5); 114.7 (C7); 134.5 (C6); 147.9 (C8) ppm.

Synthesis of 4,4'-(octa-1,3,5,7-tetrayne-1,8-diyl)dianiline (**3d**)

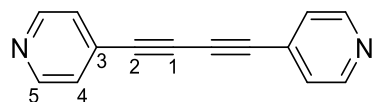


To a solution of chloroform (9 mL) and dioxane (3 mL) was added **3d-2** (210 mg, 1.5 mmol), CuCl (8 mg, 0.08 mmol), and TMEDA (0.04 mL, 0.3 mmol), and the resulting solution was stirred open to air at 50 °C for 22 h. The solvent was evaporated, and the residue purified by column chromatography (silica, dichloromethane). After evaporation of the eluent the product was obtained as an orange solid (160 mg, 77 %). IR (ATR, $\tilde{\nu}$): $\nu(\text{N-H})$ 3193, 3293, 3415; $\nu(\text{Ar-C}\equiv\text{C})$ 2183 cm^{-1} . ^1H NMR (CDCl_3 , 400 MHz): δ 3.96 (br s, 4H, NH_2); 6.58 (d, $J = 8.6$ Hz, 4H, H7); 7.34 (d, $J = 8.6$ Hz, 4H, H6) ppm. $^{13}\text{C}\{^1\text{H}\}$ NMR (CDCl_3 , 101 MHz): δ 64.3 (C1); 67.3 (C2); 73.3 (C3); 79.1 (C4); 109.4 (C5); 114.7 (C7); 135.1 (C6); 148.3 (C8) ppm. HR-MS (ESI(+)) m/z : calcd for $\text{C}_{20}\text{H}_{12}\text{N}_2+\text{H}$ 281.1079; found 281.1078 $[\text{M}+\text{H}]^+$.

2.2.4 Synthesis of Series 4 compounds

Compound **4a**¹² was synthesised according to literature procedures.

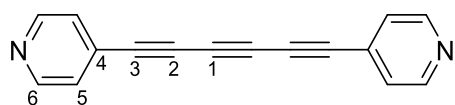
Synthesis of 1,4-di(pyridin-4-yl)buta-1,3-diyne (**4b**)



Copper chloride (50 mg, 0.5 mmol), TMEDA (0.56 mL, 3.7 mmol) and 4-ethynylpyridine hydrochloride (260 mg, 1.8 mmol) were added to acetonitrile (40 mL) and the resulting mixture stirred open to air for 15 h at room temperature. The solvent was removed in vacuo and the residue purified by flash column chromatography (silica, 1:2 hexane/ethyl acetate

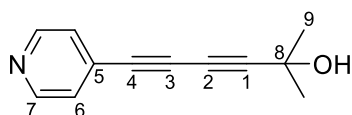
with 1 % NEt₃). After evaporation of the eluent the product was obtained as a colourless solid (150 mg, 80 %). IR (ATR, $\tilde{\nu}$): $\nu(\text{C-H})$ 2852-3025; $\nu(\text{C}\equiv\text{C})$ 2120 cm⁻¹. ¹H NMR (CDCl₃, 400 MHz): δ 7.39 (d, J = 6.0 Hz, 4H, H4); 8.65 (d, J = 6.0 Hz, 4H, H5) ppm. ¹³C {¹H} NMR (CDCl₃, 101 MHz): δ 77.3 (C1); 80.4 (C2); 126.2 (C4); 129.5 (C3); 150.1 (C5) ppm. HR-MS (ESI(+)) m/z : calcd for C₁₄H₈N₂+H 205.0766; found 205.0769 [M+H]⁺. Spectroscopic data are in agreement with literature values.¹³

Synthesis of 1,6-di(4-pyridyl)hexa-1,3,5-triyne (**4c**)



To a degassed solution of 4-iodopyridine (66 mg, 0.32 mmol), PdCl₂(PPh₃)₂ (3 mg, 0.004 mmol), and CuI (1 mg, 0.001 mmol) in dry dichloromethane (25 mL) under N₂ atmosphere was added 1,6-bis(triphenylphosphinegold(I))-hexa-1,3,5-triyne (160 mg, 0.16 mmol) and the mixture heated to 50 °C for 21 h. After completion of the reaction, the solvent was evaporated and the residue purified by column chromatography (silica, 1:1 dichloromethane/ethyl acetate with 1 % NEt₃). Evaporation of the eluent gave the product as a colourless solid (25 mg, 67 %). IR (ATR, $\tilde{\nu}$): $\nu(\text{Ar-C}\equiv\text{C})$ 2199 cm⁻¹. ¹H NMR (CDCl₃, 400 MHz): δ 7.38 (d, J = 5.8 Hz, 4H, H5); 8.64 (d, J = 5.8 Hz, 4H, H6) ppm. ¹³C {¹H} NMR (CDCl₃, 101 MHz): δ 67.5 (C1); 76.4 (C3); 78.1 (C2); 126.5 (C5); 129.1 (C4); 150.2 (C6) ppm. HR-MS (ESI(+)) m/z : calcd for C₁₆H₈N₂+H 229.0766; found 229.0765 [M+H]⁺.

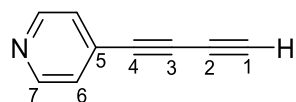
Synthesis of 6-(4-pyridyl)-2-methylhexa-3,5-diyne-2-ol (**4d-1**)



To a solution of chloroform (4 mL) and dioxane (1.5 mL) was added 4-ethynylpyridine hydrochloride (130 mg, 0.97 mmol), 2-methyl-3-butyn-2-ol (1.2 mL, 1.3 mmol), copper powder (3 mg, 0.05 mmol), and TMEDA (0.17 mL, 1.2) and the resulting mixture was stirred open to air at 50 °C for 24 h. The solvent was removed in vacuo and the residue purified by column chromatography (silica, 1:1 ethyl acetate/hexanes). Evaporation of the eluent afforded the product as a colourless solid (28 mg, 16%). IR (ATR, $\tilde{\nu}$): $\nu(\text{O-H})$

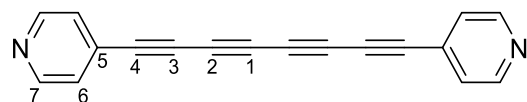
3378; $\nu(\text{C-H})$ 2374-2976; $\nu(\text{Ar-C}\equiv\text{C})$ 2237 cm^{-1} . $^1\text{H NMR}$ (CDCl_3 , 400 MHz): δ 1.59 (s, 6H, H9); 2.15 (s, 1H, OH); 7.32 (d, $J = 6.0$ Hz, 2H, H6); 8.60 (d, $J = 6.0$ Hz, 2H, H7) ppm. $^{13}\text{C}\{^1\text{H}\}$ NMR (CDCl_3 , 101 MHz): δ 31.2 (C9); 65.9 (C8); 66.5 (C1); 75.7 (C2); 77.7 (C3); 89.2 (C4); 126.3 (C6); 130.1 (C5); 149.9 (C7) ppm. HR-MS (ESI(+)) m/z : calcd for $\text{C}_{12}\text{H}_{11}\text{NO}+\text{H}$ 186.0919; found 186.0917 $[\text{M}+\text{H}]^+$. Spectroscopic data are in agreement with literature values.⁷

Synthesis of 4-(buta-1,3-diynyl)pyridine (**4d-2**)



To a degassed solution of **4d-1** (230 mg, 1.2 mmol) in dry toluene (20 mL), under N_2 atmosphere, was added NaOH (120 mg, 3.0 mmol) and the mixture heated to 135 $^\circ\text{C}$ for 50 min. After completion of the reaction as determined by TLC, the mixture was cooled to room temperature, and the solvent evaporated in vacuo. The residue was purified by flash column chromatography (silica, 3:1 hexanes/ethyl acetate with 1 % NEt_3). Evaporation of the eluent gave the product as a colourless solid that was immediately transferred to the subsequent reaction vessel. IR (ATR, $\tilde{\nu}$): $\nu(\text{C}\equiv\text{C})$ 3097; $\nu(\text{C-H})$ 2855-2959; $\nu(\text{Ar-C}\equiv\text{C})$ 2121 cm^{-1} . $^1\text{H NMR}$ (CDCl_3 , 400 MHz): δ 2.59 (s, 1H, H1); 7.35 (d, $J = 4.3$, 2H, H6); 8.60 (d, $J = 4.3$ Hz, 2H, H7) ppm. $^{13}\text{C}\{^1\text{H}\}$ NMR (CDCl_3 , 101 MHz): δ 67.4 (C3); 72.3 (C2); 73.6 (C1); 77.8 (C4); 126.4 (C6); 129.5 (C5); 150.0 (C7) ppm.

Synthesis 1,8-di(4-pyridyl)octa-1,3,5,7-tetrayne (**4d**)

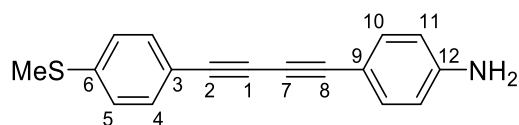


To a solution of chloroform (9 mL) and dioxane (3 mL) was added **4d-2** (160 mg, 1.2 mmol), CuCl (8 mg, 0.08 mmol), and TMEDA (0.05 mL, 0.3 mmol), and the resulting solution was stirred open to air at 50 $^\circ\text{C}$ for 16 h. The solvent was evaporated and the residue purified by column chromatography (silica, 1:1 hexanes/ethyl acetate with 1 % NEt_3). After evaporation of the eluent the product was obtained as a colourless solid (100 mg, 63 %). IR (ATR, $\tilde{\nu}$): $\nu(\text{C-H})$ 2854-2957; $\nu(\text{Ar-C}\equiv\text{C})$ 2206 cm^{-1} . $^1\text{H NMR}$ (CDCl_3 , 400 MHz): δ 7.37 (d, $J = 4.4$

Hz, 4H, H6); 8.64 (d, $J = 4.4$ Hz, 4H, H7) ppm. $^{13}\text{C}\{^1\text{H}\}$ NMR (CDCl_3 , 101 MHz): δ 63.7 (C1); 68.6 (C2); 75.0 (C3); 78.2 (C4); 126.6 (C6); 128.8 (C5); 150.2 (C7) ppm. HR-MS (ESI(+)) m/z : calcd for $\text{C}_{18}\text{H}_8\text{N}_2+\text{H}$ 253.0766; found 253.0765 $[\text{M}+\text{H}]^+$. Spectroscopic data are in agreement with literature values.⁸

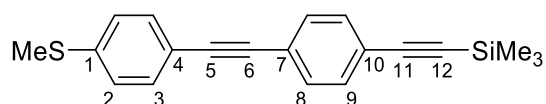
2.2.5 Synthesis of Additional Compounds

Synthesis of 4-((4-(methylthio)phenyl)buta-1,3-diyne-1-yl)aniline (5)



To a solution of chloroform (2.1 mL) and dioxane (0.7 mL) was added copper powder (3 mg, 0.05 mmol), TMEDA (0.03 mL, 0.2 mmol), 4-ethynylthioanisole (150 mg, 1.0 mmol), and 4-ethynylaniline (140 mg, 1.2 mmol) and the resulting mixture was stirred open to air at 50 °C for 24 h. The solvent was evaporated in vacuo and the resulting residue purified by column chromatography (silica, 3:1 dichloromethane/hexanes). After evaporation of the eluent the product was obtained as an orange solid (120 mg, 44 %). IR (ATR, $\tilde{\nu}$): $\nu(\text{N-H})$ 3380, 3466; $\nu(\text{C}\equiv\text{C})$ 2137, 2206 cm^{-1} . ^1H NMR (CDCl_3 , 400 MHz): δ 2.49 (s, 3H, SMe); 3.89 (br s, 2H, NH_2); 6.60 (d, $J = 8.7$ Hz, 2H, H11); 7.17 (d, $J = 8.6$ Hz, 2H, H5); 7.33 (d, $J = 8.7$ Hz, 2H, H10); 7.41 (d, $J = 8.6$ Hz, 2H, H4) ppm. $^{13}\text{C}\{^1\text{H}\}$ NMR (CDCl_3 , 101 MHz): δ 15.4 (SMe); 72.2 (C1); 74.7 (C7); 80.8 (C2); 83.0 (C8); 110.9 (C9); 114.8 (C11); 118.5 (C3); 125.8 (C5); 132.8 (C4); 134.2 (C10); 140.5 (C6); 147.6 (C12) ppm. HR-MS (ESI(+)) m/z : calcd for $\text{C}_{17}\text{H}_{14}\text{NS}$ 264.0842; found 264.0839 $[\text{M}+\text{H}]^+$.

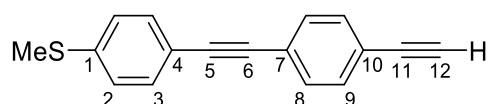
Synthesis of 4-((4-(methylthio)phenyl)ethynyl)-1-(trimethylsilylethynyl)benzene



To a degassed solution of 4-bromo-1-(trimethylsilylethynyl)benzene (890 mg, 3.5 mmol), $\text{PdCl}_2(\text{PPh}_3)_2$ (50 mg, 0.07 mmol), and CuI (10 mg, 0.05 mmol) in dry NEt_3 (20 mL) was added 4-ethynylthioanisole (40 mg, 2.7 mmol). The resulting mixture was heated to 90 °C for 18 h. The solvent was evaporated in vacuo and the residue purified by column

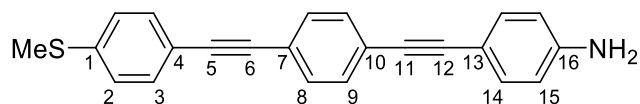
chromatography (silica, 3:1 hexanes/dichloromethane). After evaporation of the eluent the product was obtained as a pale-yellow solid (580 mg, 68 %). IR (ATR, $\tilde{\nu}$): $\nu(\text{C}\equiv\text{C})$ 2154, 2216 cm^{-1} . ^1H NMR (CDCl_3 , 400 MHz): δ 0.26 (s, 9H, SiMe_3); 2.50 (s, 3H, SMe); 7.21 (d, $J = 8.6$ Hz, 2H, H3); 7.43 (d, $J = 8.6$ Hz, 2H, H2); 7.44 (s, 4H, H8/9) ppm. $^{13}\text{C}\{^1\text{H}\}$ NMR (CDCl_3 , 101 MHz): δ 0.07 (SiMe_3); 15.5 (SMe); 89.3 (C6/11); 91.3 (C5); 96.4 (C12); 104.8 (C6/11); 119.4 (C4); 123.0 (C7/10); 123.5 (C7/10); 126.0 (C2); 131.4 (C8/9); 132.0 (C3/8/9); 132.0 (C3/8/9); 139.8 (C1) ppm. HR-MS (APCI(+)) m/z : calcd for $\text{C}_{20}\text{H}_{20}\text{SSi}$ 320.1050; found 320.1048 $[\text{M}]^+$.

Synthesis of 4-((4-(methylthio)phenyl)ethynyl)-1-(ethynyl)benzene



To a degassed solution of 4-((4-(methylthio)phenyl)ethynyl)-1-(trimethylsilylethynyl)benzene (500 mg, 1.6 mmol) in dry MeOH (25 mL) was added K_2CO_3 (320 mg, 2.3 mmol). The resulting mixture was stirred at room temperature for 19 h. The solvent was evaporated in vacuo and the residue purified by column chromatography (silica, 1:1 dichloromethane/hexanes). After evaporation of the eluent the product was obtained as a pale-yellow solid (390 mg, 99 %). IR (ATR, $\tilde{\nu}$): $\nu(\text{C}\equiv\text{C}-\text{H})$ 3267; $\nu(\text{C}\equiv\text{C})$ 2102, 2213 cm^{-1} . ^1H NMR (CDCl_3 , 400 MHz): δ 2.50 (s, 3H, SMe); 3.17 (s, 1H, H12); 7.21 (d, $J = 8.6$ Hz, 2H, H2); 7.43 (d, $J = 8.6$ Hz, 2H, H3); 7.46 (s, 4H, H8/9) ppm. $^{13}\text{C}\{^1\text{H}\}$ NMR (CDCl_3 , 101 MHz): δ 15.5 (SMe); 79.0 (C12); 83.4 (C6/11); 89.1 (C6/11); 91.4 (C5); 119.3 (C4); 121.9 (C7/10); 124.0 (C7/10); 126.0 (C2); 131.5 (C8/9); 132.0 (C3/8/9); 132.2 (C3/8/9); 139.9 (C1) ppm. HR-MS (ESI(+)) m/z : calcd for $\text{C}_{17}\text{H}_{13}\text{S}$ 249.0733; found 249.0730 $[\text{M}+\text{H}]^+$.

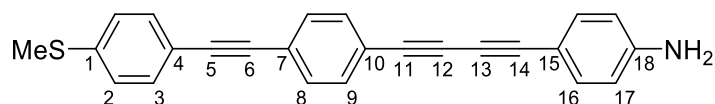
Synthesis of 4-((4-((4-(methylthio)phenyl)ethynyl)phenyl)ethynyl)aniline (6)



To a degassed solution of 4-((4-(methylthio)phenyl)ethynyl)-1-(ethynyl)benzene (100 mg, 0.40 mmol), $\text{PdCl}_2(\text{PPh}_3)_2$ (7 mg, 0.01 mmol), and CuI (2 mg, 0.01 mmol) in dry NEt_3 (5 mL) and tetrahydrofuran (5 mL) was added 4-iodoaniline (97 mg, 0.44 mmol). The resulting

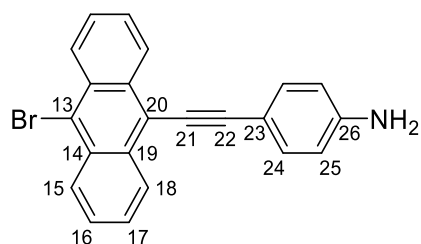
mixture was stirred at room temperature for 17 h. The solvent was evaporated in vacuo and the residue purified by column chromatography (silica, 3:1 dichloromethane/hexanes). After evaporation of the eluent the product was obtained as a pale-brown solid (66 mg, 48 %). IR (ATR, $\tilde{\nu}$): $\nu(\text{N-H})$ 3354, 3456; $\nu(\text{C}\equiv\text{C})$ 2210 cm^{-1} . ^1H NMR (CDCl_3 , 400 MHz): δ 2.50 (s, 3H, SMe); 3.84 (br s, 2H, NH_2); 6.64 (d, $J = 8.6$ Hz, 2H, H15); 7.21 (d, $J = 8.5$ Hz, 2H, H2); 7.34 (d, $J = 8.6$ Hz, 2H, H14); 7.44 (d, $J = 8.5$ Hz, 2H, H14); 7.46 (s, 4H, H8/9) ppm. $^{13}\text{C}\{^1\text{H}\}$ NMR (CDCl_3 , 101 MHz): δ 15.5 (SMe); 87.4 (6/11); 89.6 (6/11); 90.9 (C5); 92.3 (C12); 112.5 (C13); 114.9 (C15); 119.6 (C4); 122.5 (C7/10); 123.9 (C7/10); 126.0 (C2); 131.4 (C8/9); 131.5 (C8/9); 132.0 (C3); 133.2 (C14); 139.7 (C1); 147.0 (C16) ppm. HR-MS (ESI(+)) m/z : calcd for $\text{C}_{23}\text{H}_{18}\text{NS}$ 340.1155; found 340.1153 $[\text{M}+\text{H}]^+$.

Synthesis of 4-((4-((4-(methylthio)phenyl)ethynyl)phenyl)buta-1,3-diyne-1-yl)aniline (7)



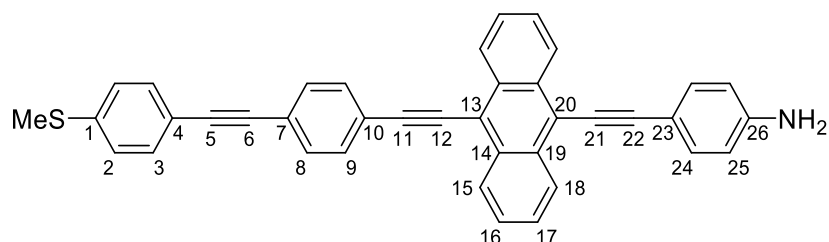
To a solution of chloroform (2.1 mL) and dioxane (0.7 mL) was added copper powder (2 mg, 0.03 mmol), TMEDA (0.02 mL, 0.1 mmol), 4-((4-(methylthio)phenyl)ethynyl)-1-(ethynyl)benzene (150 mg, 0.6 mmol), and 4-ethynylaniline (85 mg, 0.7 mmol) and the resulting mixture was stirred open to air at 50 °C for 24 h. The solvent was evaporated in vacuo and the resulting residue purified by column chromatography (silica, 3:1 dichloromethane/hexanes). After evaporation of the eluent the product was obtained as a pale-yellow solid (41 mg, 19 %). IR (ATR, $\tilde{\nu}$): $\nu(\text{N-H})$ 3379, 3475; $\nu(\text{C}\equiv\text{C})$ 2135, 2204 cm^{-1} . ^1H NMR (CDCl_3 , 400 MHz): δ 2.50 (s, 3H, SMe); 3.92 (s, 2H, NH_2); 6.60 (d, $J = 8.6$ Hz, 2H, H17); 7.21 (d, $J = 8.5$ Hz, 2H, H2); 7.34 (d, $J = 8.6$ Hz, 2H, H16); 7.43 (d, $J = 8.5$ Hz, 2H, H3); 7.46 (s, 4H, H8/9) ppm. $^{13}\text{C}\{^1\text{H}\}$ NMR (DMSO-d_6 , 125 MHz): δ 14.7 (SMe); 71.2; 77.2; 89.6; 92.7; 106.2 (C15); 114.5 (C17); 118.3 (C4); 121.7 (C7/10); 123.8 (C7/10); 126.2 (C2); 132.3 (C8/9); 132.6 (C8/9); 133.1 (C3); 134.7 (C16); 141.0 (C1); 151.3 (C18) ppm (Due to low solubility ^{13}C NMR spectra were recorded as solution in DMSO-d_6 ; only 4 distinguishable acetylene carbons resonances were observed). HR-MS (ESI(+)) m/z : calcd for $\text{C}_{25}\text{H}_{18}\text{NS}$ 364.1152; found 364.1152 $[\text{M}+\text{H}]^+$.

Synthesis of 9-bromo-10-((4-aminophenyl)ethynyl)anthracene



To a degassed solution of 9,10-dibromoanthracene (260 mg, 0.78 mmol), PdCl₂(PPh₃)₂ (14 mg, 0.02 mmol), and CuI (4 mg, 0.02 mmol) in dry NEt₃ (20 mL) was added 4-ethynylaniline (100 mg, 0.85 mmol). The resulting mixture was stirred at 50 °C for 18 h. The solvent was evaporated in vacuo and the residue purified by column chromatography (silica, 3:1 dichloromethane/hexanes). After evaporation of the eluent the product was obtained as an orange solid (130 mg, 44 %). IR (ATR, $\tilde{\nu}$): ν (N–H) 3354, 3433; ν (C≡C) 2194 cm⁻¹. ¹H NMR (CDCl₃, 400 MHz): δ 3.92 (br s, 2H, NH₂); 6.74 (d, J = 8.6 Hz, 2H, H25); 7.61 (m, 6H, H16/17/24); 8.56 (m, 2H, H15/18); 8.70 (m, 2H, H15/18) ppm. ¹³C{¹H} NMR (CDCl₃, 101 MHz): δ 84.2 (C21); 103.1 (C22); 112.8 (C23); 115.0 (C25); 119.4 (C13/20); 123.3 (C13/20); 126.6 (C16/17); 127.5 (C15/16/17/18); 127.6 (C15/16/17/18); 128.3 (C15/18); 130.5 (C14/19); 132.9 (C14/19); 133.2 (C24); 147.3 (C26) ppm. HR-MS (ESI(+)) m/z : calcd for C₂₂H₁₅BrN 372.0382, 374.0362; found 372.0375, 374.0354 [M+H]⁺.

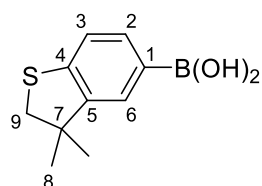
Synthesis of 9-((4-aminophenyl)ethynyl)-10-(((4-methylthiophenyl)ethynyl)phenyl)ethynyl)anthracene (8)



To a degassed solution of 9-bromo-10-((4-aminophenyl)ethynyl)anthracene (110 mg, 0.29 mmol), PdCl₂(PPh₃)₂ (5 mg, 0.01 mmol) and CuI (1 mg, 0.01 mmol) in dry NEt₃ (5 mL) and tetrahydrofuran (5 mL) was added 4-(((4-(methylthio)phenyl)ethynyl)-1-(ethynyl)benzene (100 mg, 0.40 mmol). The resulting mixture was stirred at 90 °C for 18 h. The solvent was evaporated in vacuo and the residue purified by column chromatography (silica, 3:1 dichloromethane/hexanes). After evaporation of the eluent the product was washed with

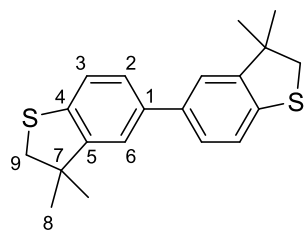
diethyl ether to obtain the product as a red solid (74 mg, 47 %). IR (ATR, $\tilde{\nu}$): $\nu(\text{N-H})$ 3378, 3472; $\nu(\text{C}\equiv\text{C})$ 2177 cm^{-1} . ^1H NMR (CDCl_3 , 400 MHz): δ 2.52 (s, 3H, SMe); 3.92 (br s, 2H, NH_2); 6.74 (d, $J = 8.4$ Hz, 2H, H25); 7.23 (d, $J = 8.4$ Hz, 2H, H2); 7.48 (d, $J = 8.4$ Hz, 2H, H3); 7.63 (m, 8H, H8/9/16/17/24); 7.75 (d, $J = 8.4$ Hz, 2H, H8/9); 8.69 (m, 4H, H15/18) ppm. $^{13}\text{C}\{^1\text{H}\}$ NMR (CDCl_3 , 101 MHz): δ 15.5 (SMe); 84.9 (C12/21); 88.8 (C12/21); 89.5 (C6/11); 91.6 (C5); 102.0 (C6/11); 104.1 (C22); 112.9 (C23); 115.0 (C25); 117.3 (C13/20); 119.4 (C4); 120.0 (C13/20); 123.4 (C7/10); 123.6 (C7/10); 126.0 (C2); 126.7 (C16/17); 127.0 (C16/17); 127.2 (C15/18); 127.7 (C15/18); 131.7 (C8/9); 131.8 (C8/9); 132.0 (C14/19); 132.1 (C3); 132.4 (C14/19); 133.3 (C24); 139.9 (C1); 147.3 (C26) ppm. HR-MS (ESI(+)) m/z : calcd for $\text{C}_{39}\text{H}_{26}\text{NS}$ 540.1781; found 540.1779 $[\text{M}+\text{H}]^+$.

Synthesis of (3,3-dimethyl-2,3-dihydrobenzo[b]thiophen-5-yl)boronic acid



To a degassed solution of 5-bromo-3,3-dimethyl-2,3-dihydrobenzo[b]thiophene (300 mg, 1.2 mmol) in dry tetrahydrofuran (10 mL), under N_2 atmosphere at -78 $^\circ\text{C}$, was added $n\text{-BuLi}$ (2.5 M in hexanes, 0.54 mL, 1.4 mmol) dropwise over 5 min. After 15 min, triisopropylborate (0.34 mL, 1.5 mmol) was added and the solution allowed to warm to room temperature over 18 h. The reaction was quenched with water (50 mL) and treated with concentrated HCl (5 mL). The resulting mixture was extracted with diethyl ether (3×20 mL), and the organic phases combined, washed with brine, dried over MgSO_4 and filtered. The solvent was evaporated and hexanes (20 mL) was added forming a white precipitate. The mixture was filtered, washing with hexanes, to obtain the product as a white solid (58 mg, 23 %). IR (ATR, $\tilde{\nu}$): $\nu(\text{O-H})$ 3284 cm^{-1} . ^1H NMR (CDCl_3 , 400 MHz): δ 1.48 (s, 6H, H8); 3.25 (s, 2H, H9); 7.34 (d, $J = 7.7$ Hz, 1H, H3); 7.84 (s, 1H, H6); 7.99 (d, $J = 7.7$ Hz, 1H, H2) ppm. $^{13}\text{C}\{^1\text{H}\}$ NMR (CDCl_3 , 101 MHz): δ 27.7 (C8); 47.2 (C9); 47.4 (C7); 122.2 (C3); 129.4 (C6); 135.2 (C2); 147.0 (C4); 147.7 (C5) ppm. HR-MS (ESI(+)) m/z : calcd for $\text{C}_{10}\text{H}_{13}\text{BOS}$ 208.0729; found 208.0723 $[\text{M}]^+$.

Synthesis of 3,3,3',3'-tetramethyl-2,2',3,3'-tetrahydro-5,5'-bibenzo[*b*]thiophene



To a degassed solution of 5-bromo-3,3-dimethyl-2,3-dihydrobenzo[*b*]thiophene (44 mg, 0.18 mmol), K_2CO_3 (113 mg, 0.36 mmol), $Pd_2(dba)_3$ (10 mg, 0.01 mmol), JohnPhos (8 mg, 0.02 mmol), and water (1 mL) in dry toluene (10 mL), under N_2 atmosphere, was added (3,3-dimethyl-2,3-dihydrobenzo[*b*]thiophen-5-yl)boronic acid (45 mg, 0.22 mmol) and the reaction stirred at 105 °C for 21 h. The solvent was evaporated and the residue purified by column chromatography (silica, 9:1 hexanes:ethyl acetate). After evaporation of the eluent the product was obtained as a colourless solid (21 mg, 36 %). 1H NMR ($CDCl_3$, 400 MHz): δ 1.42 (s, 12H, H8); 3.22 (s, 4H, H9); 7.19 (d, J = 1.8 Hz, 2H, H6); 7.23 (d, J = 8.0 Hz, 2H, H3); 7.31 (dd, J = 1.8, 8.0 Hz, 2H, H2) ppm. $^{13}C\{^1H\}$ NMR ($CDCl_3$, 101 MHz): δ 27.6 (C8); 47.5 (C9); 47.6 (C7); 121.4 (C6); 122.8 (C3); 126.4 (C2); 138.1 (C5); 139.6 (C4); 148.7 (C1) ppm. HR-MS (ESI(+)) m/z : calcd for $C_{20}H_{22}S_2$ 326.1163; found 326.1158 $[M]^+$

2.3 Molecular and Crystal Structures

Single crystal X-ray diffraction. Crystallographic data were collected at 100(2) K on a Rigaku-Oxford Diffraction XtaLAB Synergy-S, single source HyPix diffractometer using a micro-focus sealed Cu K α radiation ($\lambda = 1.54184 \text{ \AA}$) X-ray source. Structures were solved using ShelXT 2018/2¹⁴ solution program with Olex2 1.3¹⁵ as the graphical interface. The models were refined with ShelXL¹⁴ using full matrix least squares minimization on F^2 . Anisotropic displacement parameters were employed for non-hydrogen atoms. All hydrogen atoms were added at calculated positions and refined by use of a riding model with isotropic displacement parameters based on those of the parent atom. Graphics of the molecular structures have been created by using DIAMOND 4.6.7.¹⁶ Crystallographic data have been deposited at the Cambridge Crystallographic Data Centre. Copies of the data with CCDC numbers 2244309–2244317.

Single crystals of **1d-1**, **1d**, **3d-1**, **4c**, and **4d-1** were obtained by slow evaporation in dichloromethane, **3d** and **5** were obtained by slow diffusion of hexanes into dichloromethane solutions; **1c** was obtained by crystallisation from hot toluene, and **2d** was obtained by slow diffusion of pentane into a dichloromethane solution. The compounds crystallise in triclinic $P\bar{1}$ (**1c**, **1d-1**, **1d**), monoclinic $I2/a$ (**3d-1**), monoclinic $P2_1/c$ (**2d**, **4d-1**), orthorhombic $Pca2_1$ (**3d**), monoclinic $P2_1/n$ (**4c**), and orthorhombic $Pna2_1$ (**5**) space groups.

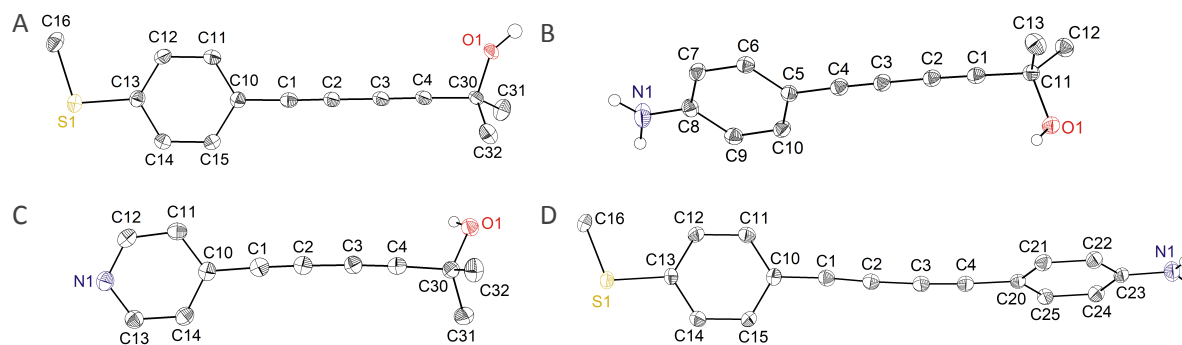


Figure S9: ORTEP drawings (50 % probability level) of the molecular structures of A) **1d-1**, B) **3d-1**, C) **4d-1**, and D) **5** with their atom numbering schemes. A second molecule in the asymmetric unit of **1d-1** (see Figure S10), one molecule of water in the asymmetric unit of **4d-1** (see Figure S10), and C-bonded H atoms are omitted for clarity. Selected bond properties are summarized in Table S1.

Table S5: Selected bond lengths (Å) and plane intersections (°) of **1d-1**, **3d-1**, **4d-1**, and **5**.

	1d-1	3d-1	4d-1	5
Bond Lengths (Å)				
C10–C1	1.4296(16) ¹ 1.4313(16) ²	1.4282(13)	1.4349(15)	1.432(4)
C1≡C2	1.2066(17) ² 1.2076(17) ¹	1.2057(14)	1.1957(16)	1.214(4)
C2–C3	1.3742(17) ² 1.3768(17) ¹	1.3750(13)	1.3792(15)	1.366(4)
C3≡C4	1.2017(17) ² 1.2054(17) ¹	1.2021(14)	1.2024(15)	1.208(4)
C4–C20	–	–	–	1.429(4)
C4–C30	1.4809(16) ² 1.4814(16) ¹	1.4765(13)	1.4812(14)	–
C30–O1	1.4315(14) ¹ 1.4320(14) ²	1.4489(11)	1.4292(12)	–
S···N	–	–	–	15.3718(27)
Plane Intersections (°)				
Ar···Ar	–	–	–	84.959(88)

^{1,2} The value relates to the associated bond length from molecule 1 or 2 of the asymmetric unit.

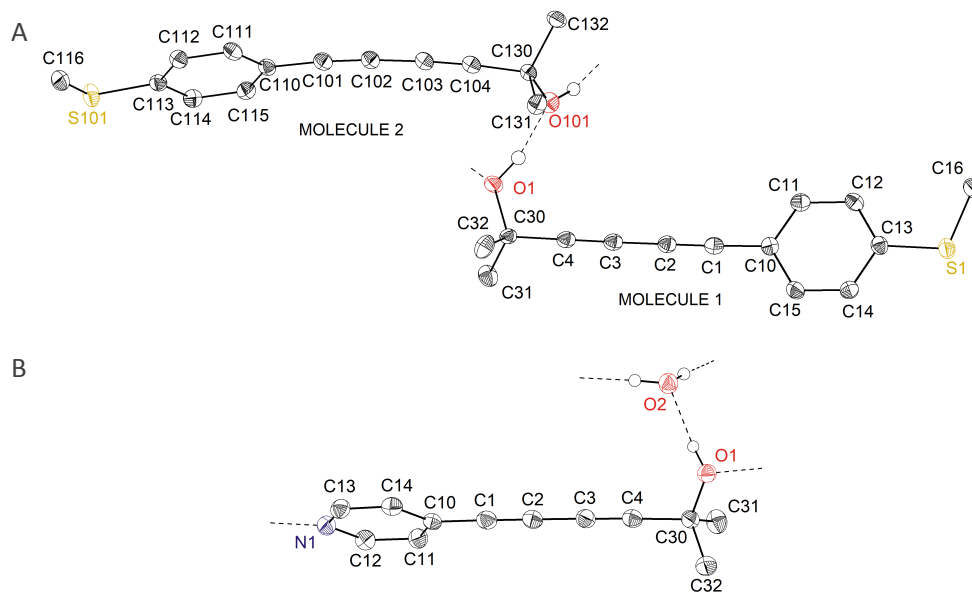


Figure S10: ORTEP drawings (50 % probability level) of the asymmetric unit for the crystal structures of A) **1d-1**, and B) **4d-1** with their atom numbering scheme. C-bonded H atoms are omitted for clarity. Dashed lines represent hydrogen bonding between molecules of the crystal lattice.

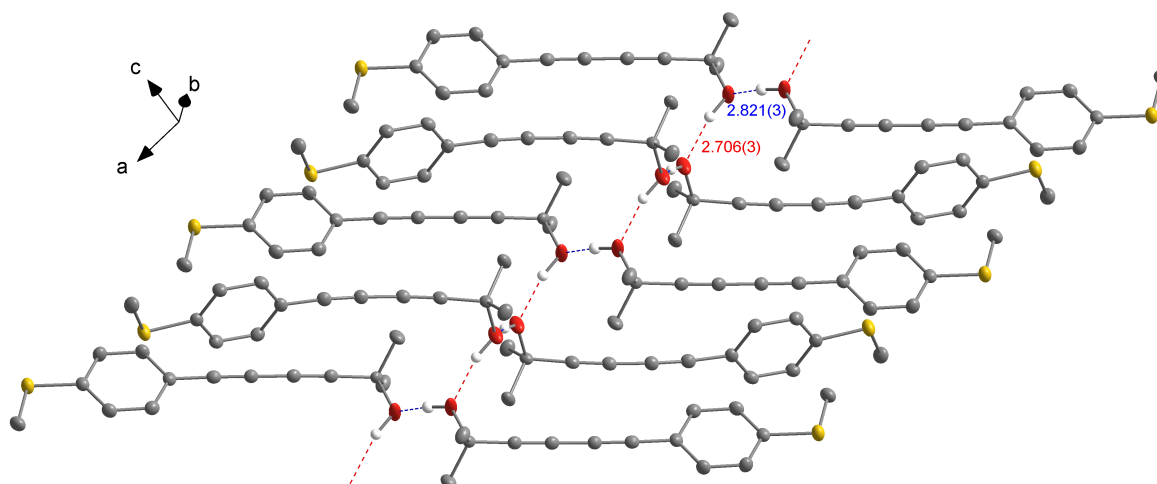


Figure S11: Ball-and-stick representation of the crystal packing of **1d-1** showing the hydrogen bond network formed by O–H \cdots O interactions (red and blue). C-bonded H atoms are omitted for clarity. Values (Å) refer to the corresponding O \cdots O distances.

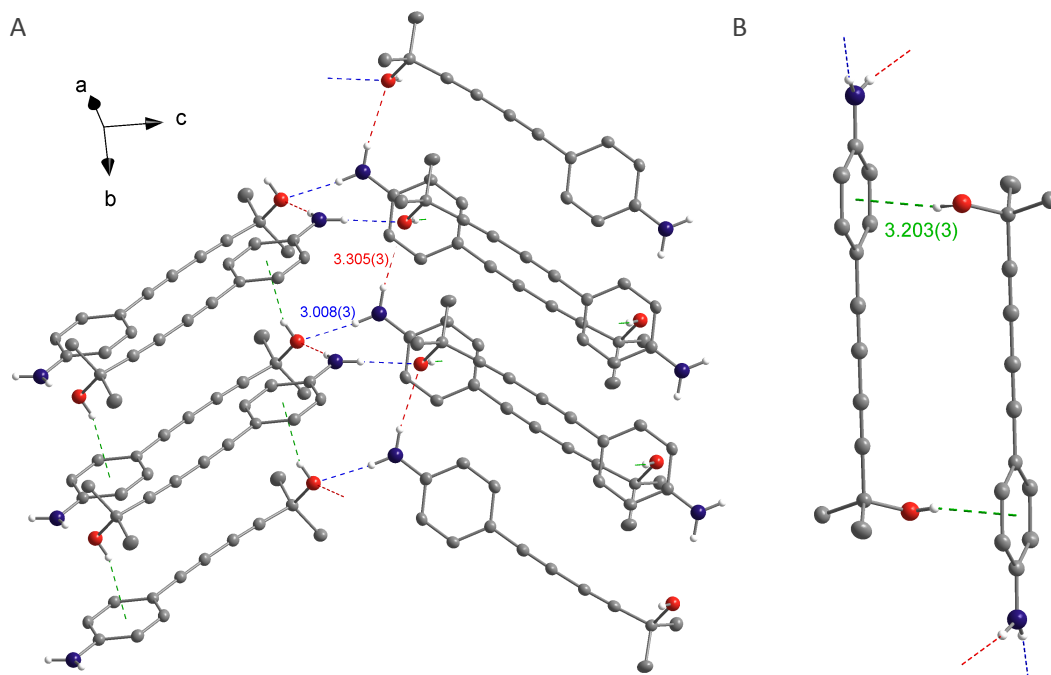


Figure S12: A) Ball-and-stick representation of the crystal packing of **3d-1** showing the hydrogen bond network formed by N–H···O (red and blue) and O–H··· π interactions (green). B) Dimer of **3d-1** formed by O–H··· π interactions. C-bonded H atoms are omitted for clarity. Values (Å) refer to the corresponding N···O or O···centroid distances.

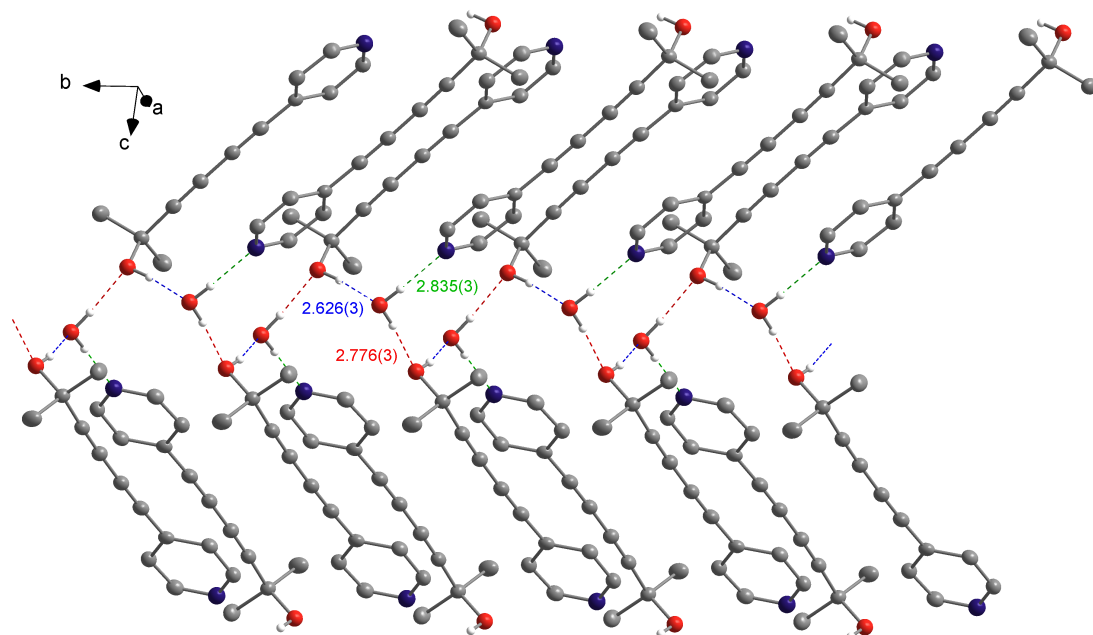


Figure S13: Ball-and-stick representation of the crystal packing of **4d-1** showing the hydrogen bond network formed by O–H \cdots O (red and blue) and O–H \cdots N (green) interactions. C-bonded H atoms are omitted for clarity. Values (Å) refer to the corresponding corresponding O \cdots O or O \cdots N distances.

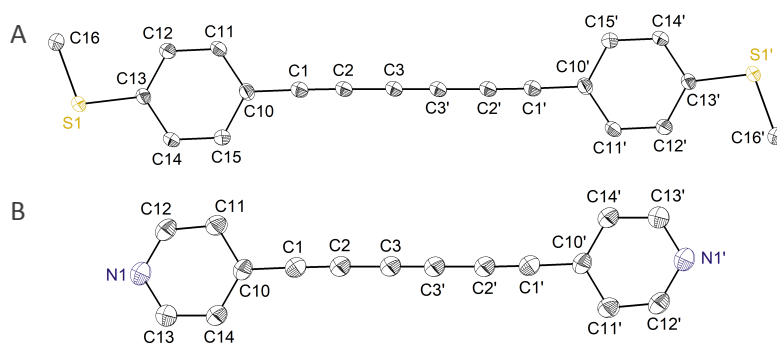


Figure S14: ORTEP drawings (50 % probability level) of the molecular structures of **1c** (A), and **4c** (B) with their atom numbering schemes. C-bonded H atoms are omitted for clarity. Selected bond properties are summarized in Table S2.

Table S6: Selected bond lengths (Å) and plane intersections (°) of **1c** and **4c**.

	1c	4c
	X = S	X = N
Bond Lengths		
C10–C1	1.429(2)	1.431(2)
C1≡C2	1.211(3)	1.208(2)
C2–C3	1.362(3)	1.364(2)
C3≡C3'	1.213(4)	1.210(3)
X⋯X	18.3263(7)	14.8240(4)
Plane Intersections		
Ar⋯Ar	0.0(2)	0.0(2)

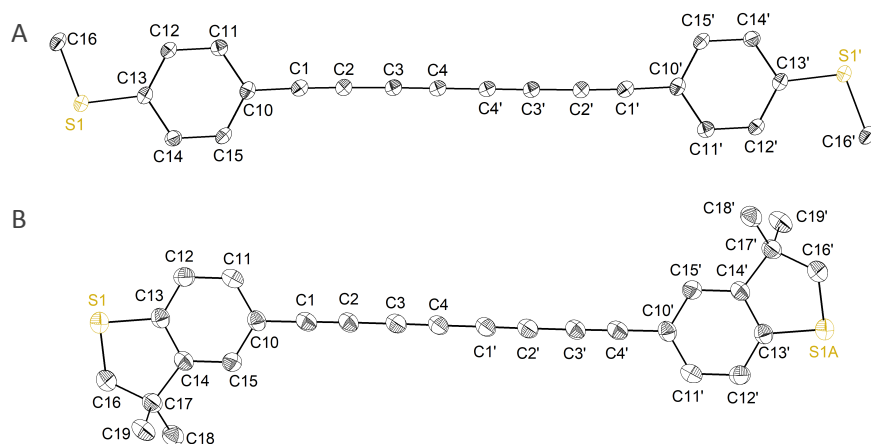


Figure S15: ORTEP drawings (50 % probability level) of the molecular structures of **1d** (A), and **2d** (B) with their atom numbering scheme. Disordered atoms in the structure of **2d**, and C-bonded H atoms are omitted for clarity. Selected bond properties are summarized in Table S3.

Table S7: Selected bond lengths (Å) and plane intersections (°) of **1d** and **4d**.

	1d	2d
Bond Lengths		
C10–C1	1.423(2)	1.424(4)
C1≡C2	1.213(2)	1.207(5)
C2–C3	1.359(2)	1.362(5)
C3≡C4	1.215(2)	1.208(5)
C4–C4'	1.357(3)	1.362(6)
S⋯S	20.8665(8)	20.7935(38)
Plane Intersections		
Ar⋯Ar	0.0(2)	0.0(2)

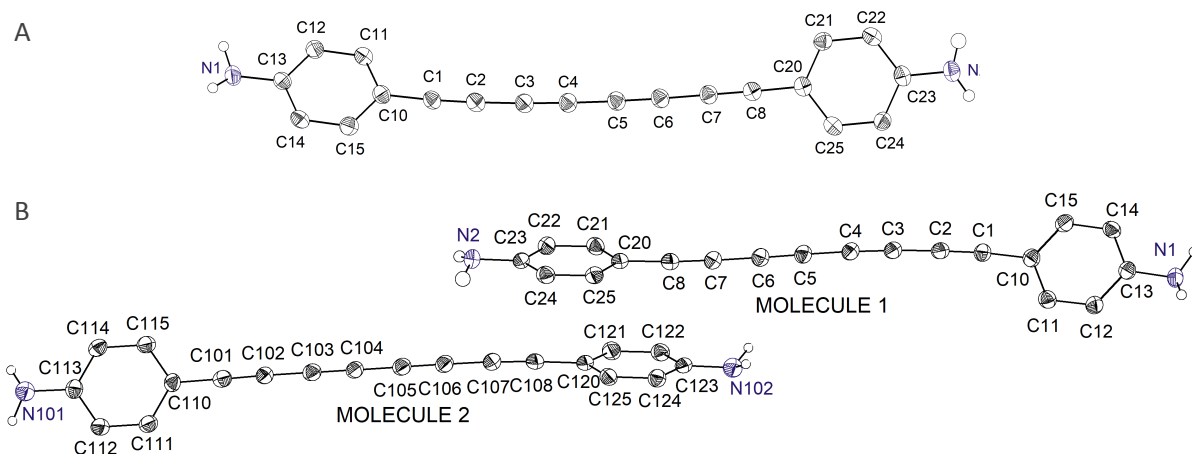


Figure S16: ORTEP drawings (50 % probability level) of the molecular structure of **3d** (A), and the asymmetric unit for the crystal structure of **3d** (B). C-bonded H atoms are omitted for clarity. Selected bond properties are summarized in Table S3.

Table S8: Selected bond lengths (Å) and plane intersections (°) of **3d**.

3d			
Bond Lengths (Å)			
C10–C1	1.424(4) ¹	C5≡C6	1.221(4) ²
	1.425(4) ²		1.223(4) ¹
C1≡C2	1.213(4) ²	C6–C7	1.352(4) ¹
	1.219(4) ¹		1.356(4) ²
C2–C3	1.355(4) ²	C7≡C8	1.218(4) ¹
	1.357(4) ¹		1.219(4) ²
C3≡C4	1.215(4) ¹	C8–C20	1.423(4) ²
	1.227(4) ²		1.424(4) ¹
C4–C5	1.353(4) ²	N···N	20.0812(38) ¹
	1.356(4) ¹		20.1593(38) ²
Plane Intersections (°)			
Ar···Ar	44.338(109) ¹		
	51.614(85) ²		

^{1,2} The value relates to the associated bond length from molecule 1 or 2 of the asymmetric unit.

2.4 Crystallographic Data

	1d-1	3d-1	4d-1
Empirical formula	C ₁₄ H ₁₄ OS	C ₁₃ H ₁₃ NO	C ₁₂ H ₁₃ NO ₂
Formula weight	230.31	199.24	203.23
Temperature/K	100.01(10)	100.15	100.15
Crystal system	triclinic	monoclinic	monoclinic
Space group	<i>P</i> -1	<i>I</i> 2/a	<i>P</i> 2 ₁ /c
<i>a</i> /Å	7.39700(10)	16.2725(2)	7.81540(10)
<i>b</i> /Å	9.82200(10)	5.97010(10)	6.00420(10)
<i>c</i> /Å	18.7581(3)	23.8665(3)	24.4944(4)
α /°	94.6200(10)	90	90
β /°	98.4700(10)	103.1140(10)	98.117(2)
γ /°	110.8710(10)	90	90
<i>V</i> /Å ³	1246.41(3)	2258.13(6)	1137.89(3)
<i>Z</i>	4	8	4
ρ_{calc} g/cm ³	1.227	1.172	1.186
μ /mm ⁻¹	2.099	0.586	0.657
<i>F</i> (000)	488	848	432
Crystal size/mm ³	0.1×0.02×0.001	0.68×0.09×0.07	0.166×0.102×0.069
Radiation	Cu K α (λ = 1.54184)	Cu K α (λ = 1.54184)	CuK α (λ = 1.54184)
2 θ range for data collection/°	9.634 to 150.732	7.606 to 150.576	7.292 to 151.096
Index ranges	-9 ≤ <i>h</i> ≤ 9, -9 ≤ <i>k</i> ≤ 12, -23 ≤ <i>l</i> ≤ 23	-20 ≤ <i>h</i> ≤ 20, -5 ≤ <i>k</i> ≤ 7, -29 ≤ <i>l</i> ≤ 29	-9 ≤ <i>h</i> ≤ 9, -7 ≤ <i>k</i> ≤ 5, -30 ≤ <i>l</i> ≤ 30
Reflections collected	23701	12608	8892
Independent reflections	5032 [<i>R</i> _{int} = 0.0277, <i>R</i> _{sigma} = 0.0203]	2276 [<i>R</i> _{int} = 0.0284, <i>R</i> _{sigma} = 0.0189]	2249 [<i>R</i> _{int} = 0.0204, <i>R</i> _{sigma} = 0.0189]
Data/restraints /parameters	5032/4/311	2276/0/147	2249/0/142
Goodness-of-fit on <i>F</i> ²	1.048	1.07	1.054
Final <i>R</i> indexes [<i>I</i> ≥ 2 σ (<i>I</i>)]	<i>R</i> ₁ = 0.0315, <i>wR</i> ₂ = 0.0833	<i>R</i> ₁ = 0.0342, <i>wR</i> ₂ = 0.0906	<i>R</i> ₁ = 0.0332, <i>wR</i> ₂ = 0.0859
Final <i>R</i> indexes [all data]	<i>R</i> ₁ = 0.0330, <i>wR</i> ₂ = 0.0845	<i>R</i> ₁ = 0.0360, <i>wR</i> ₂ = 0.0920	<i>R</i> ₁ = 0.0371, <i>wR</i> ₂ = 0.0884
Largest diff. peak/hole / e Å ⁻³	0.27/-0.28	0.20/-0.22	0.14/-0.18

	5	1c	4c
Empirical formula	C ₁₇ H ₁₃ NS	C ₂₀ H ₁₄ S ₂	C ₁₆ H ₈ N ₂
Formula weight	263.34	318.43	228.24
Temperature/K	100.01(10)	100.01(10)	103(4)
Crystal system	orthorhombic	triclinic	monoclinic
Space group	<i>Pna</i> 2 ₁	<i>P</i> -1	<i>P</i> 2 ₁ / <i>n</i>
<i>a</i> /Å	9.17990(10)	4.0180(2)	3.80550(10)
<i>b</i> /Å	6.90650(10)	7.9129(3)	25.5128(10)
<i>c</i> /Å	20.6965(2)	12.2528(5)	5.9500(2)
α /°	90	84.363(3)	90
β /°	90	87.988(4)	93.327(3)
γ /°	90	84.405(4)	90
<i>V</i> /Å ³	1312.18(3)	385.71(3)	576.71(3)
<i>Z</i>	4	1	2
ρ_{calc} g/cm ³	1.333	1.371	1.314
μ /mm ⁻¹	2.036	3.046	0.621
<i>F</i> (000)	552	166	236
Crystal size/mm ³	0.27 × 0.19 × 0.15	0.256 × 0.167 × 0.069	0.23 × 0.11 × 0.06
Radiation	Cu K α (λ = 1.54184)	Cu K α (λ = 1.54184)	Cu K α (λ = 1.54184)
2 θ range for data collection/°	8.544 to 150.06	7.252 to 149.558	6.93 to 150.834
Index ranges	-11 ≤ <i>h</i> ≤ 10, -8 ≤ <i>k</i> ≤ 8, -25 ≤ <i>l</i> ≤ 25	-5 ≤ <i>h</i> ≤ 3, -9 ≤ <i>k</i> ≤ 9, -14 ≤ <i>l</i> ≤ 15	-4 ≤ <i>h</i> ≤ 4, -31 ≤ <i>k</i> ≤ 29, -7 ≤ <i>l</i> ≤ 7
Reflections collected	22761	4800	4195
Independent reflections	2619 [<i>R</i> _{int} = 0.0465, <i>R</i> _{sigma} = 0.0284]	1496 [<i>R</i> _{int} = 0.0294, <i>R</i> _{sigma} = 0.0273]	1152 [<i>R</i> _{int} = 0.0338, <i>R</i> _{sigma} = 0.0280]
Data/restraints /parameters	2619/1/224	1496/0/101	1152/0/82
Goodness-of-fit on <i>F</i> ²	1.054	1.059	1.107
Final <i>R</i> indexes [<i>I</i> ≥ 2 σ (<i>I</i>)]	<i>R</i> ₁ = 0.0317, <i>wR</i> ₂ = 0.0836	<i>R</i> ₁ = 0.0382, <i>wR</i> ₂ = 0.1016	<i>R</i> ₁ = 0.0508, <i>wR</i> ₂ = 0.1408
Final <i>R</i> indexes [all data]	<i>R</i> ₁ = 0.0331, <i>wR</i> ₂ = 0.0855	<i>R</i> ₁ = 0.0403, <i>wR</i> ₂ = 0.1033	<i>R</i> ₁ = 0.0586, <i>wR</i> ₂ = 0.1459
Largest diff. peak/hole / e Å ⁻³	0.38/-0.19	0.47/-0.36	0.19/-0.18

	1d	2d	3d
Empirical formula	C ₂₂ H ₁₄ S ₂	C ₂₈ H ₂₂ S ₂	C ₄₀ H ₂₄ N ₄
Formula weight	342.45	422.57	560.63
Temperature/K	102.15	111(16)	100.01(10)
Crystal system	triclinic	monoclinic	orthorhombic
Space group	<i>P</i> -1	<i>P</i> 2 ₁ / <i>c</i>	<i>Pca</i> 2 ₁
<i>a</i> /Å	4.0524(2)	7.3018(3)	7.8557(3)
<i>b</i> /Å	8.0222(3)	8.2369(3)	9.7053(3)
<i>c</i> /Å	13.5176(7)	19.0284(7)	38.6997(9)
α /°	75.943(4)	90	90
β /°	84.880(4)	100.137(4)	90
γ /°	83.356(4)	90	90
<i>V</i> /Å ³	422.57(4)	1126.58(8)	2950.54(16)
<i>Z</i>	1	2	4
ρ_{calc} g/cm ³	1.346	1.246	1.262
μ /mm ⁻¹	2.822	2.214	0.583
<i>F</i> (000)	178	444	1168
Crystal size/mm ³	0.29×0.07×0.03	0.17 × 0.1 × 0.04	0.23×0.074×0.053
Radiation	CuK α (λ = 1.54184)	Cu K α (λ = 1.54184)	Cu K α (λ = 1.54184)
2 θ range for data collection/°	6.754 to 150.96	9.444 to 152.066	9.112 to 150.876
Index ranges	-5 ≤ <i>h</i> ≤ 5, -8 ≤ <i>k</i> ≤ 9, -16 ≤ <i>l</i> ≤ 16	-8 ≤ <i>h</i> ≤ 9, -9 ≤ <i>k</i> ≤ 9, -23 ≤ <i>l</i> ≤ 23	-9 ≤ <i>h</i> ≤ 8, -11 ≤ <i>k</i> ≤ 12, -48 ≤ <i>l</i> ≤ 19
Reflections collected	4532	8490	11859
Independent reflections	1637 [<i>R</i> _{int} = 0.0302, <i>R</i> _{sigma} = 0.0326]	2195 [<i>R</i> _{int} = 0.0291, <i>R</i> _{sigma} = 0.0226]	3862 [<i>R</i> _{int} = 0.0469, <i>R</i> _{sigma} = 0.0473]
Data/restraints /parameters	1637/0/110	2195/14/156	3862/1/494
Goodness-of-fit on <i>F</i> ²	1.103	1.082	1.057
Final <i>R</i> indexes [<i>I</i> ≥ 2 σ (<i>I</i>)]	<i>R</i> ₁ = 0.0330, <i>wR</i> ₂ = 0.0904	<i>R</i> ₁ = 0.0690, <i>wR</i> ₂ = 0.1974	<i>R</i> ₁ = 0.0407, <i>wR</i> ₂ = 0.1097
Final <i>R</i> indexes [all data]	<i>R</i> ₁ = 0.0358, <i>wR</i> ₂ = 0.0919	<i>R</i> ₁ = 0.0720, <i>wR</i> ₂ = 0.1995	<i>R</i> ₁ = 0.0448, <i>wR</i> ₂ = 0.1136
Largest diff. peak/hole / e Å ⁻³	0.33/-0.35	0.86/-0.30	0.15/-0.21

2.5 NMR Spectra

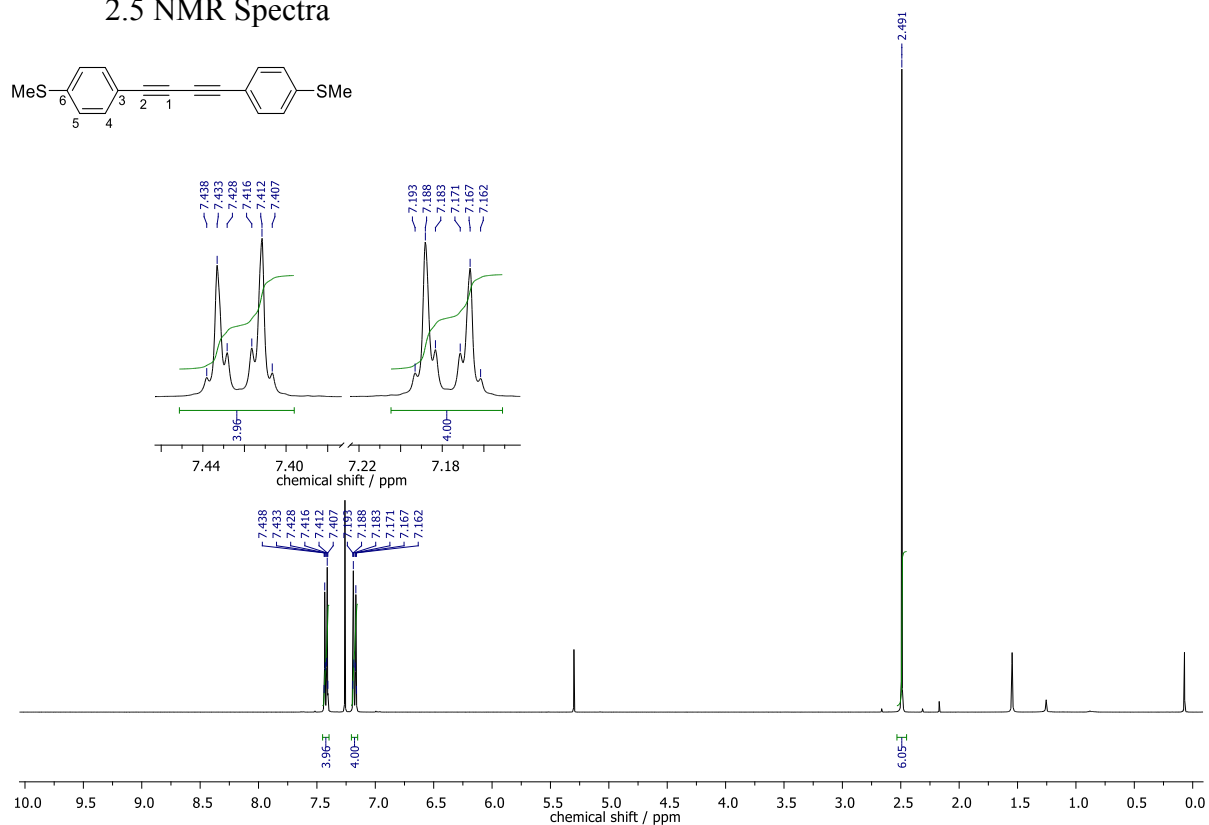


Figure S17: The ^1H NMR spectrum of **1b**.

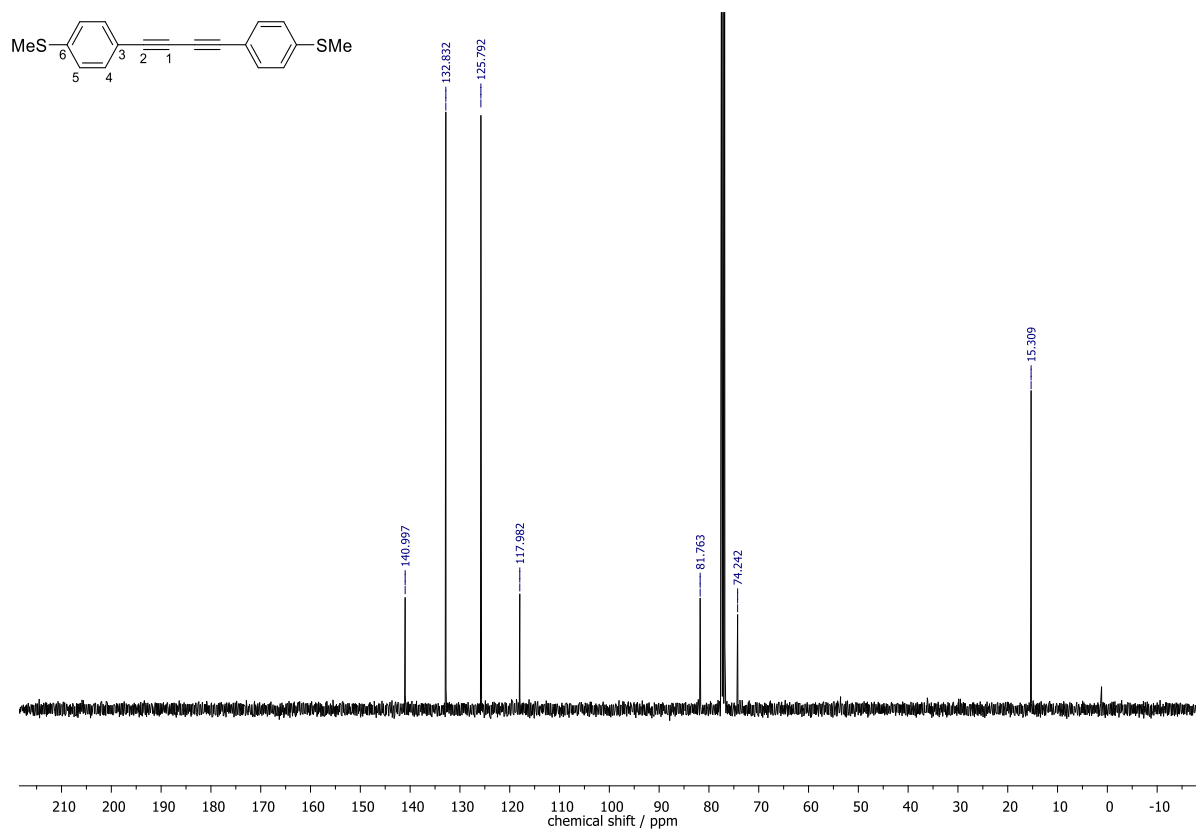


Figure S18: The $^{13}\text{C}\{^1\text{H}\}$ NMR spectrum of **1b**.

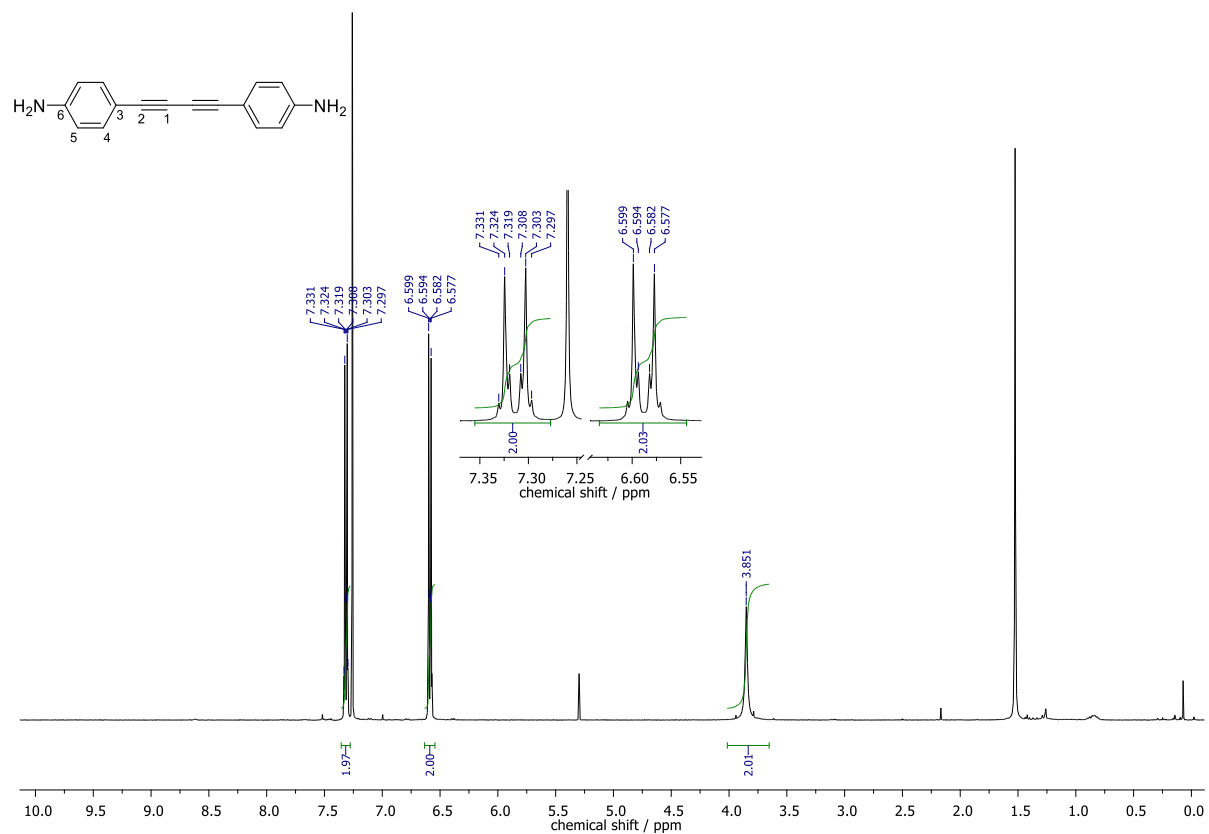


Figure S19: The ^1H NMR spectrum of **3b**.

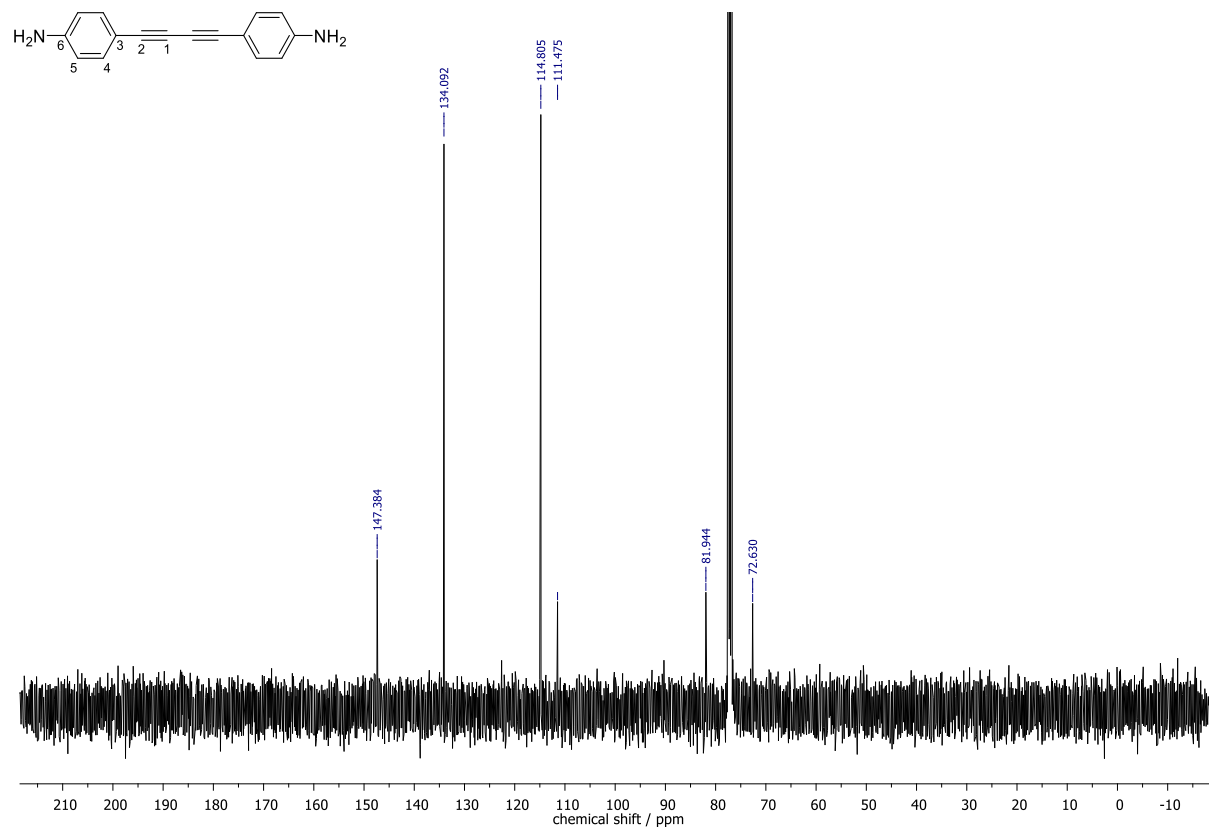


Figure S20: The $^{13}\text{C}\{^1\text{H}\}$ NMR spectrum of **3b**.

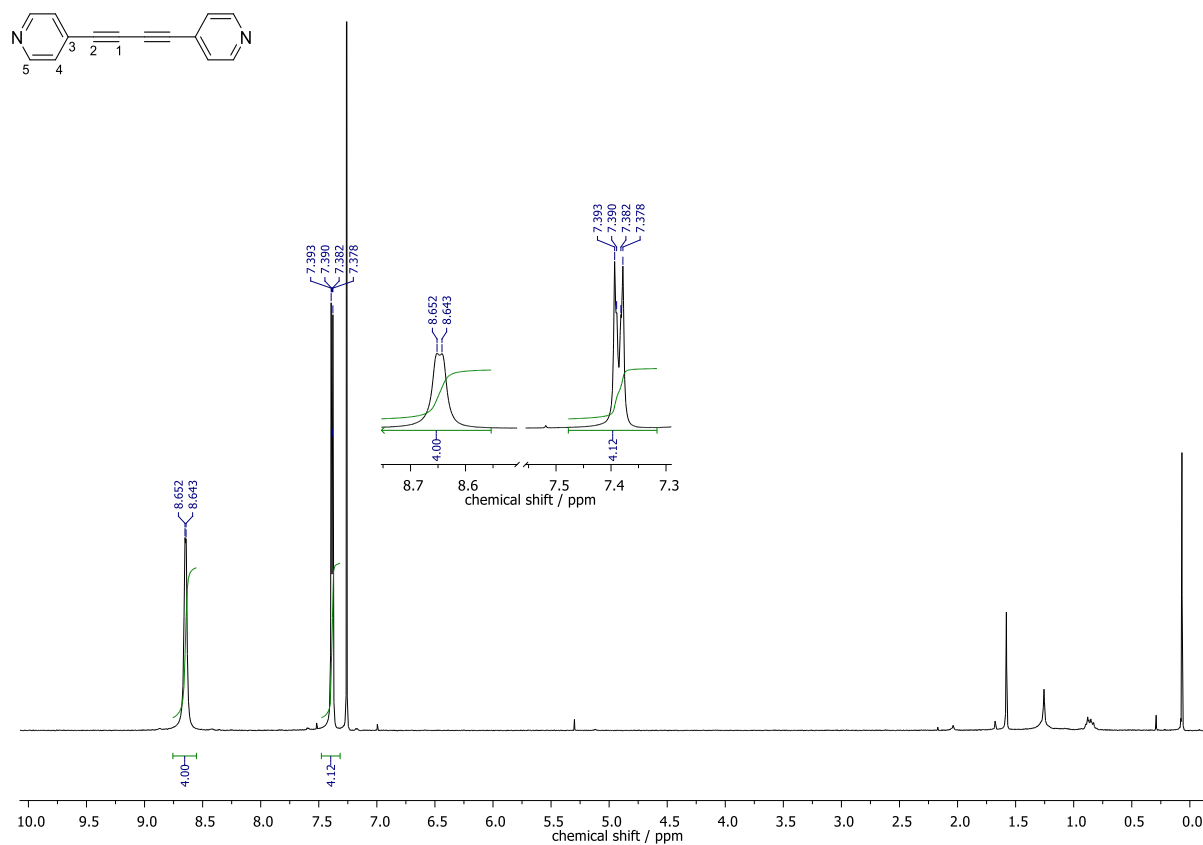


Figure S21: The ^1H NMR spectrum of **4b**.

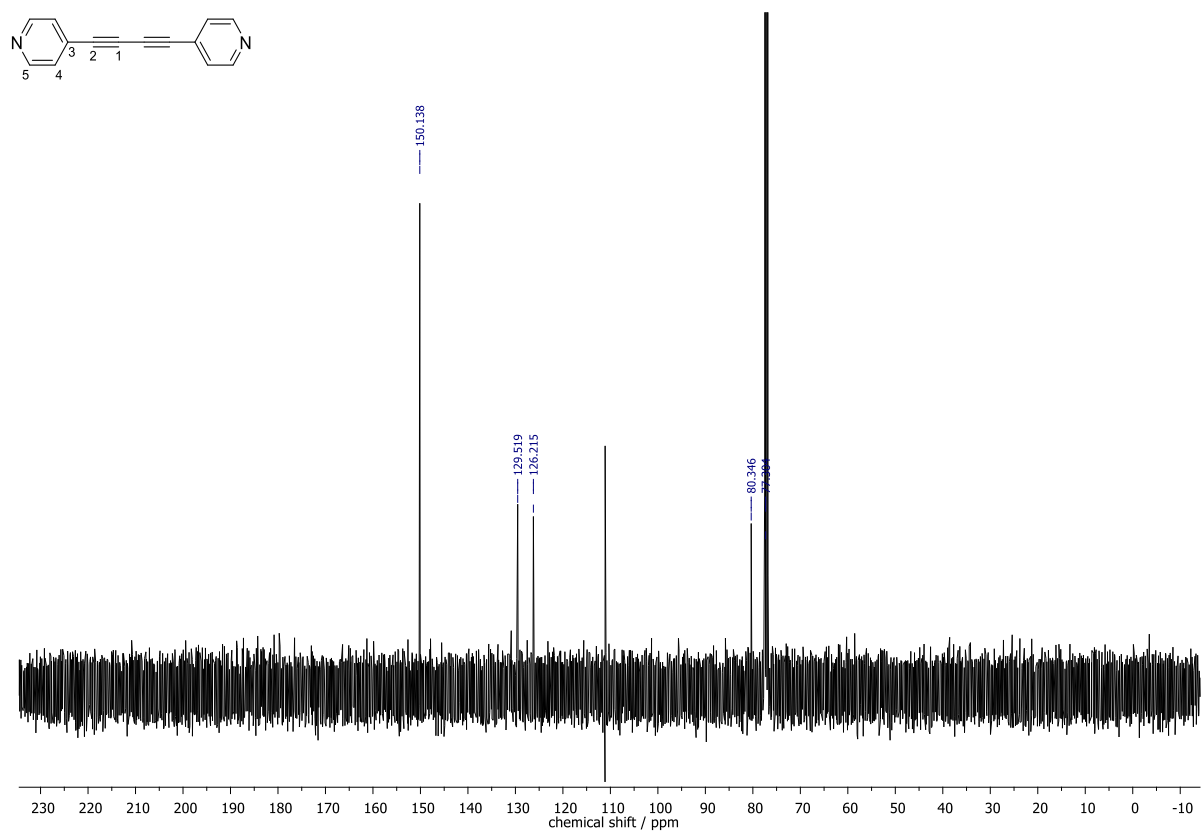


Figure S22: The $^{13}\text{C}\{^1\text{H}\}$ NMR spectrum of **4b**.

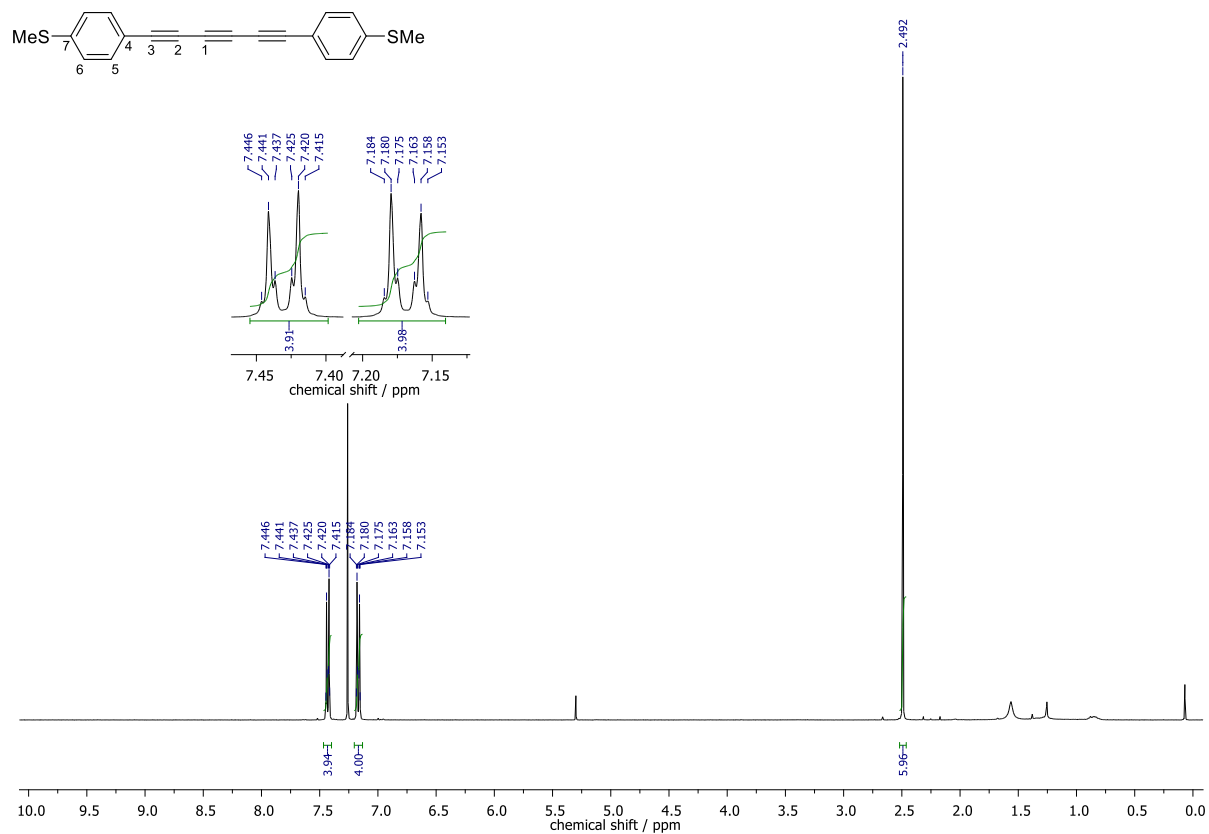


Figure S23: The ^1H NMR spectrum of **1c**.

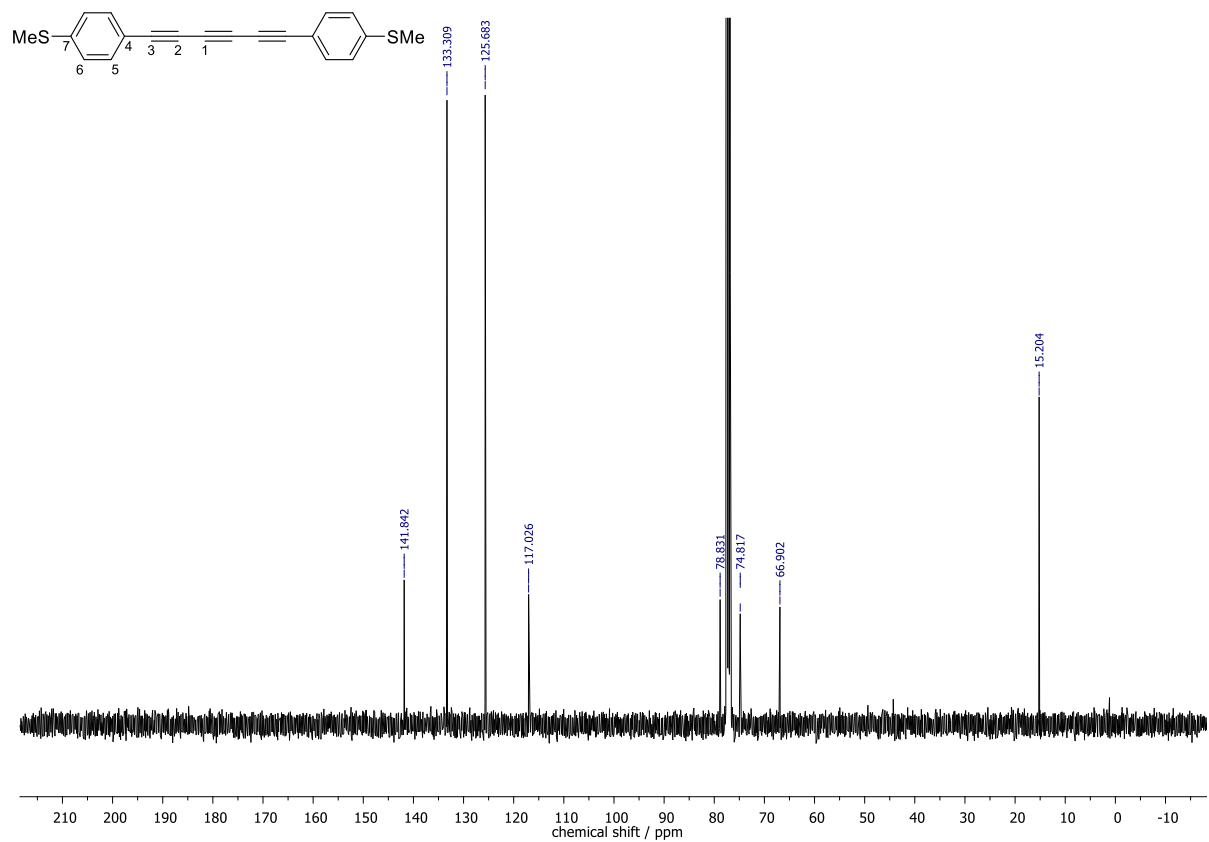


Figure S24: The $^{13}\text{C}\{^1\text{H}\}$ NMR spectrum of **1c**.

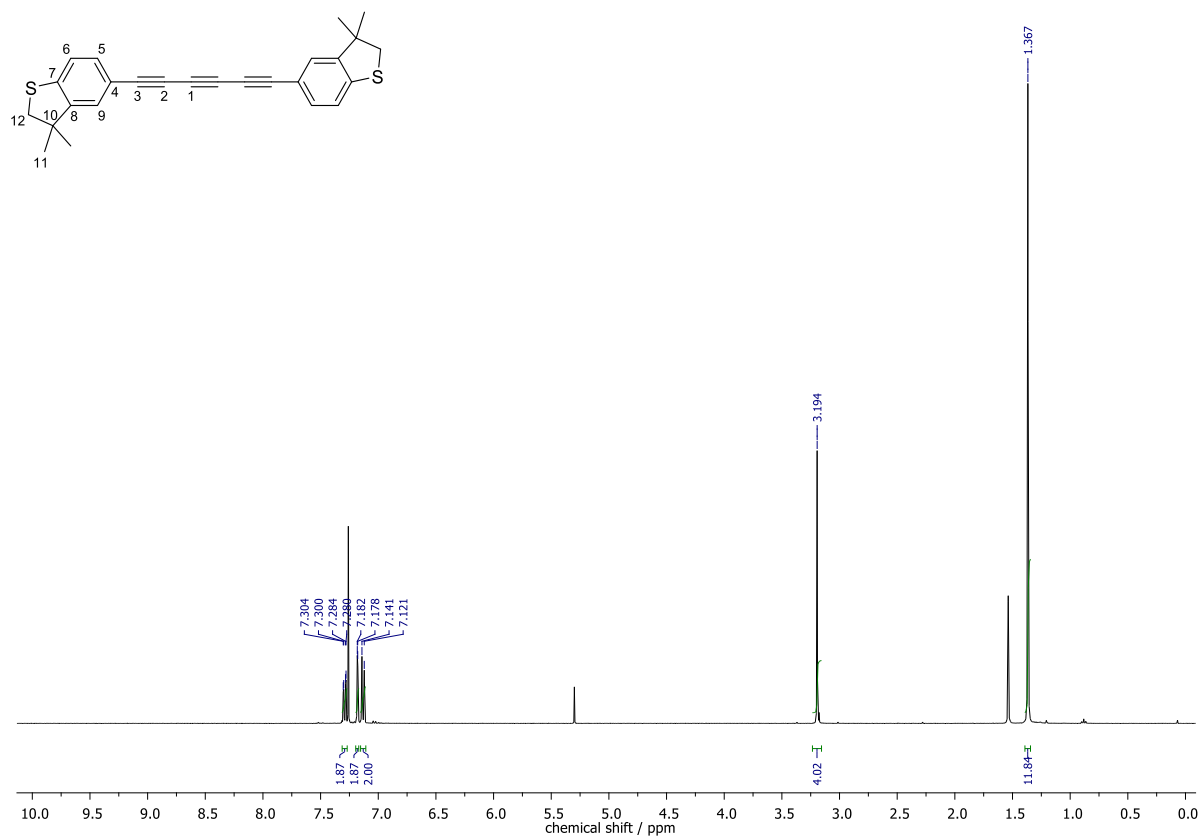


Figure S25: The ^1H NMR spectrum of **2c**.

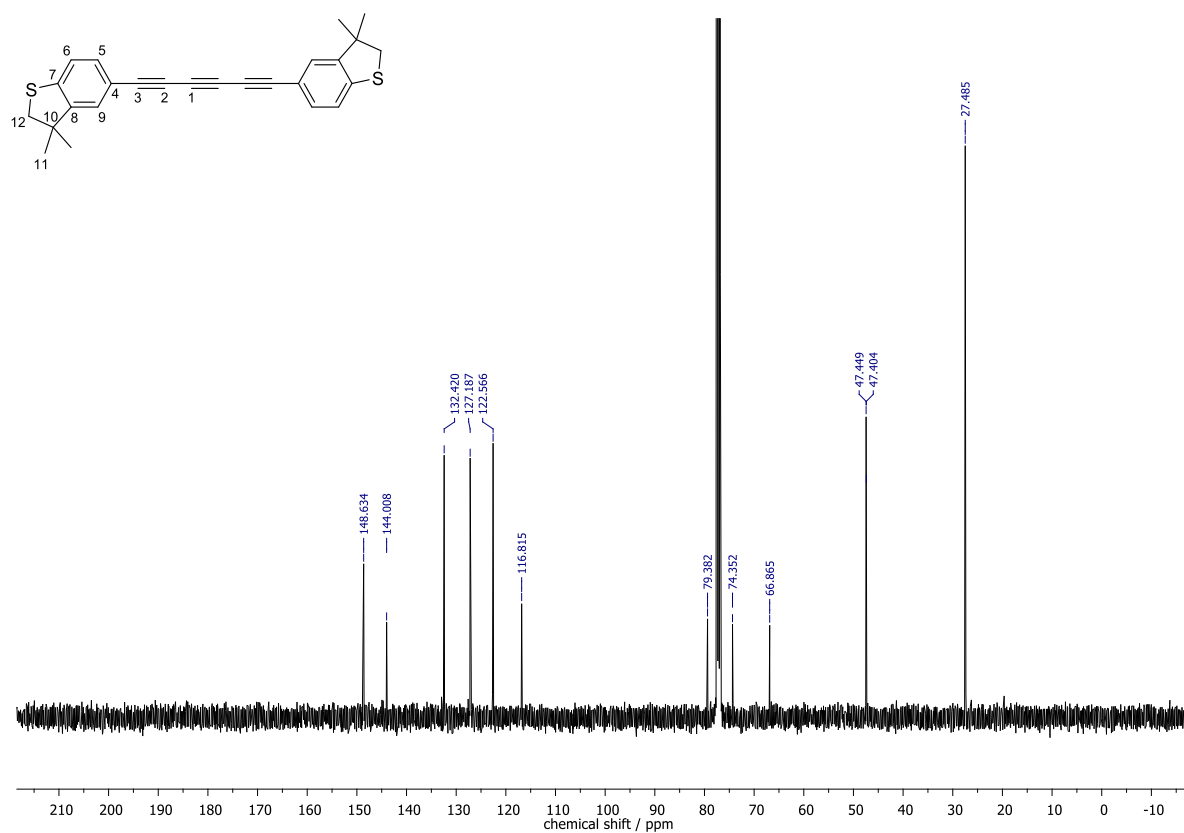


Figure S26: The $^{13}\text{C}\{^1\text{H}\}$ NMR spectrum of **2c**.

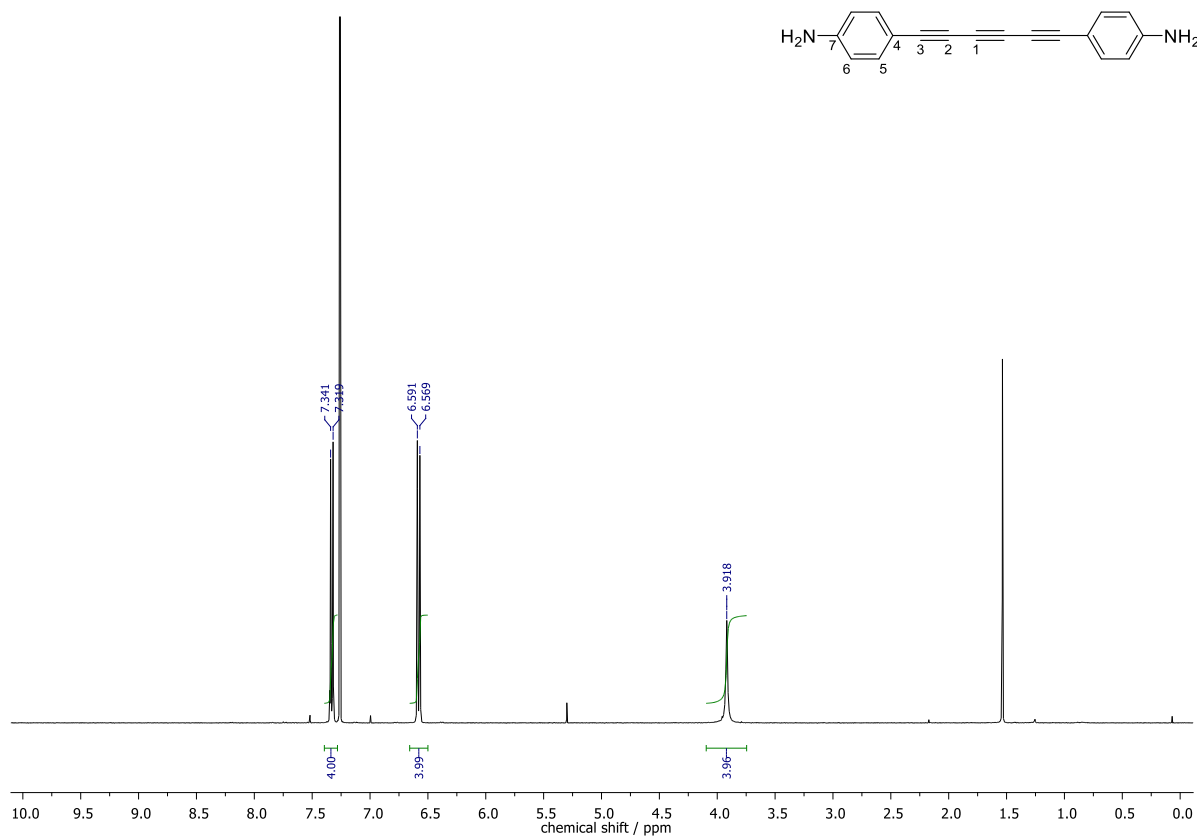


Figure S27: The ^1H NMR spectrum of **3c**.

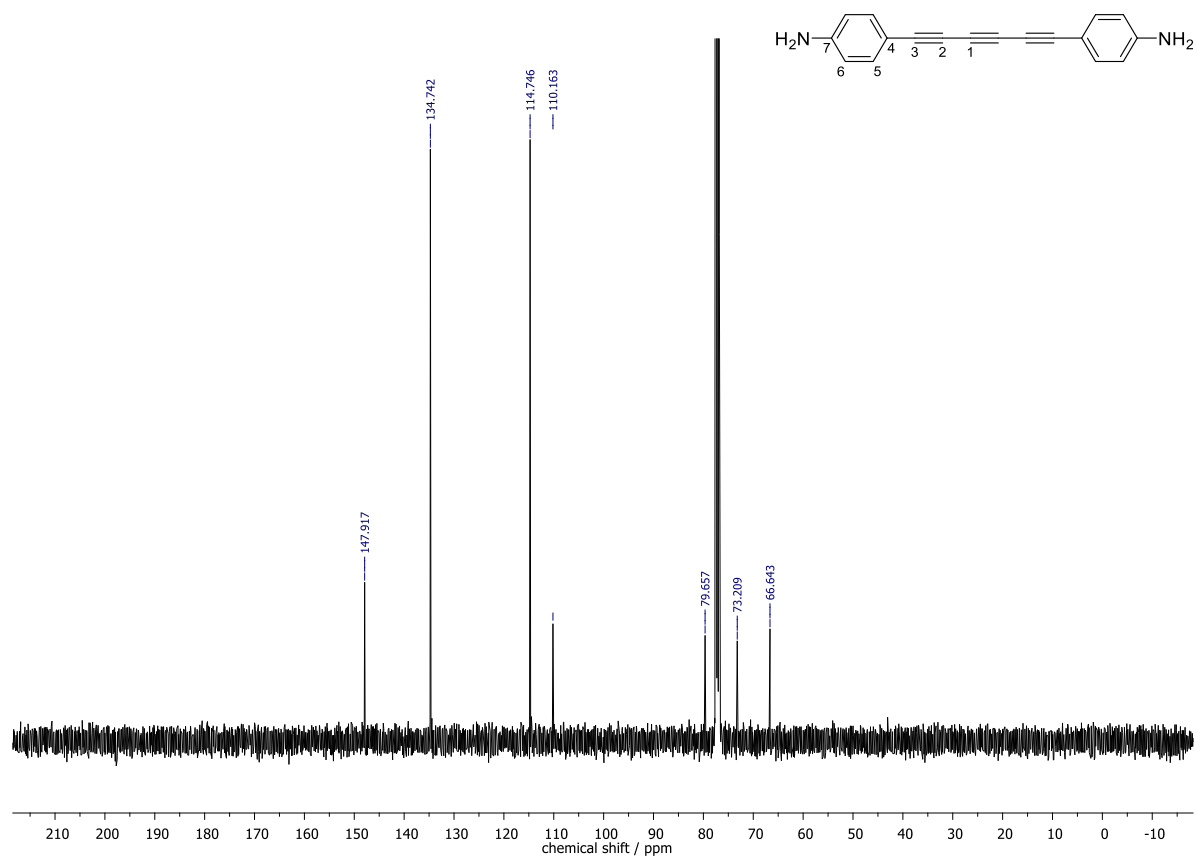


Figure S28: The $^{13}\text{C}\{^1\text{H}\}$ NMR spectrum of **3c**.

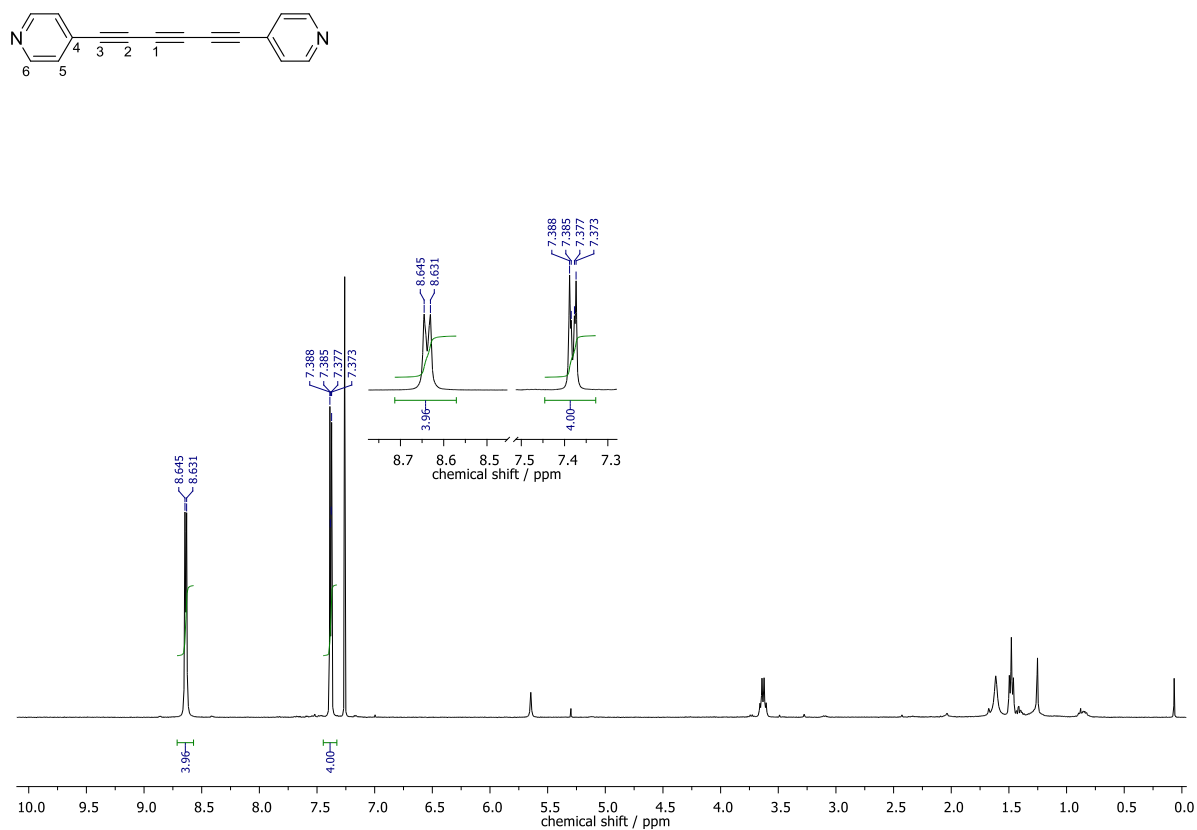


Figure S29: The ^1H NMR spectrum of **4c**.

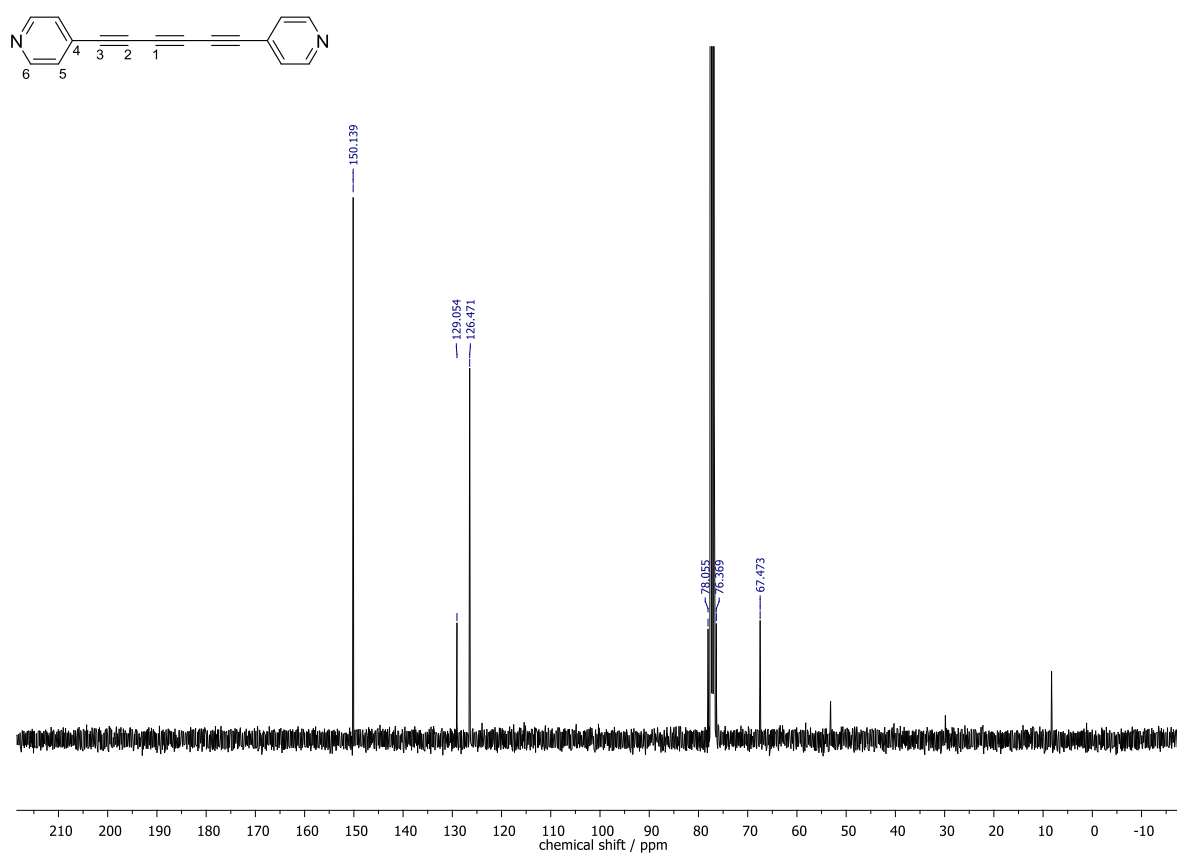


Figure S30: The $^{13}\text{C}\{^1\text{H}\}$ NMR spectrum of **4c**.

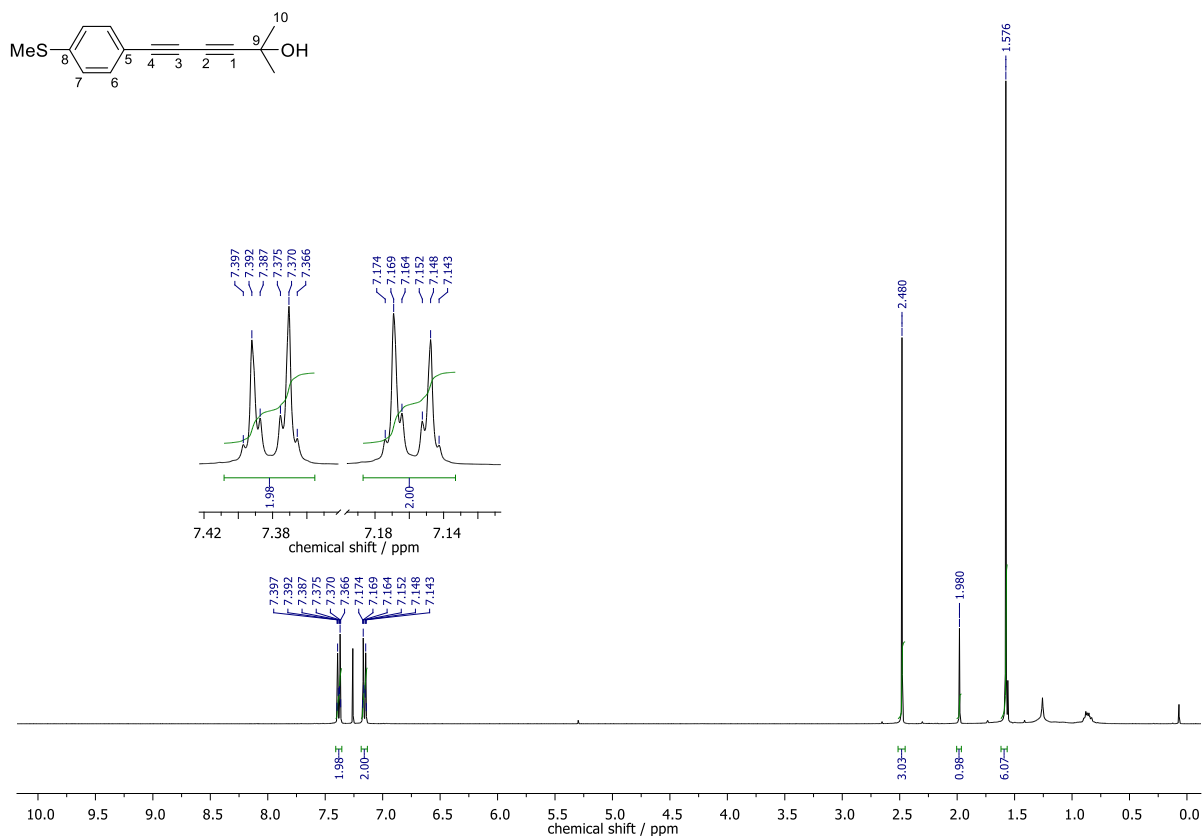


Figure S31: The ¹H NMR spectrum of **1d-1**.

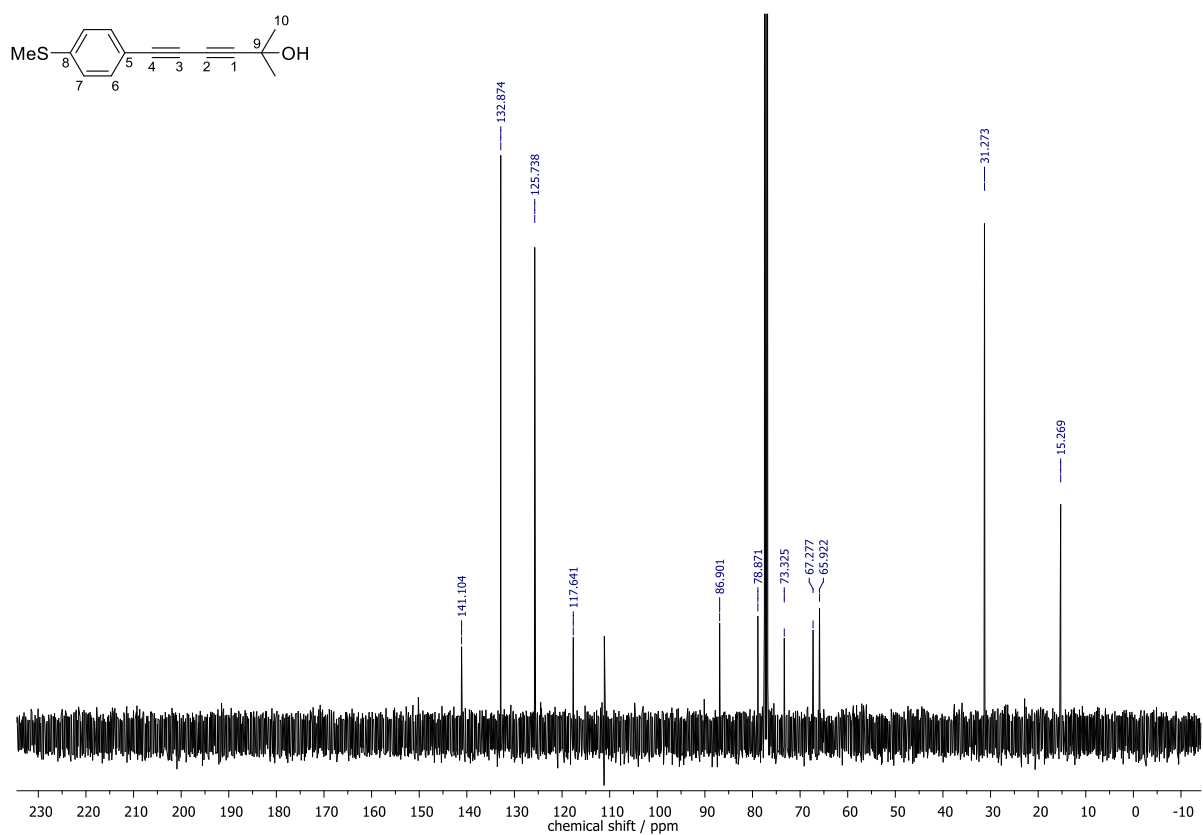


Figure S32: The ¹³C{¹H} NMR spectrum of **1d-1**.

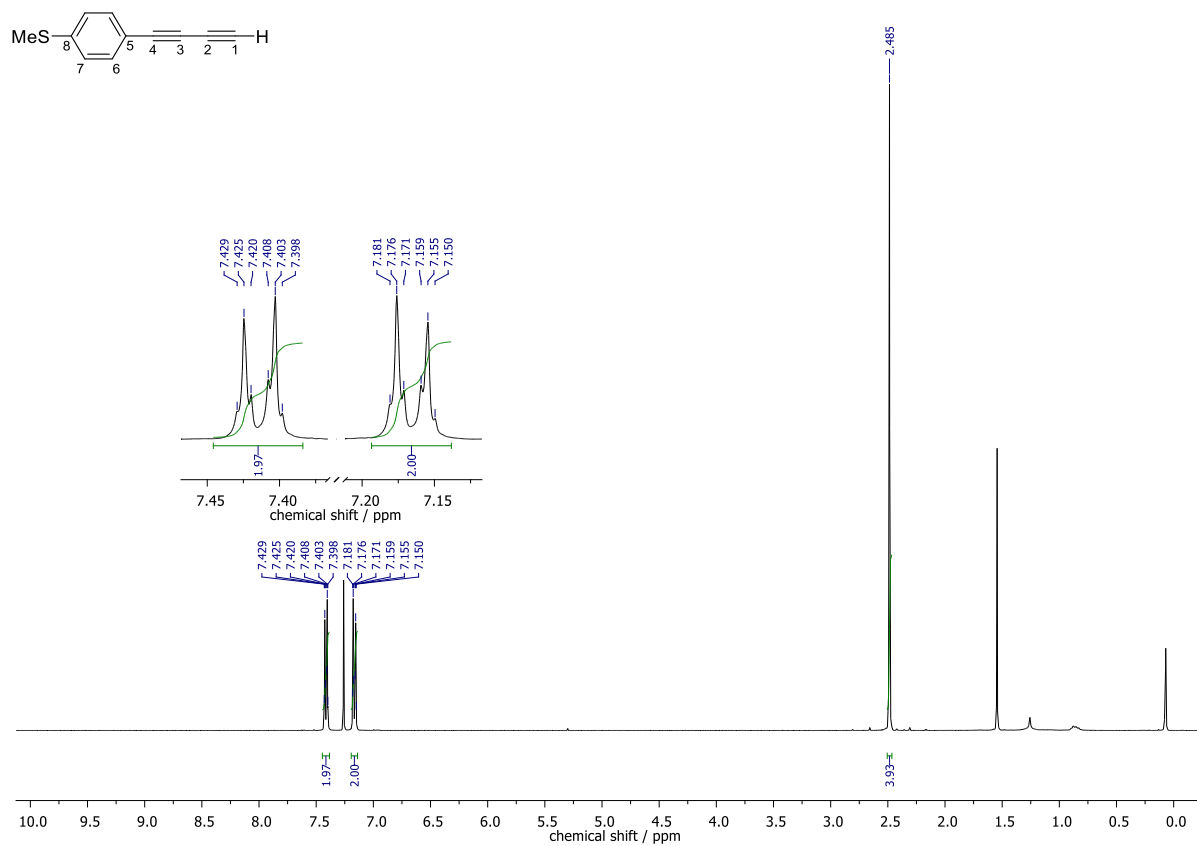


Figure S33: The ¹H NMR spectrum of **1d-2**.

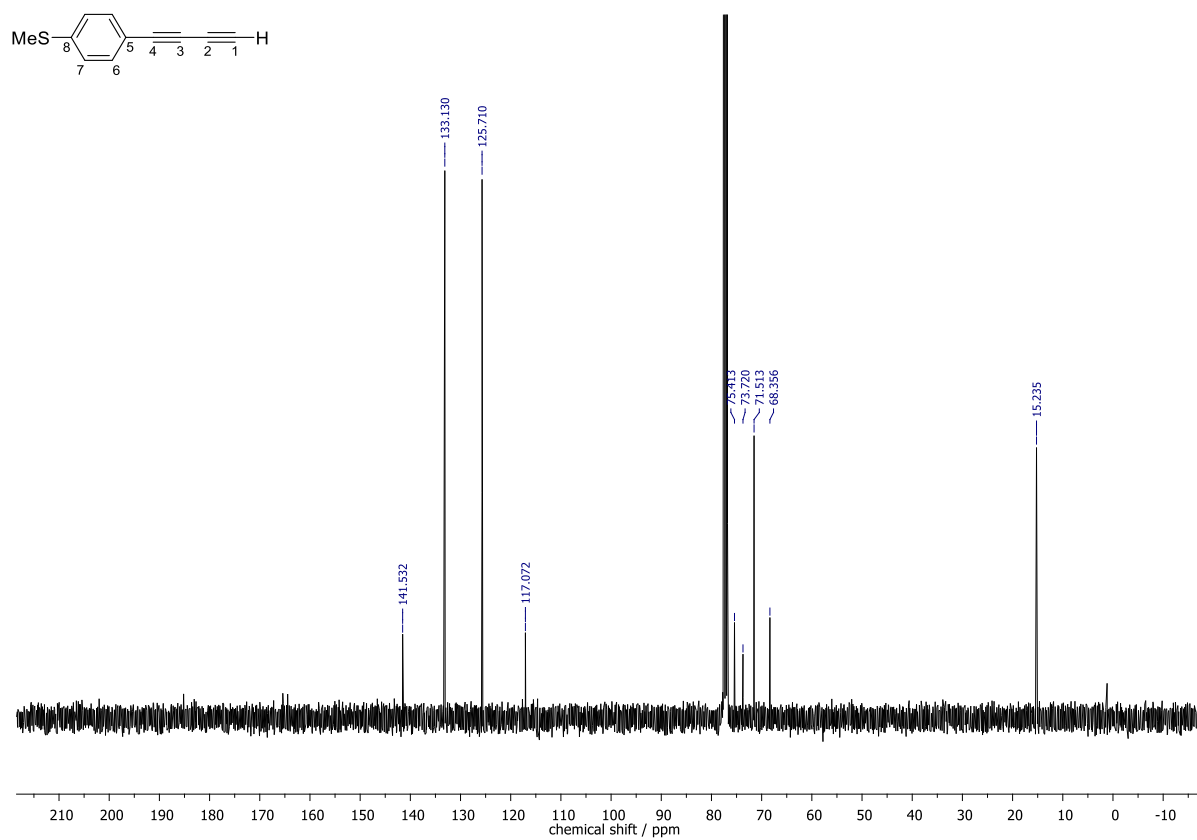


Figure S34: The ¹³C{¹H} NMR spectrum of **1d-2**.

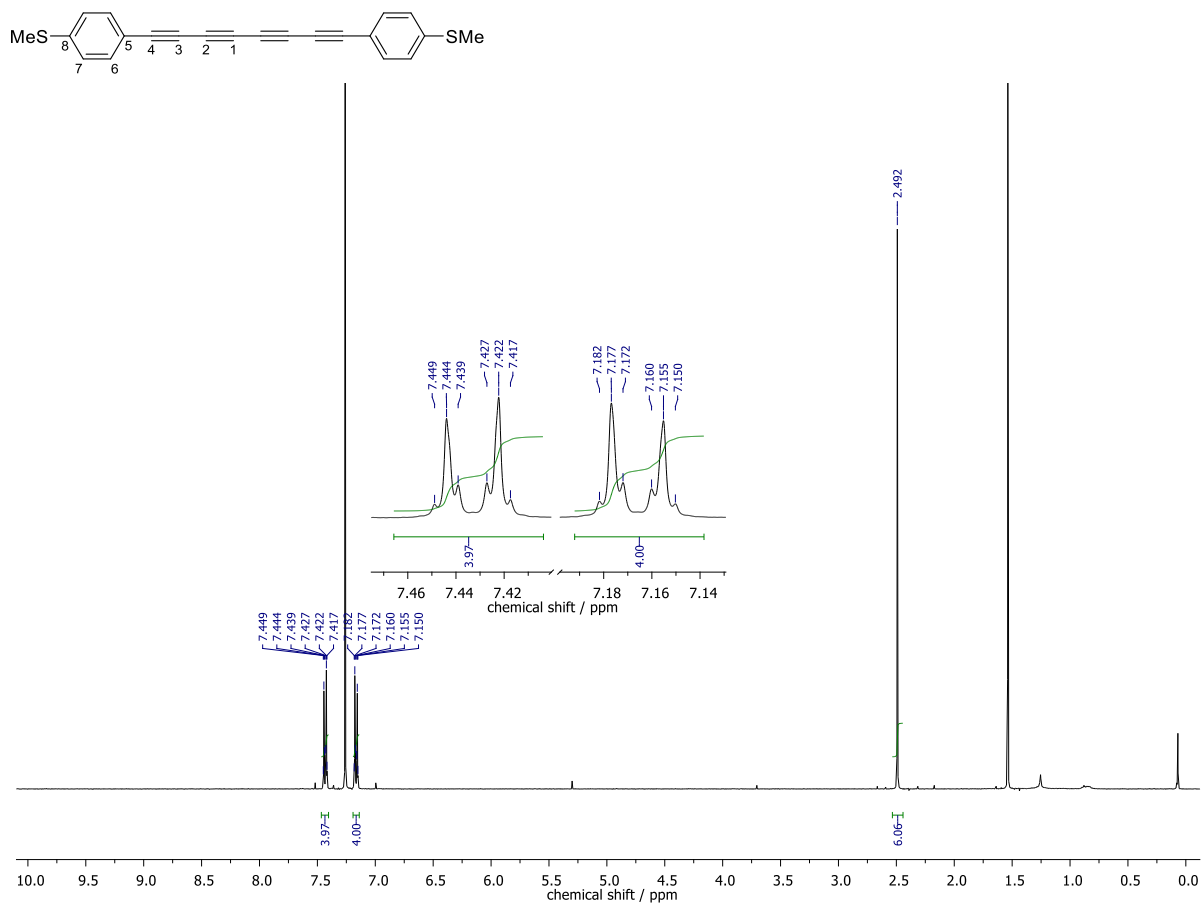


Figure S35: The ¹H NMR spectrum of **1d**.

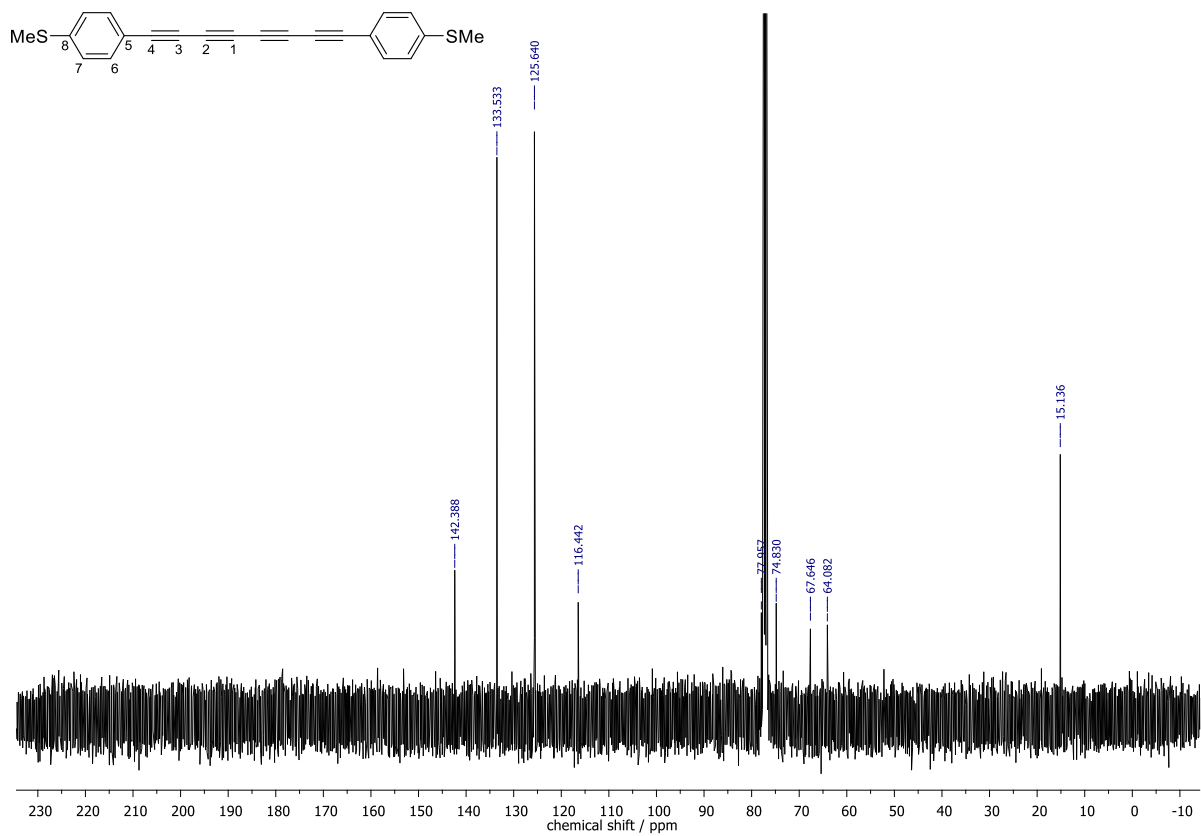


Figure S36: The ¹³C{¹H} NMR spectrum of **1d**.

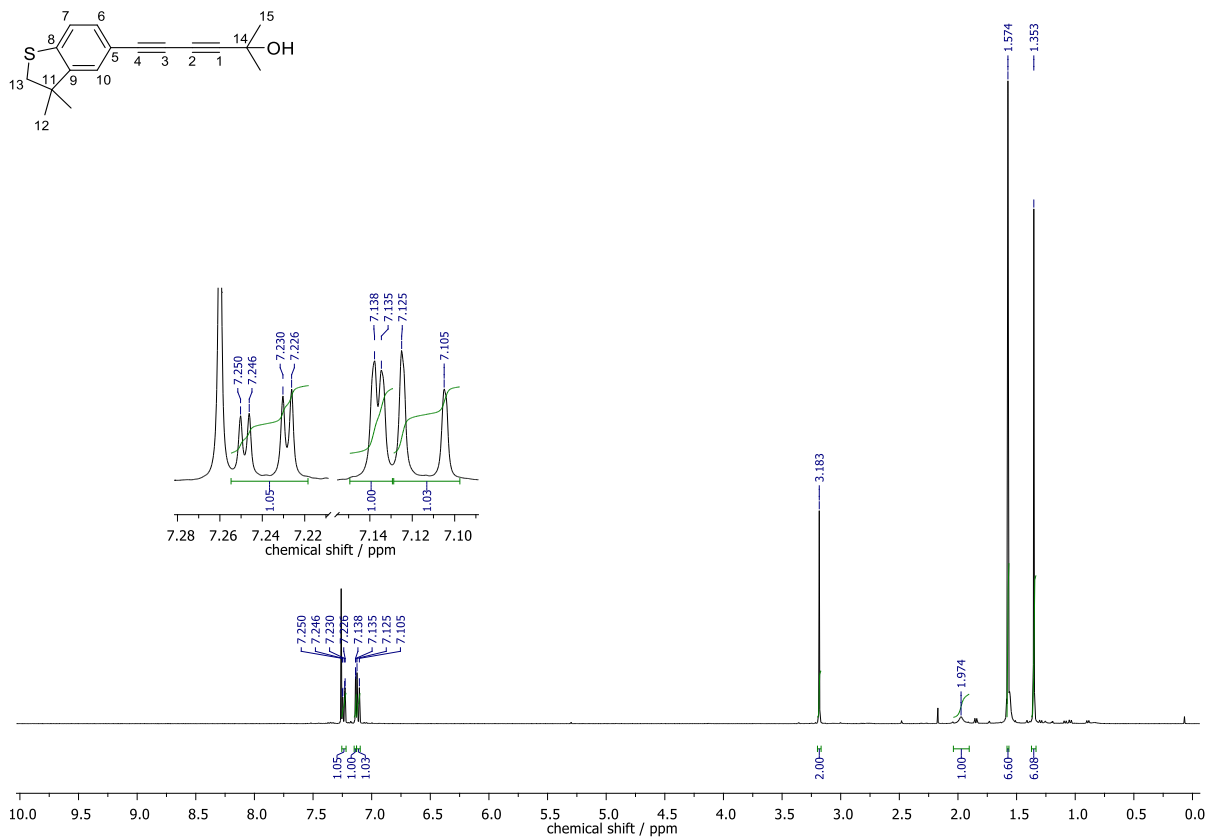


Figure S37: The ^1H NMR spectrum of **2d-1**.

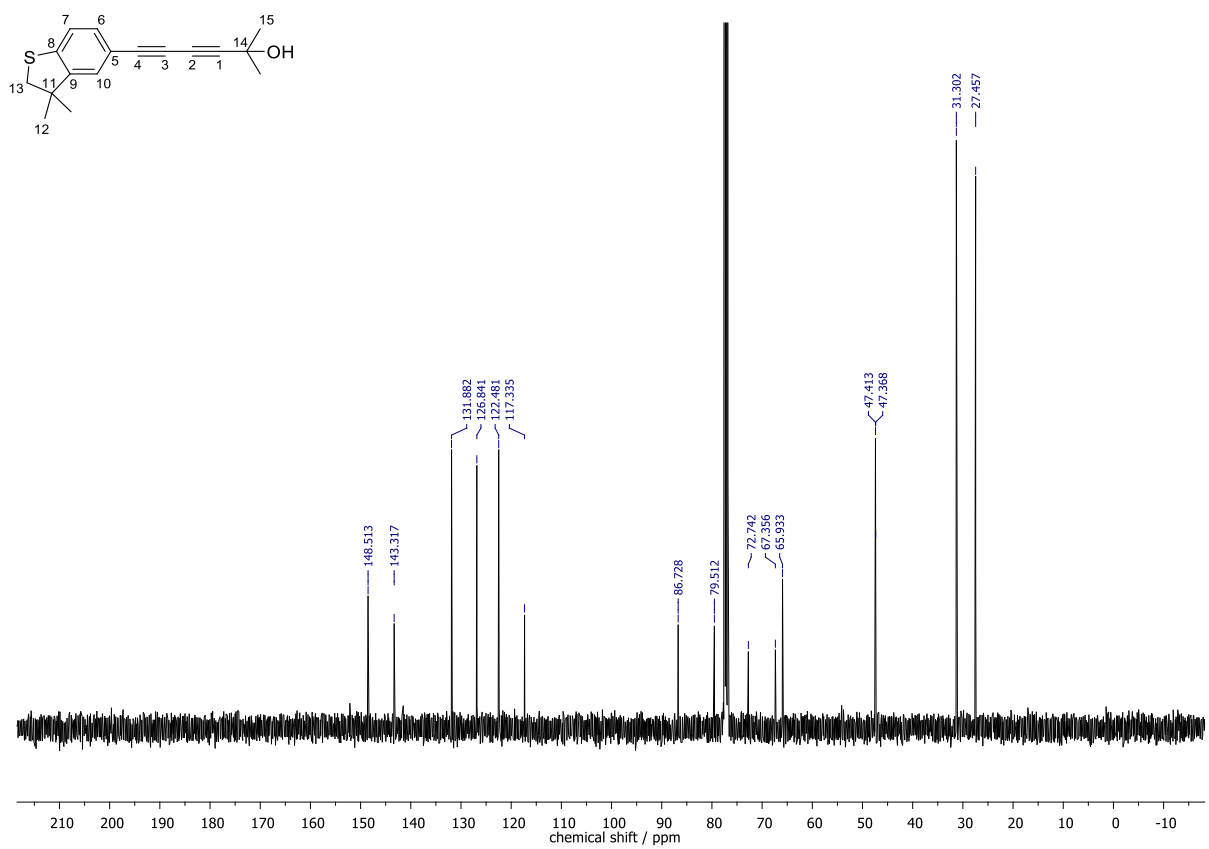


Figure S38: The $^{13}\text{C}\{^1\text{H}\}$ NMR spectrum of **2d-1**.

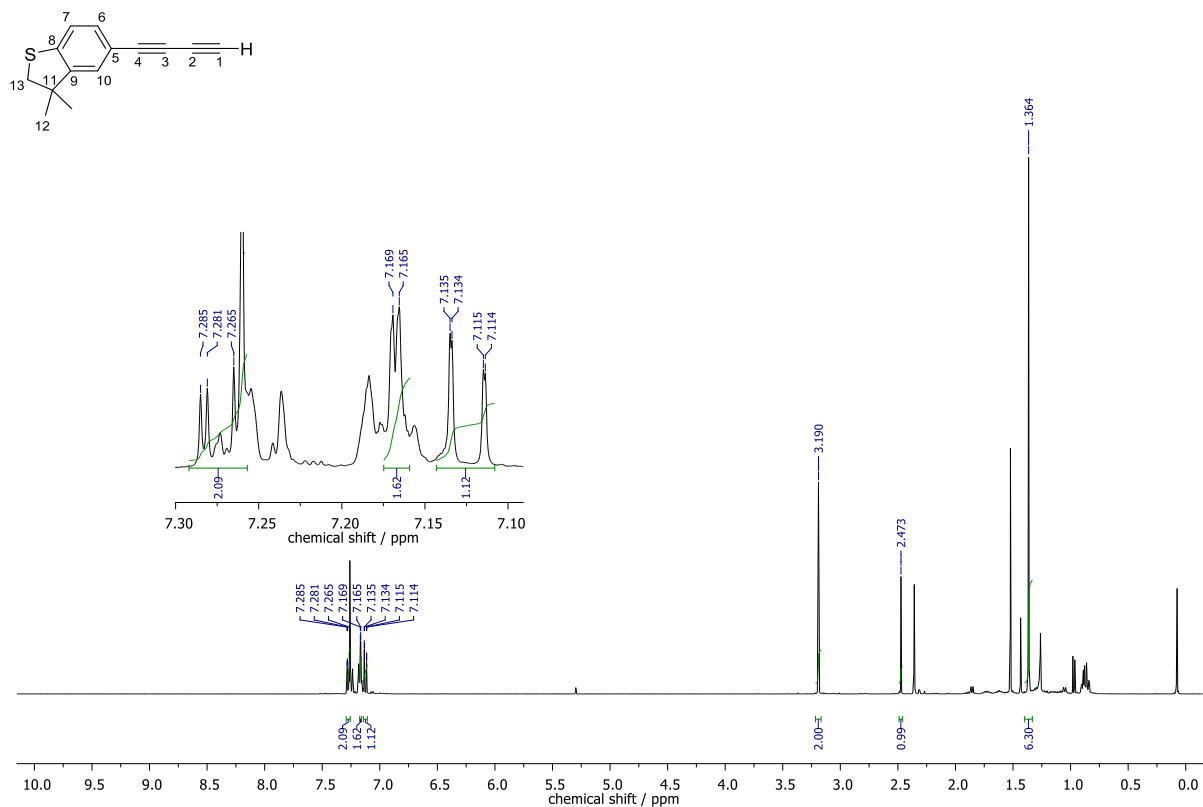


Figure S39: The ^1H NMR spectrum of **2d-2**.

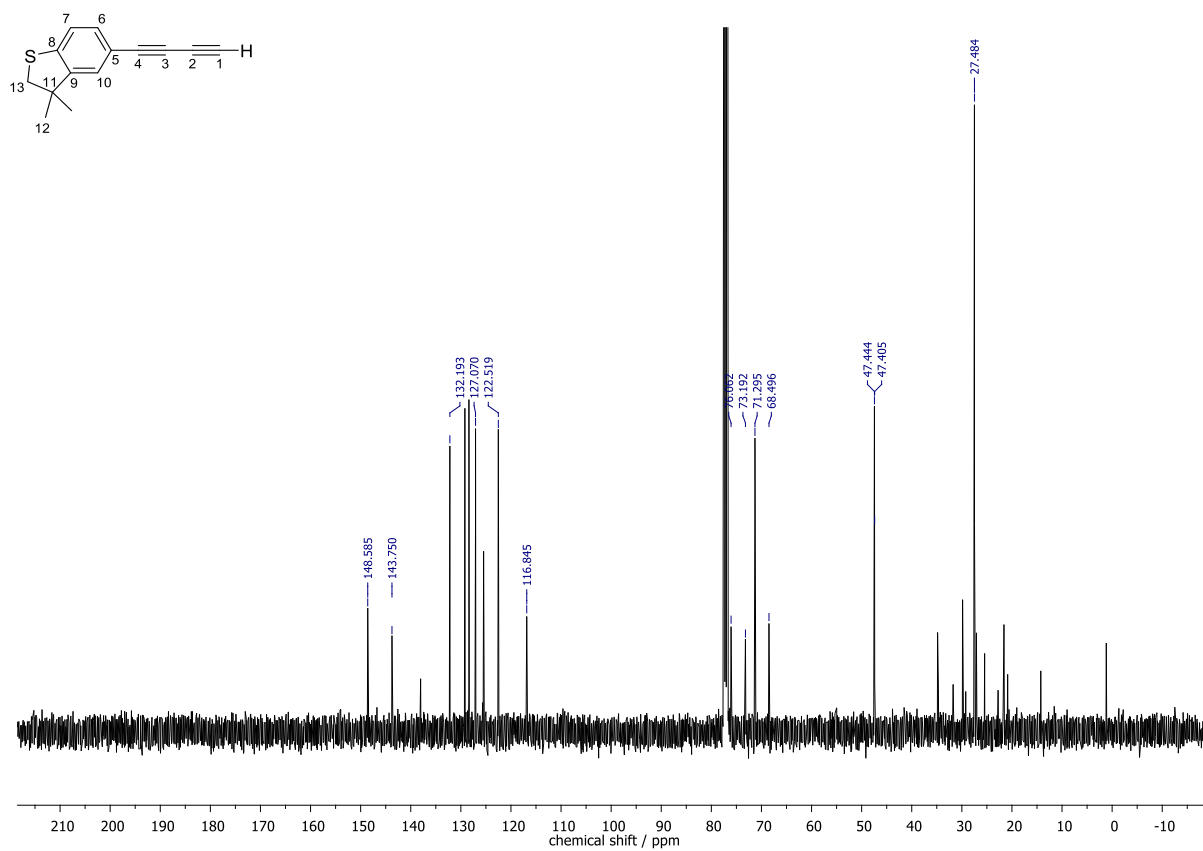


Figure S40: The $^{13}\text{C}\{^1\text{H}\}$ NMR spectrum of **2d-2**.

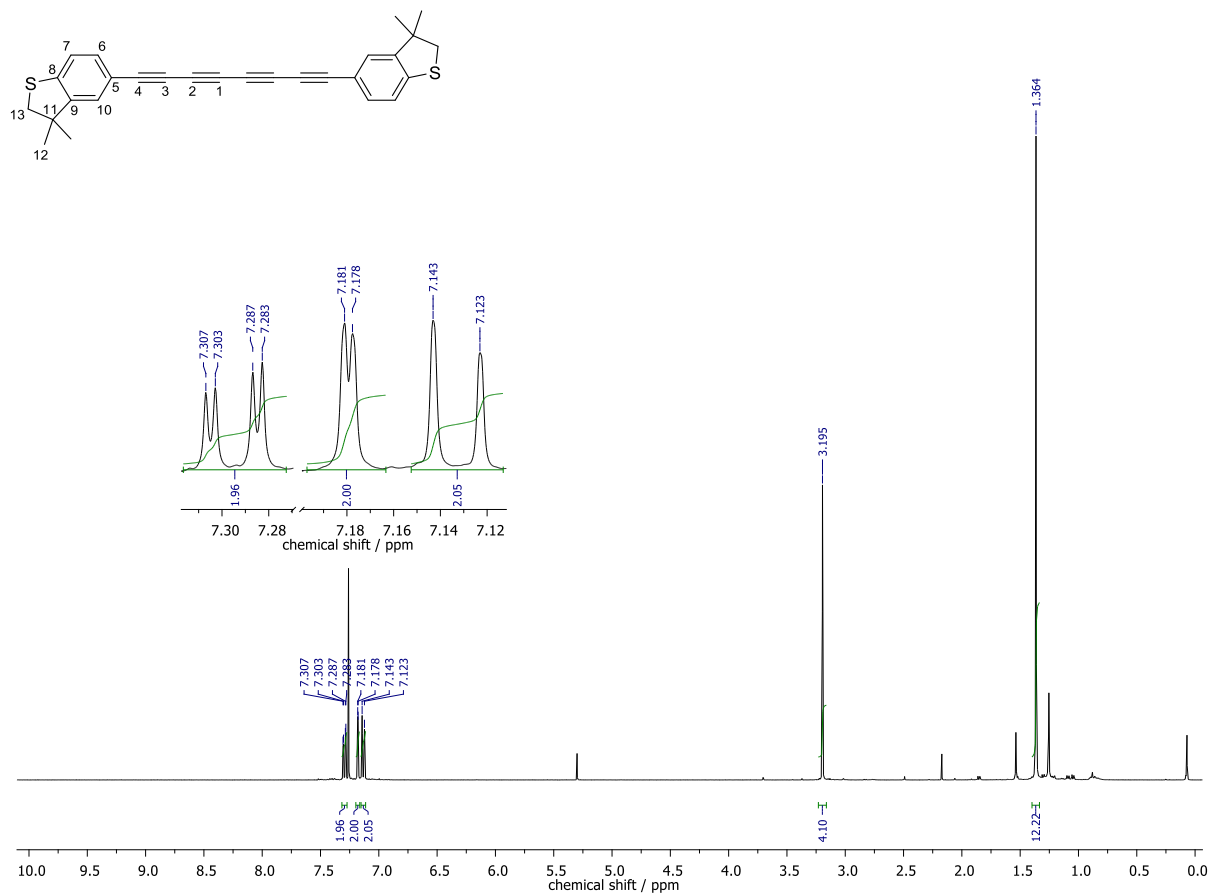


Figure S41: The ^1H NMR spectrum of **2d**.

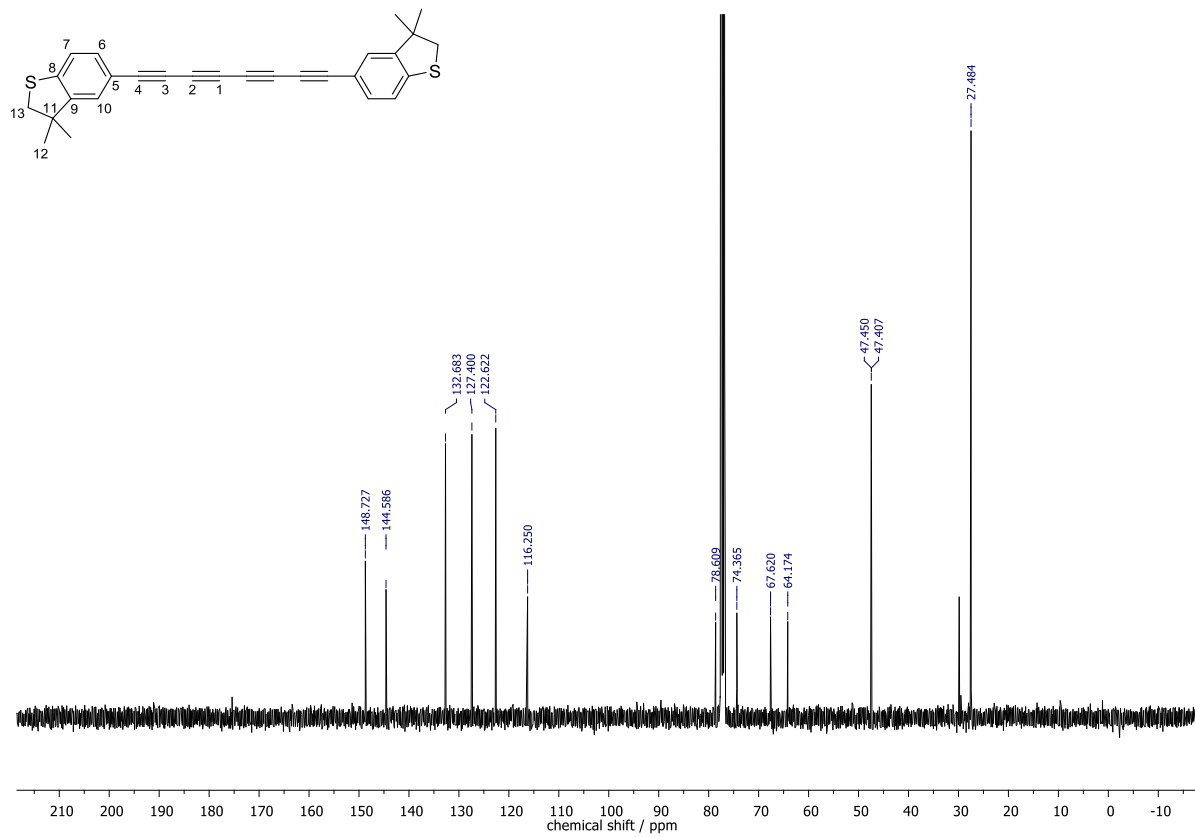


Figure S42: The $^{13}\text{C}\{^1\text{H}\}$ NMR spectrum of **2d**.

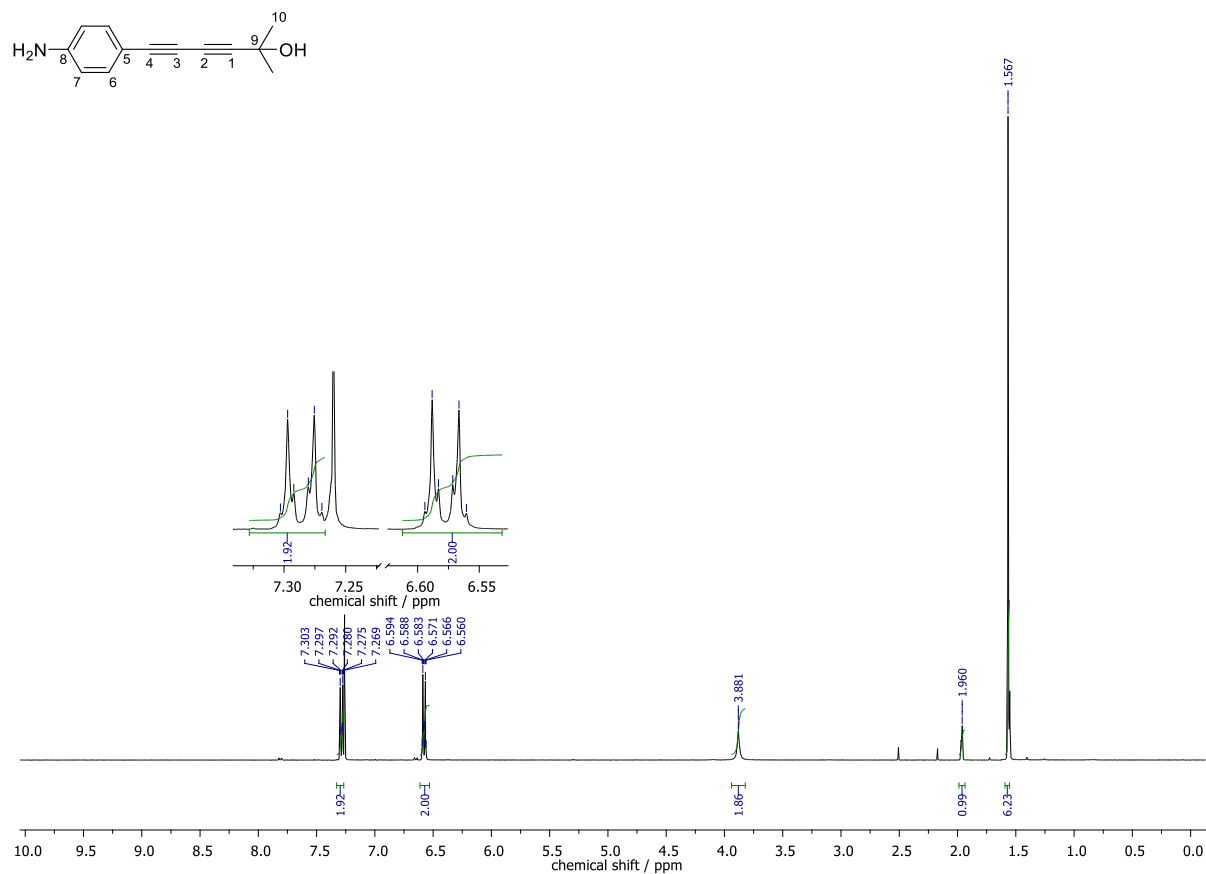


Figure S43: The ^1H NMR spectrum of **3d-1**.

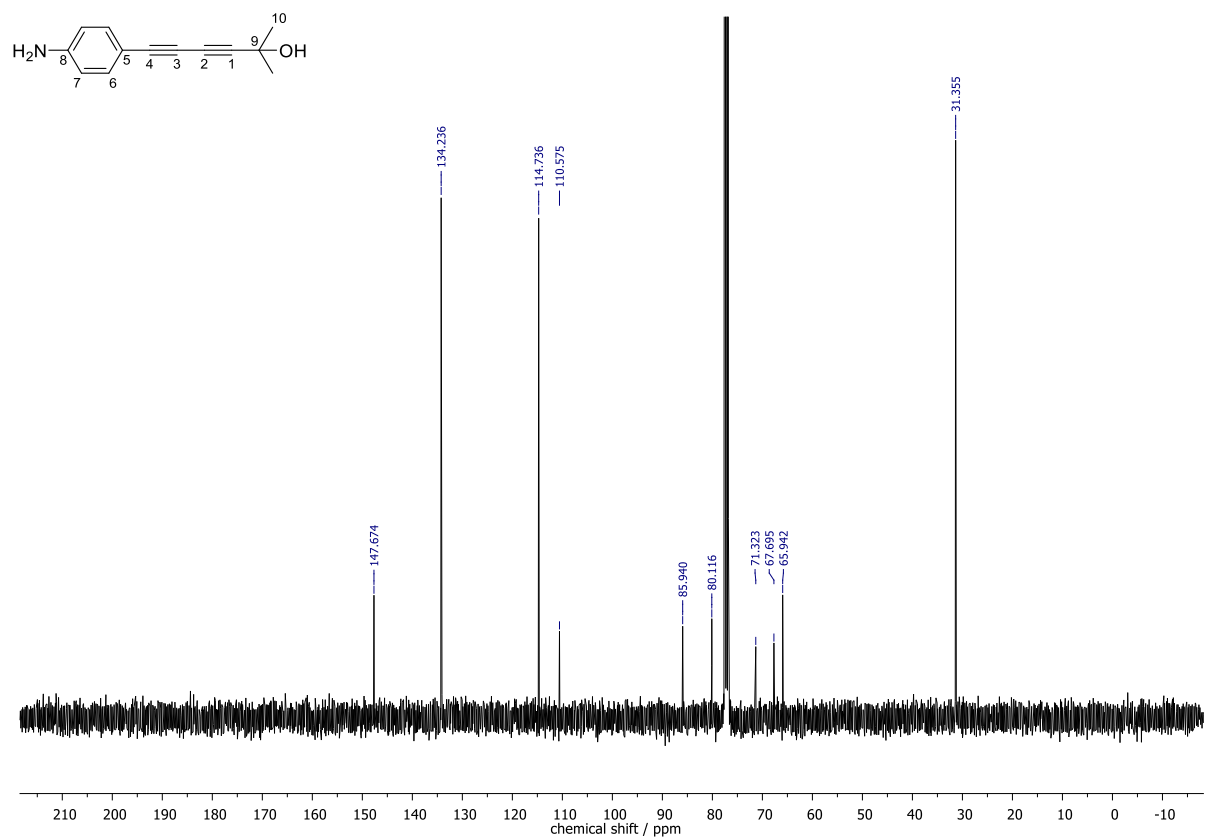


Figure S44: The $^{13}\text{C}\{^1\text{H}\}$ NMR spectrum of **3d-1**.

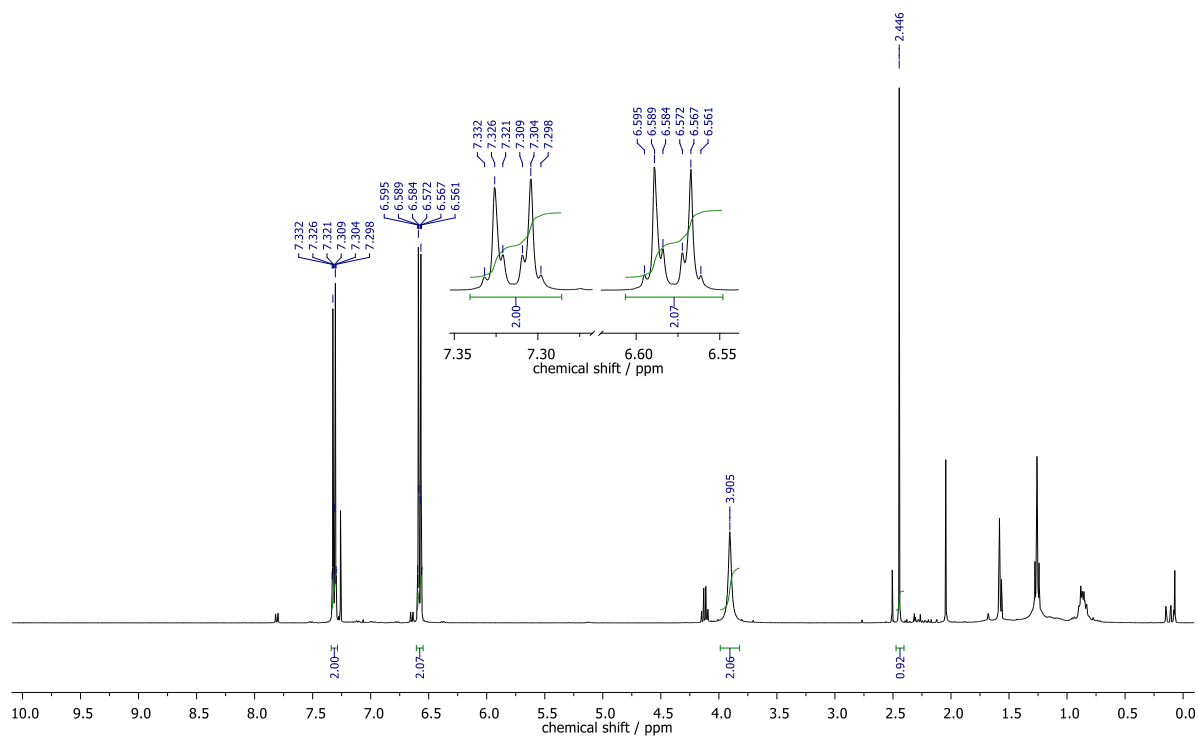
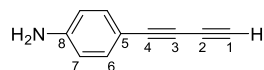


Figure S45: The ^1H NMR spectrum of **3d-2**.

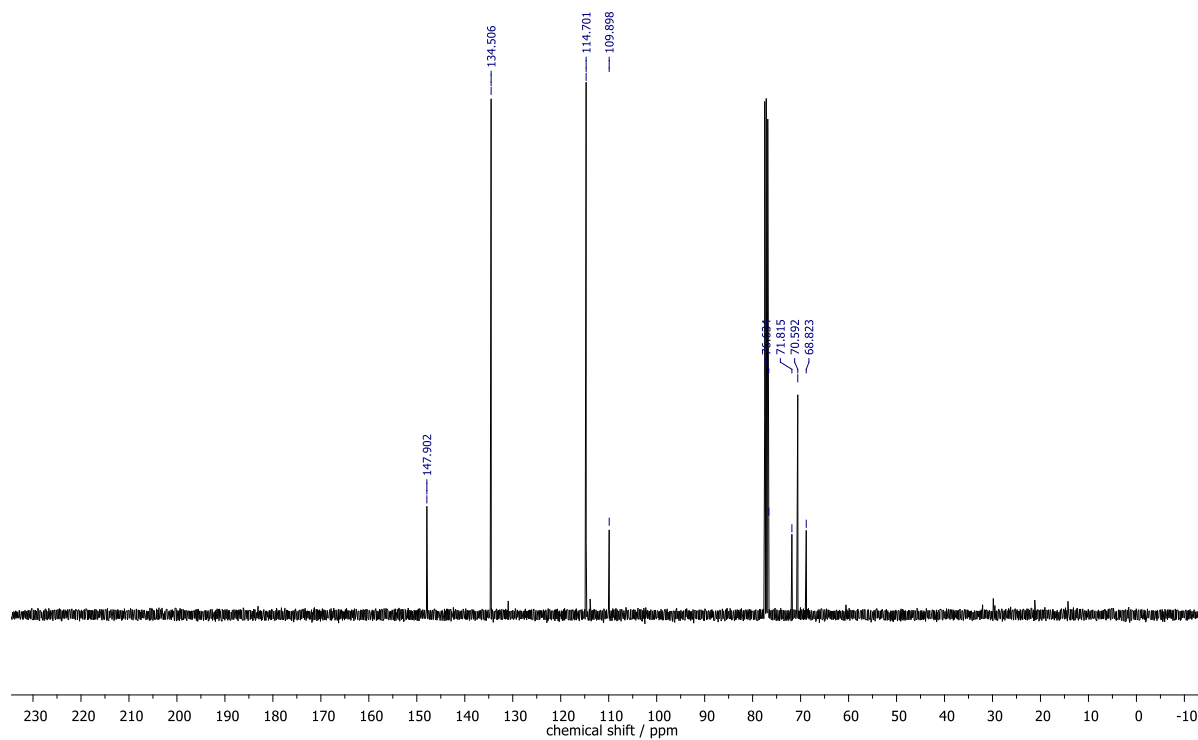
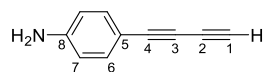


Figure S46: The $^{13}\text{C}\{^1\text{H}\}$ NMR spectrum of **3d-2**.

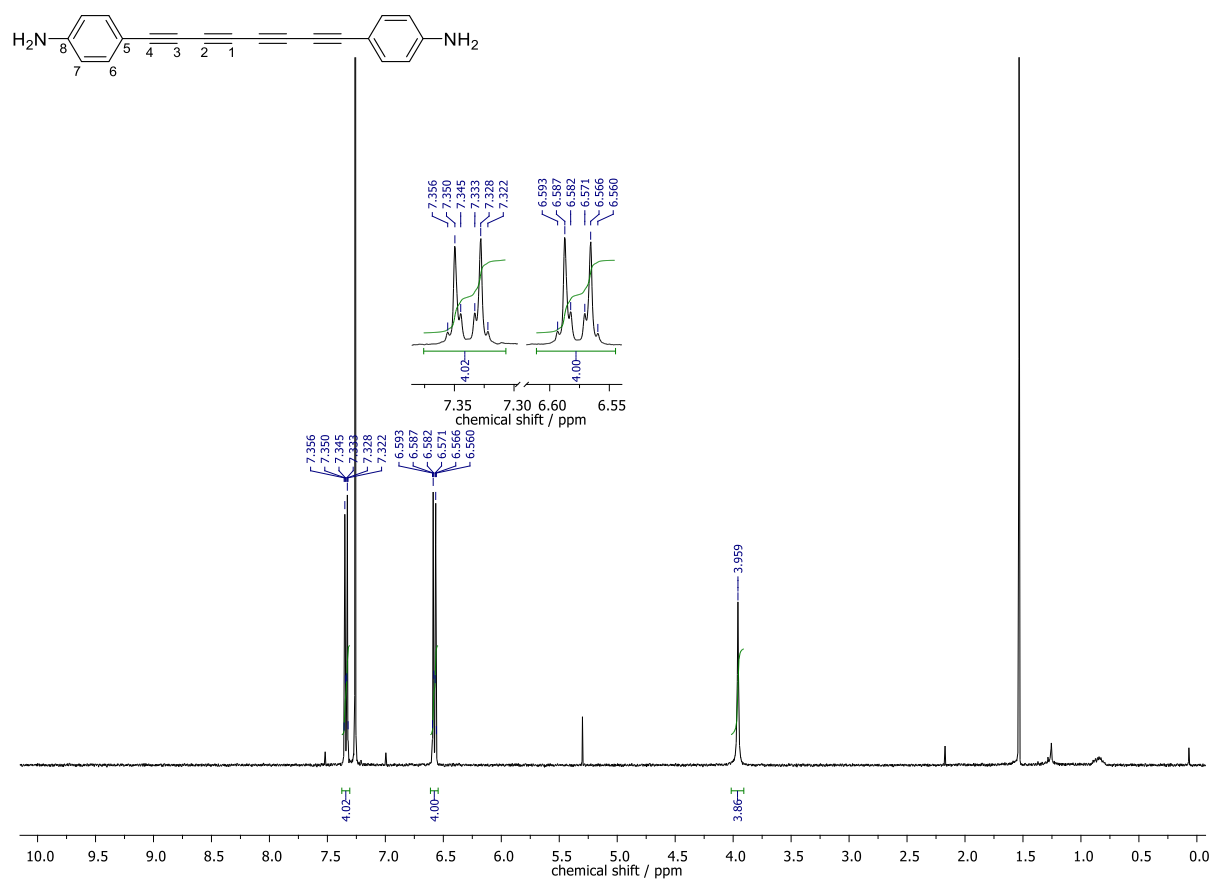


Figure S47: The ^1H NMR spectrum of **3d**.

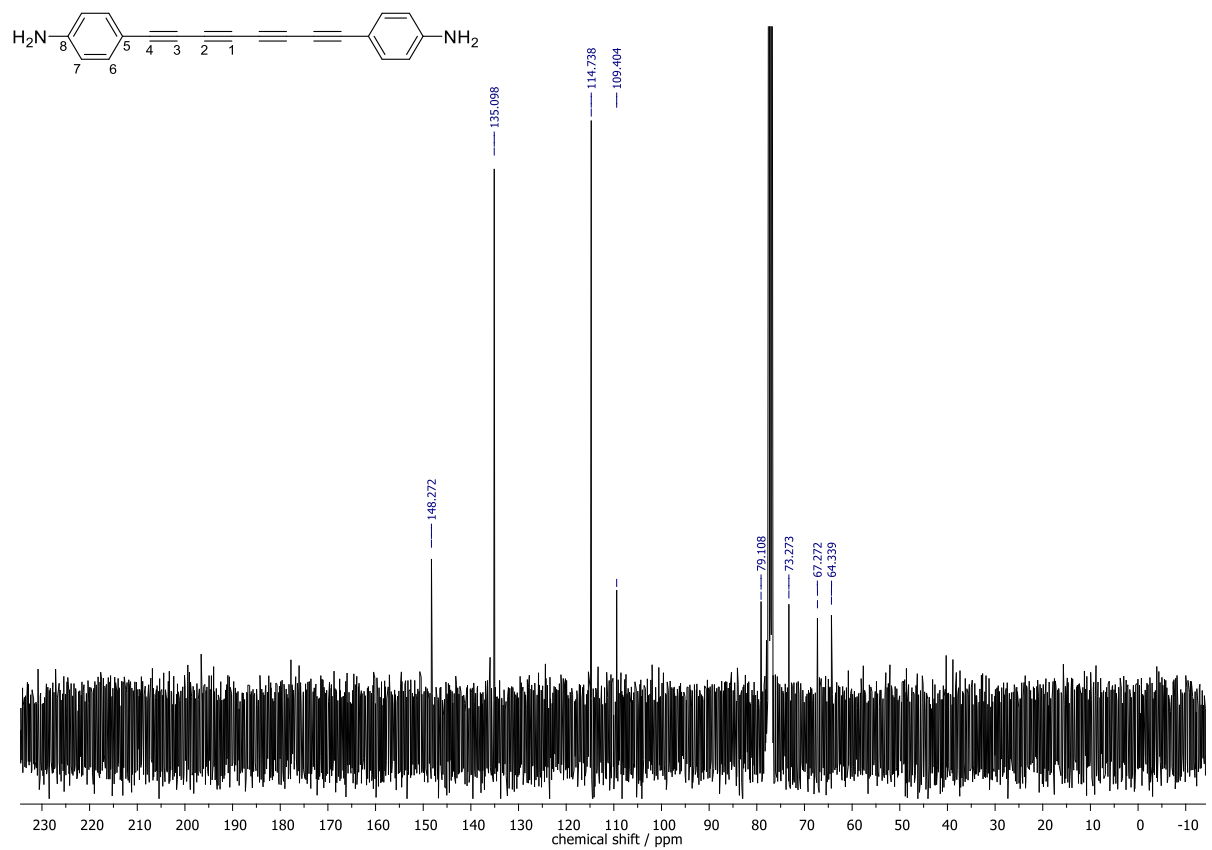


Figure S48: The $^{13}\text{C}\{^1\text{H}\}$ NMR spectrum of **3d**.

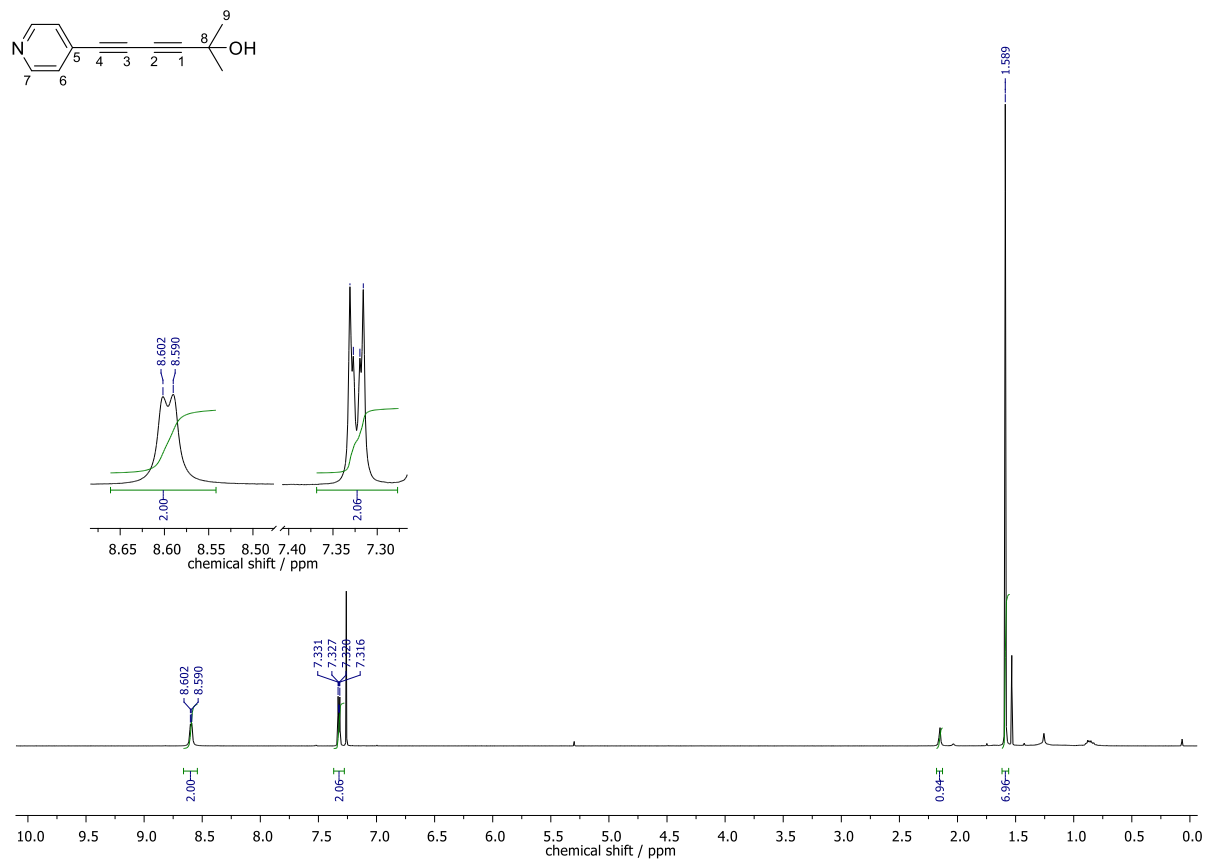


Figure S49: The ^1H NMR spectrum of 4d-1.

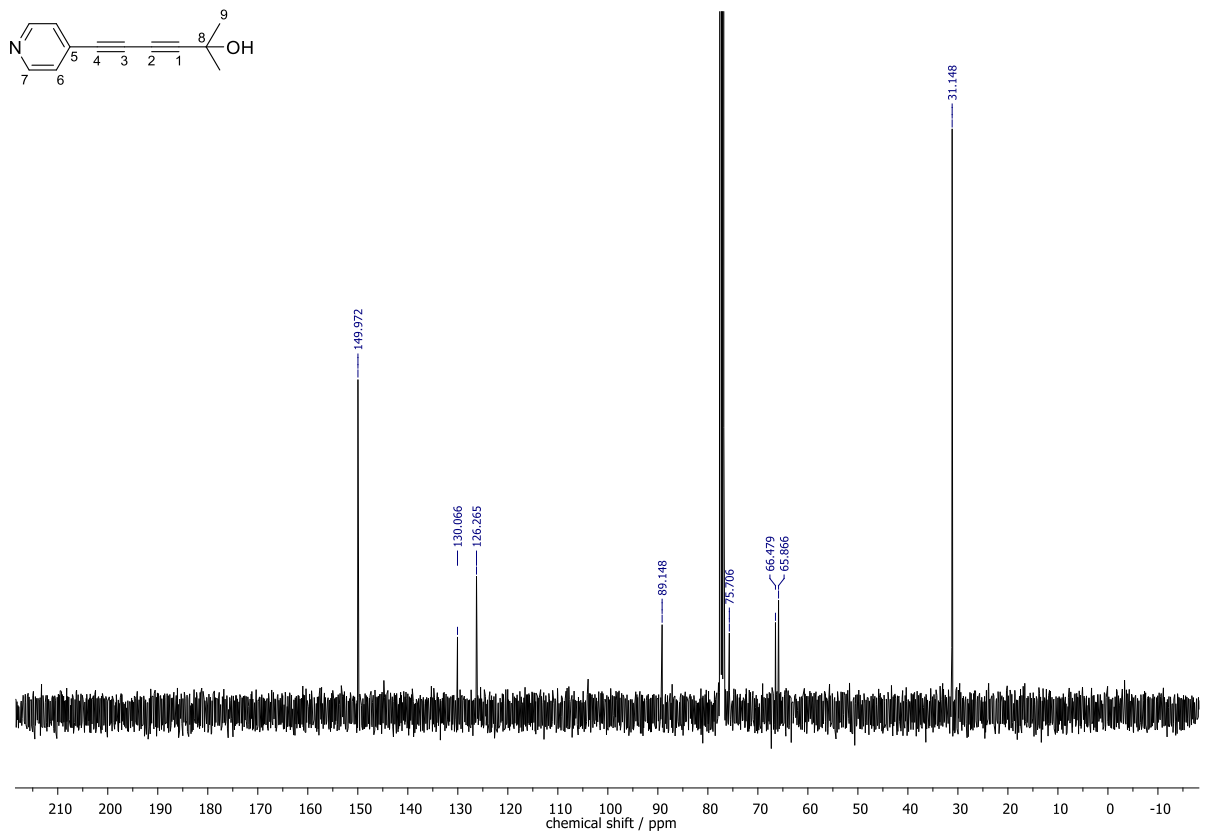


Figure S50: The $^{13}\text{C}\{^1\text{H}\}$ NMR spectrum of 4d-1.

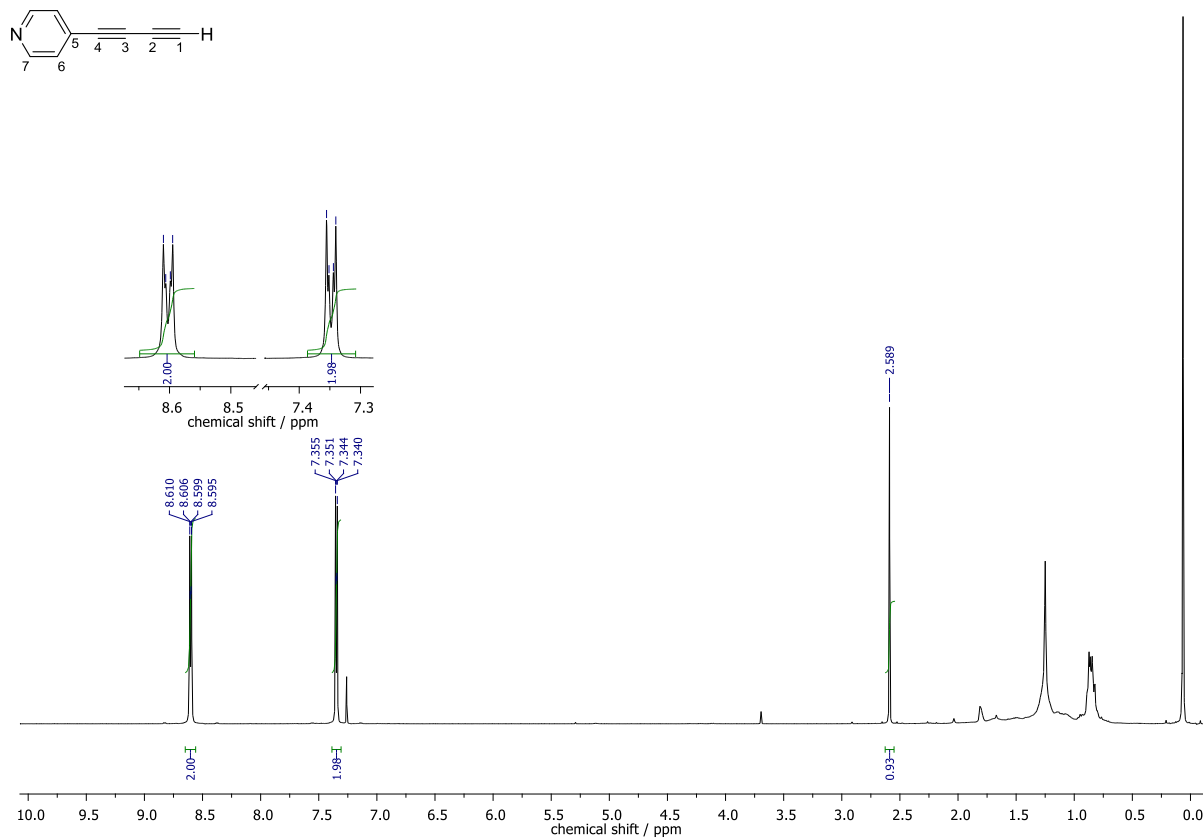


Figure S51: The ^1H NMR spectrum of **4d-2**.

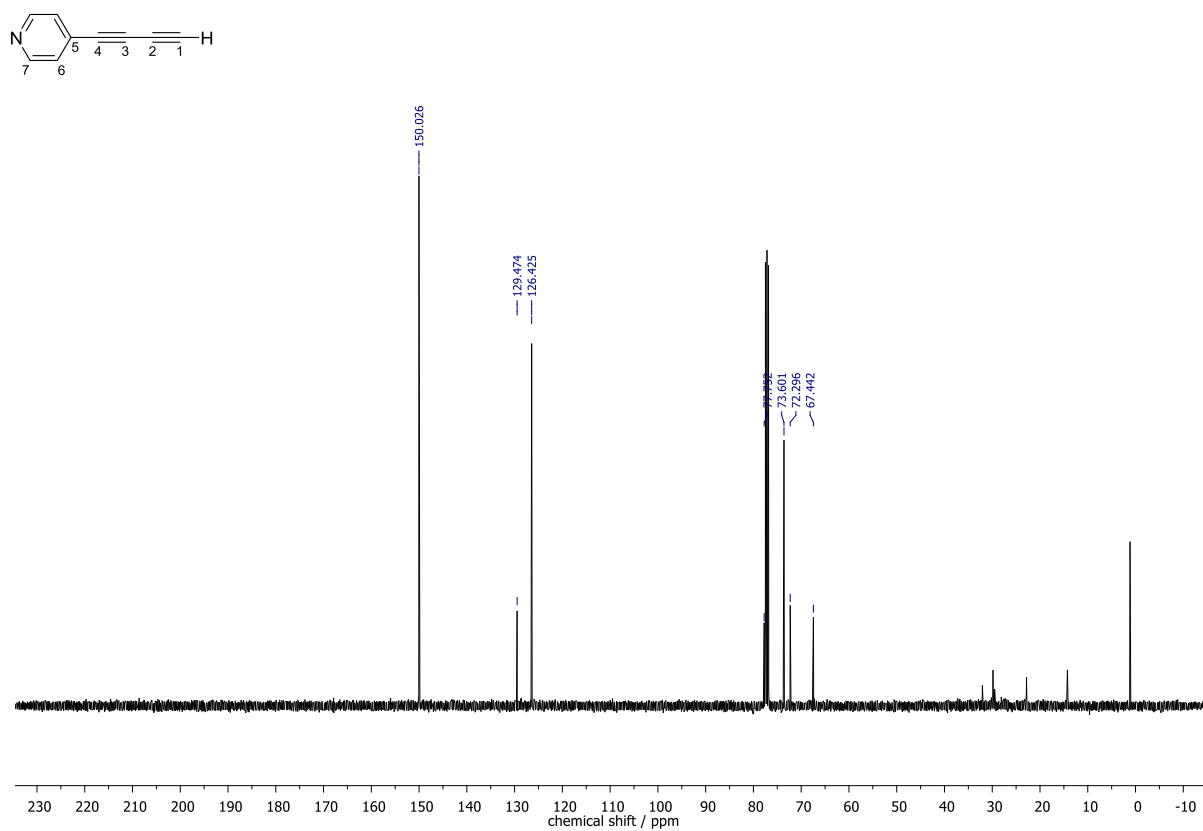


Figure S52: The $^{13}\text{C}\{^1\text{H}\}$ NMR spectrum of **4d-2**.

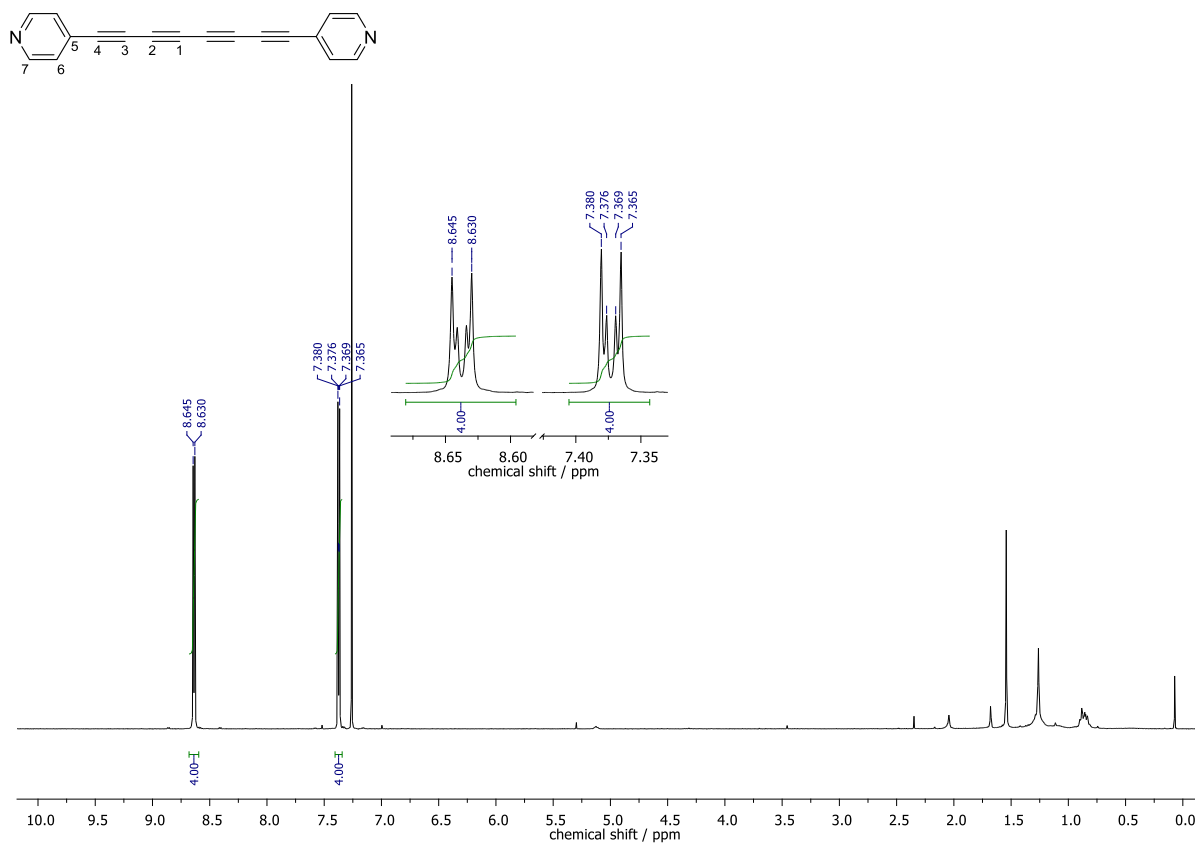


Figure S53: The ¹H NMR spectrum of **4d**.

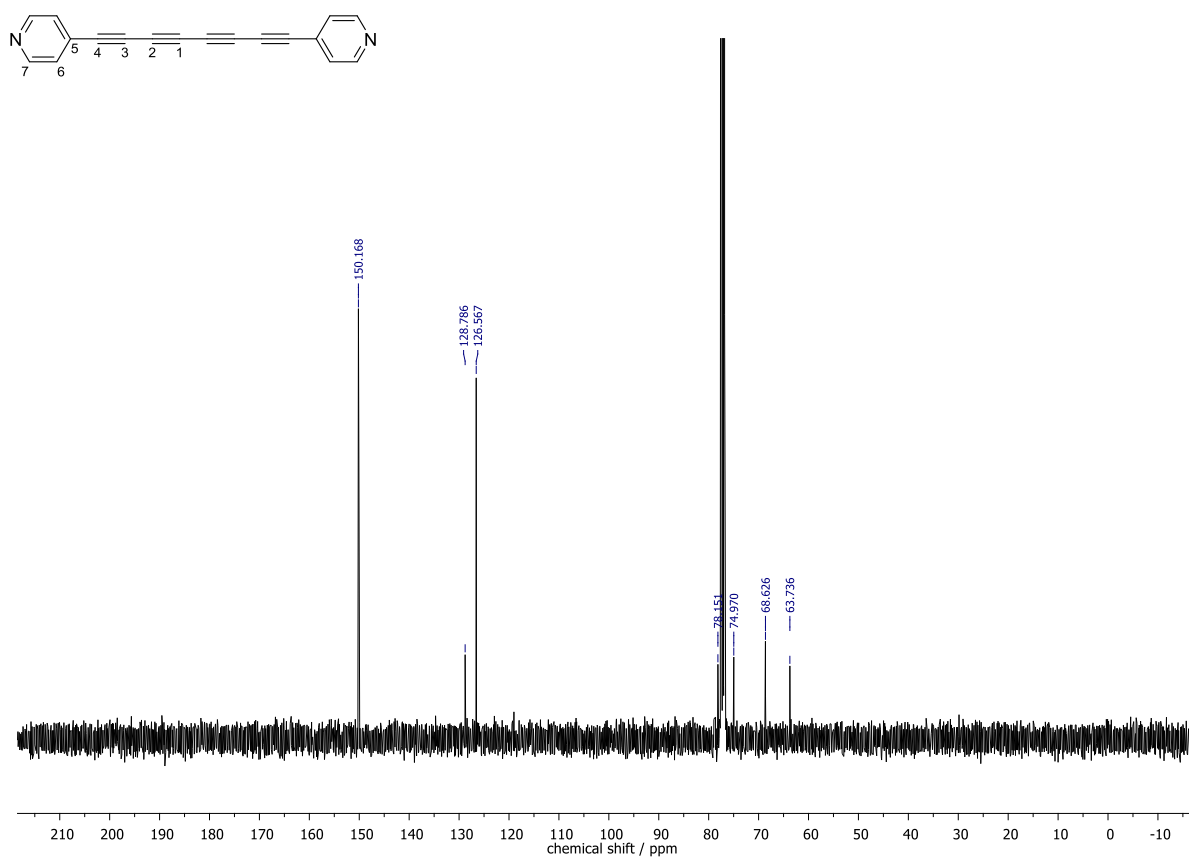


Figure S54: The ¹³C{¹H} NMR spectrum of **4d**.

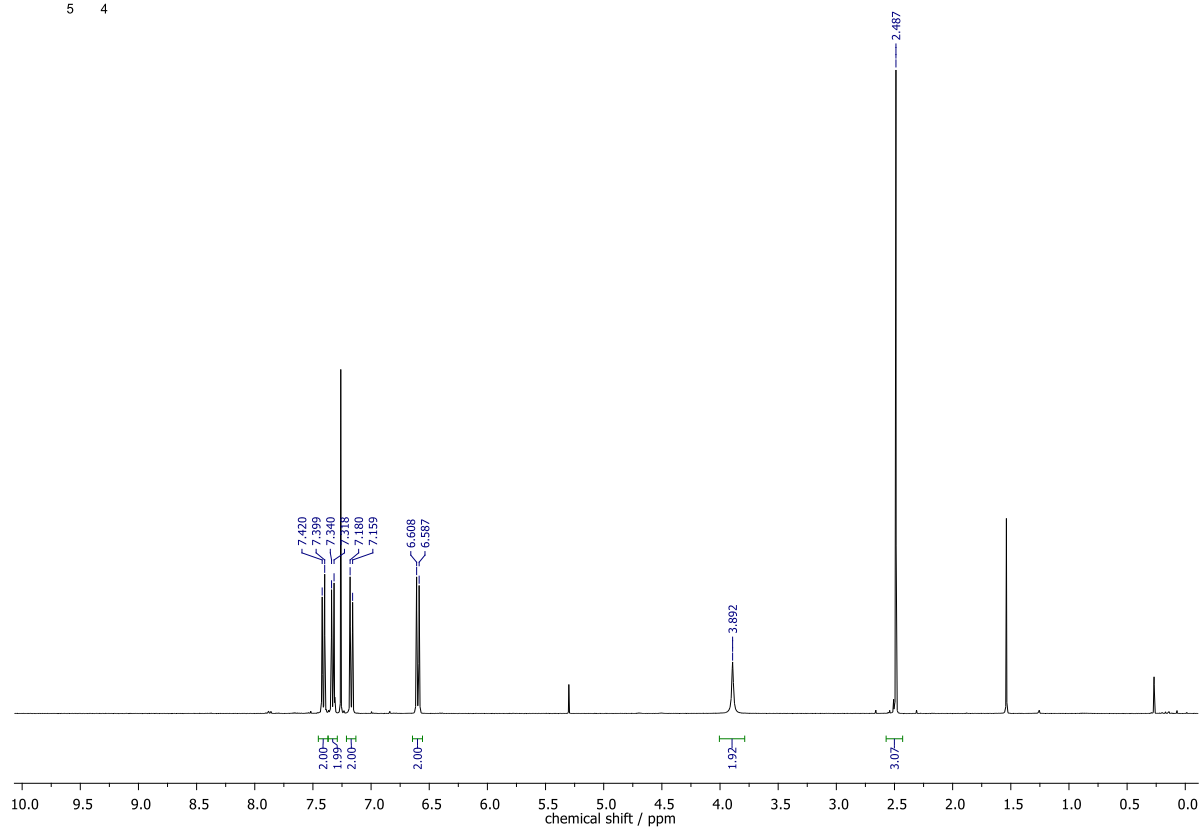
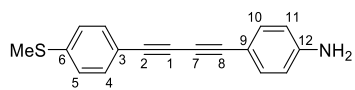


Figure S55: The ^1H NMR spectrum of **5**.

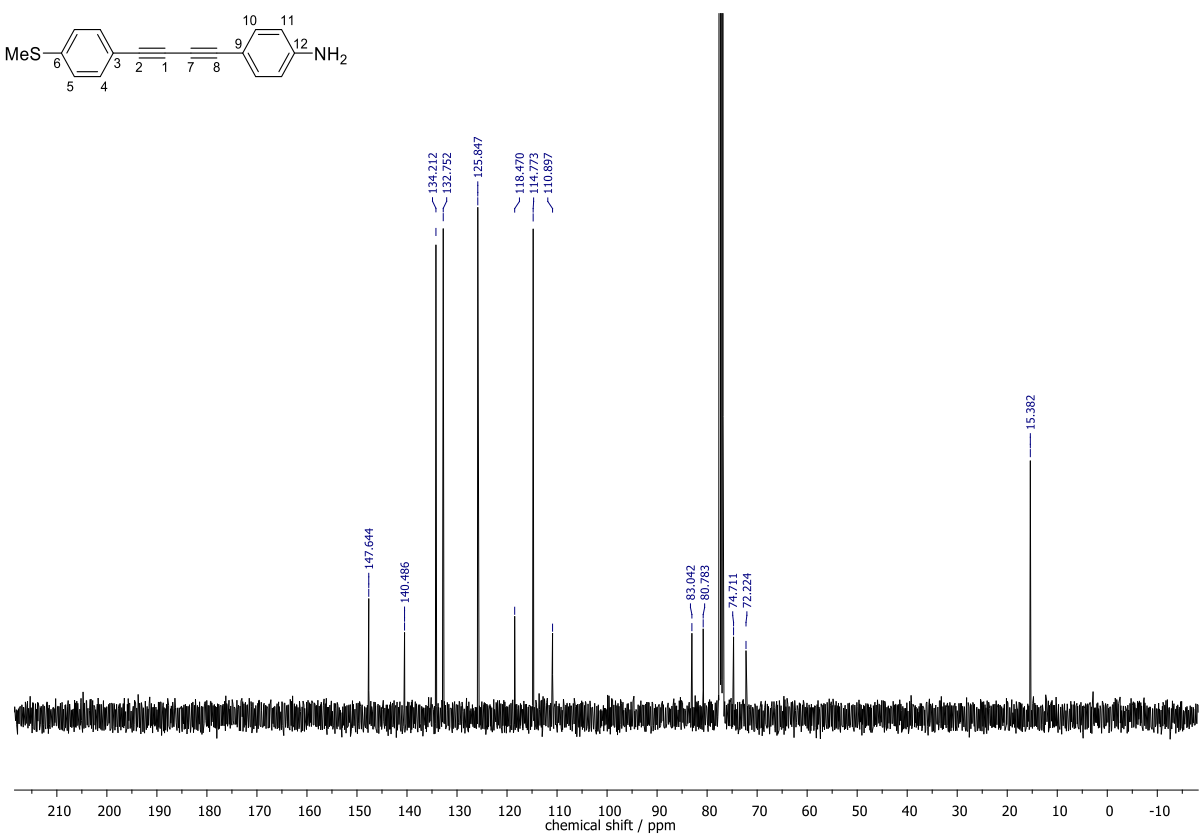
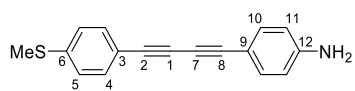


Figure S56: The $^{13}\text{C}\{^1\text{H}\}$ NMR spectrum of **5**.

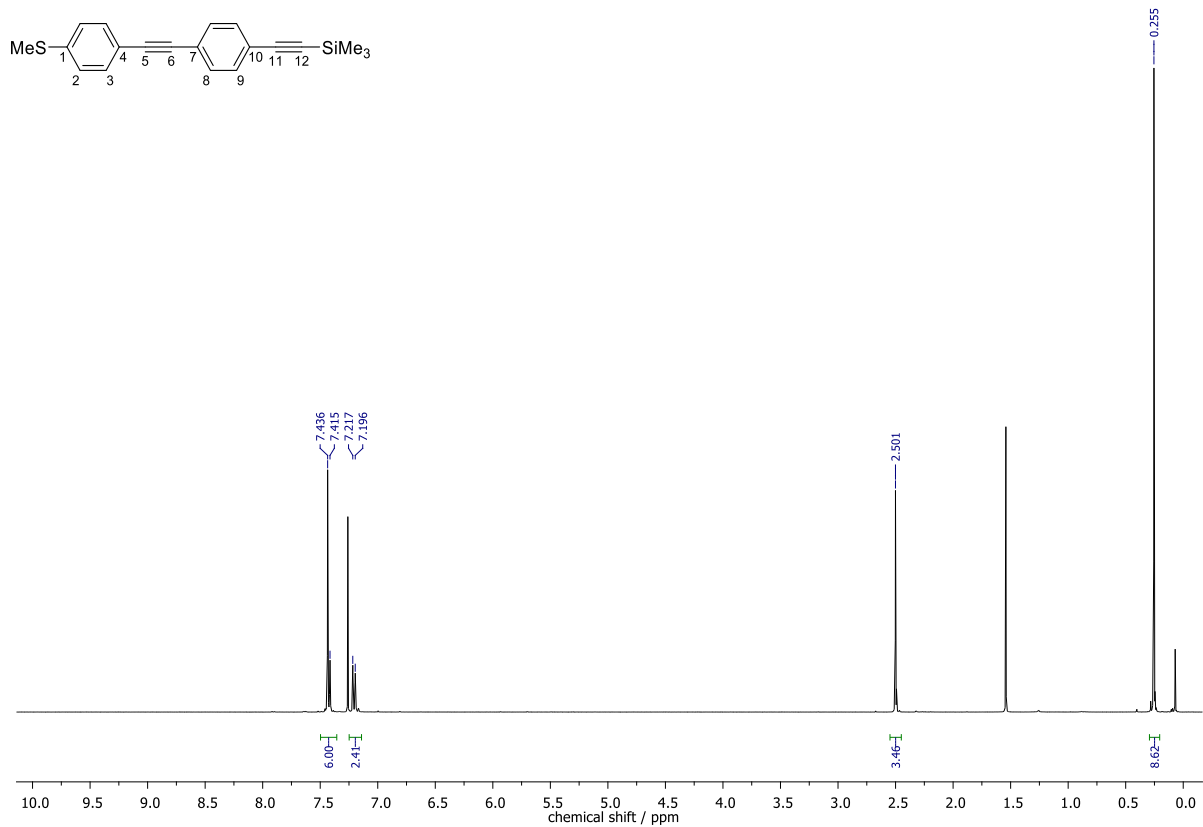


Figure S57: The ¹H NMR spectrum of 4-((4-(methylthio)phenyl)ethynyl)-1-(trimethylsilylethynyl)benzene.

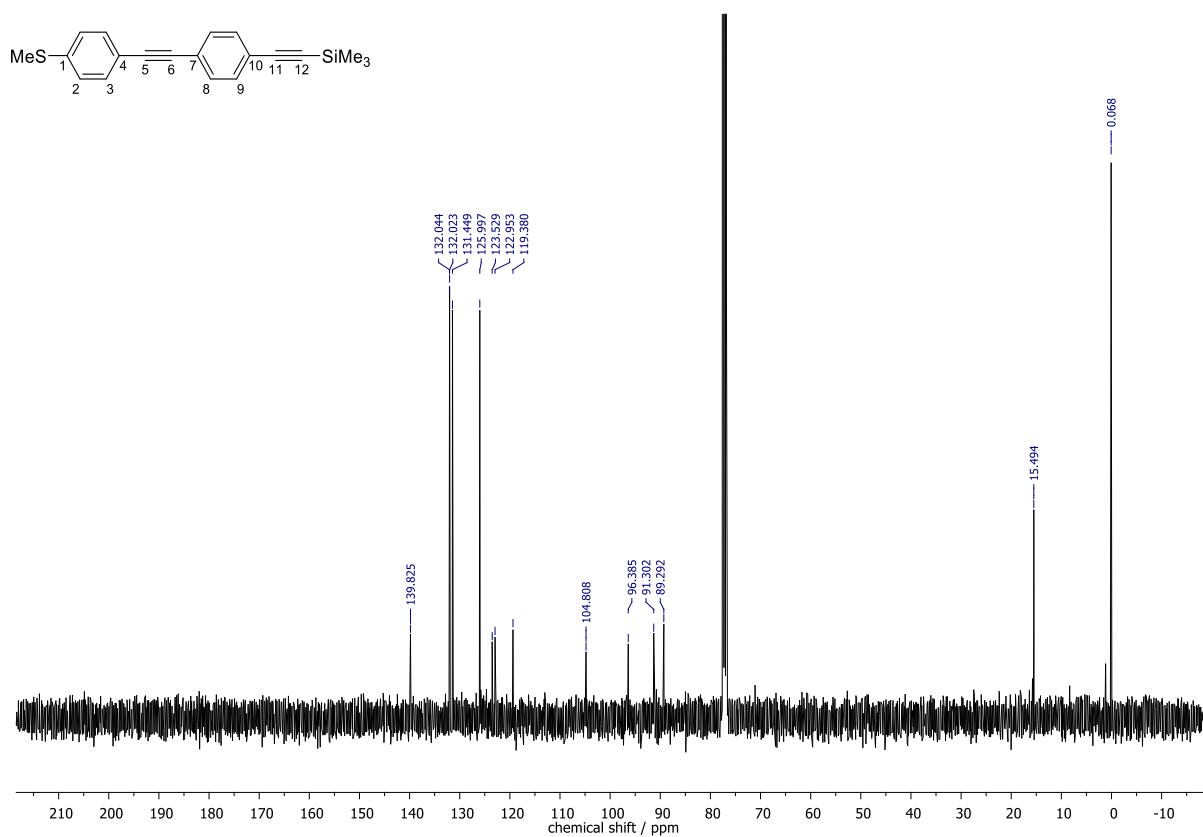


Figure S58: The ¹³C{¹H} NMR spectrum of 4-((4-(methylthio)phenyl)ethynyl)-1-(trimethylsilylethynyl)benzene.

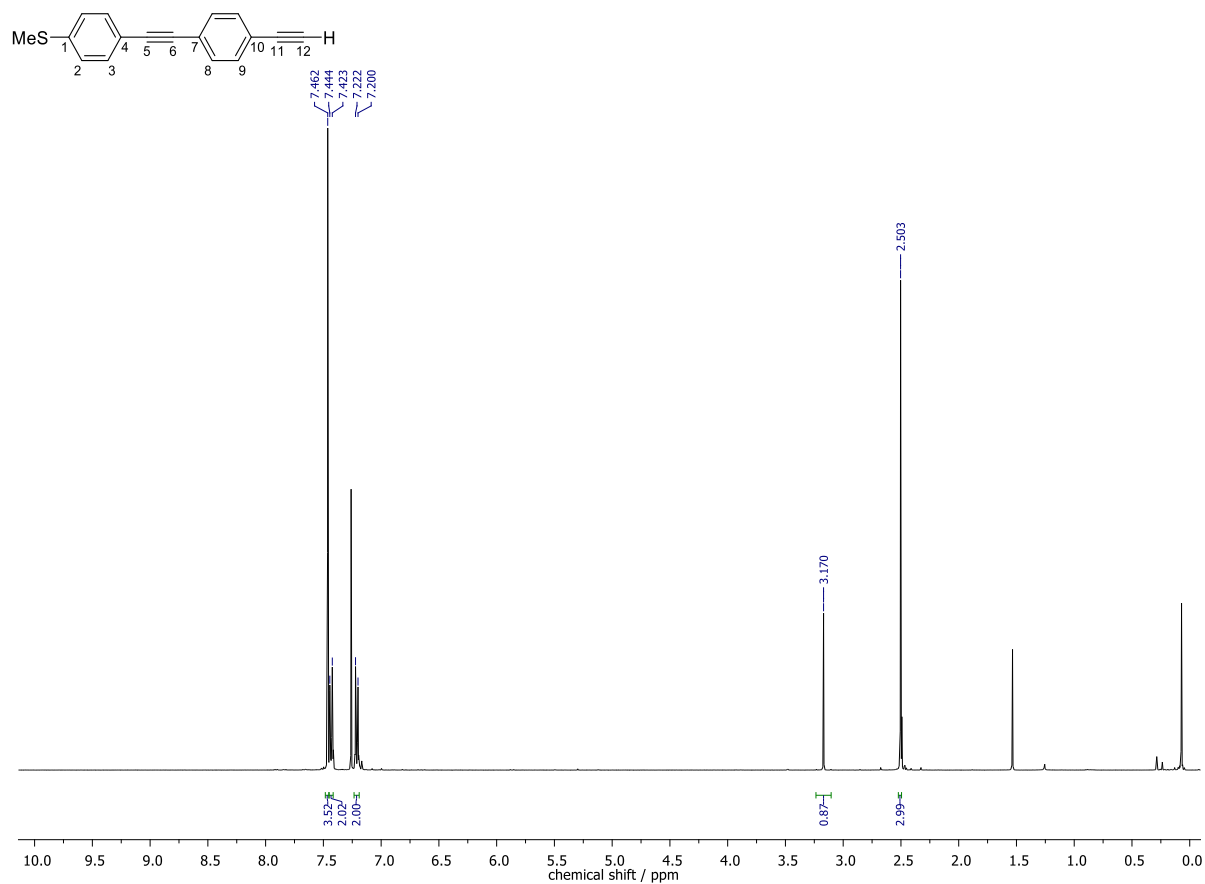


Figure S59: The ¹H NMR spectrum of 4-((4-(methylthio)phenyl)ethynyl)-1-(ethynyl)benzene.

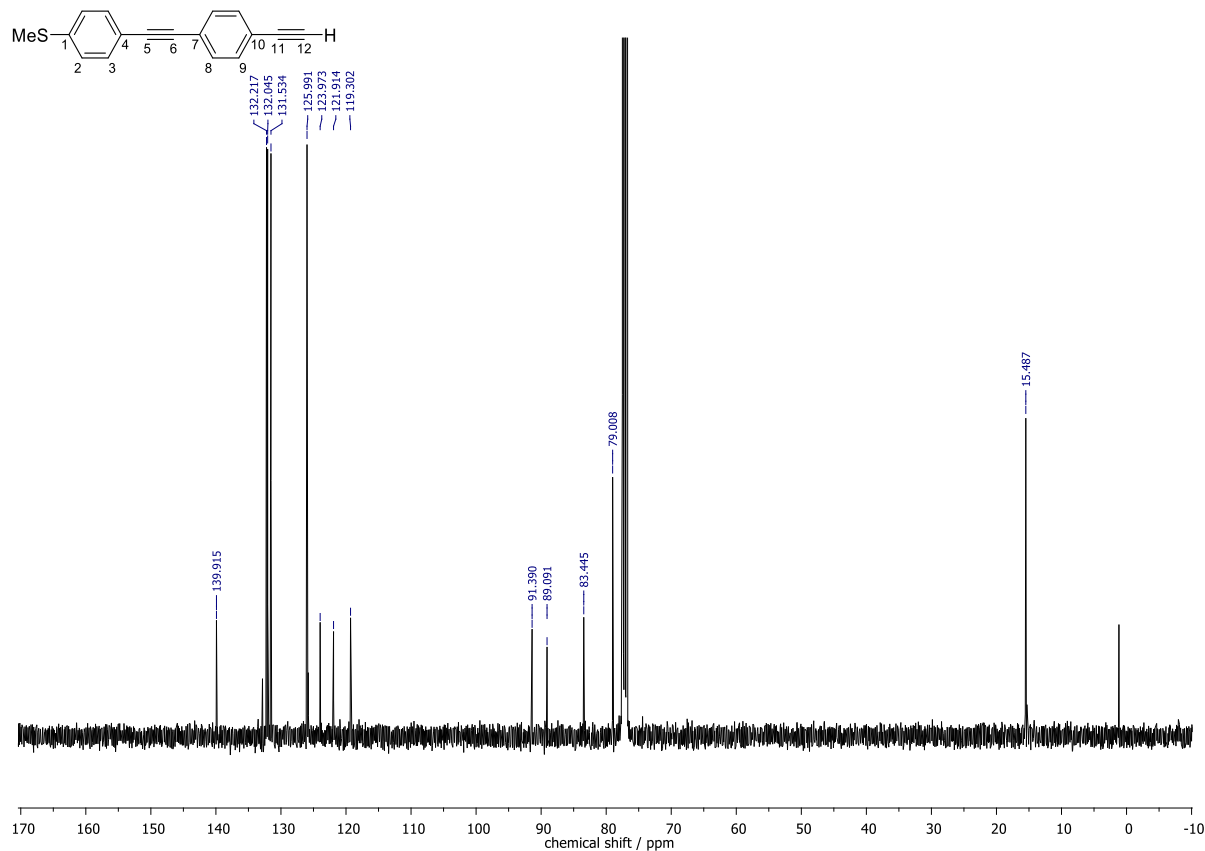


Figure S60: The ¹³C {¹H} NMR spectrum of 4-((4-(methylthio)phenyl)ethynyl)-1-(ethynyl)benzene.

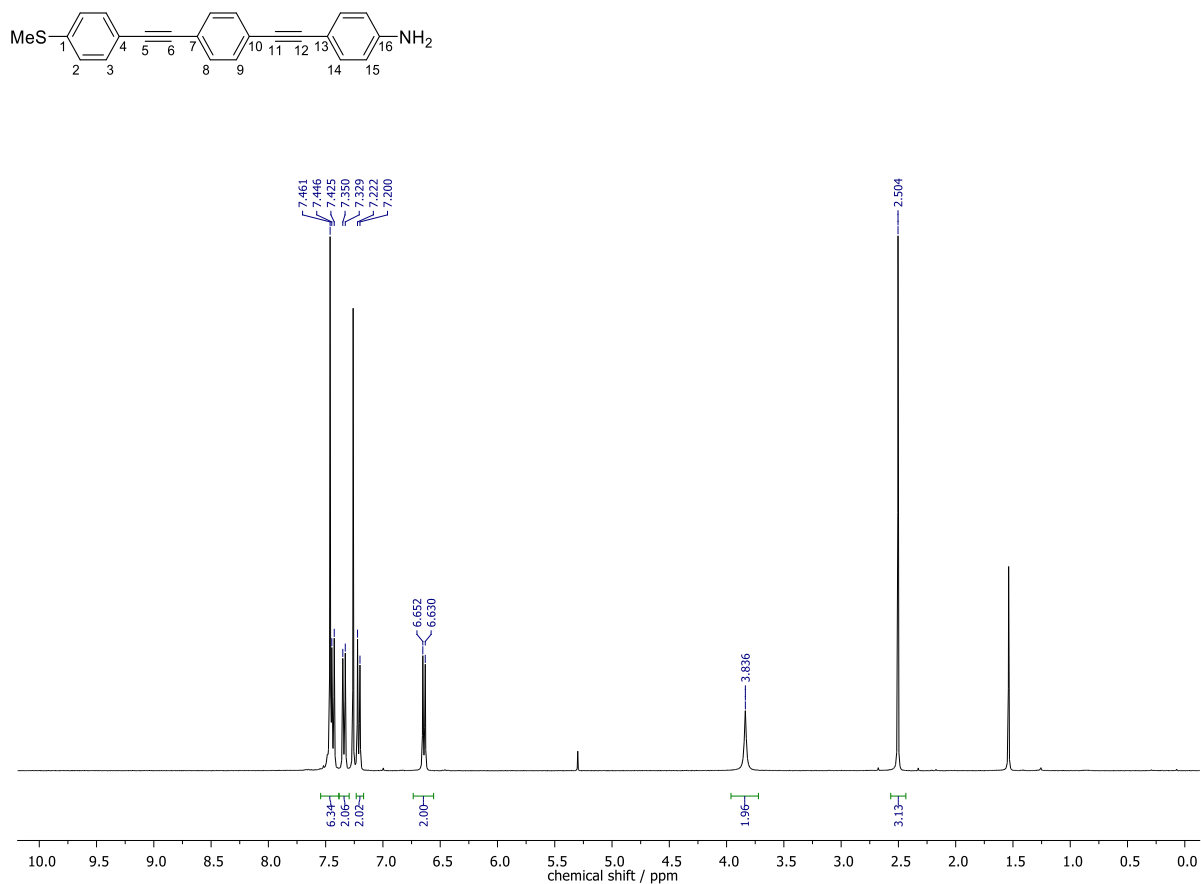


Figure S61: The ¹H NMR spectrum of 6.

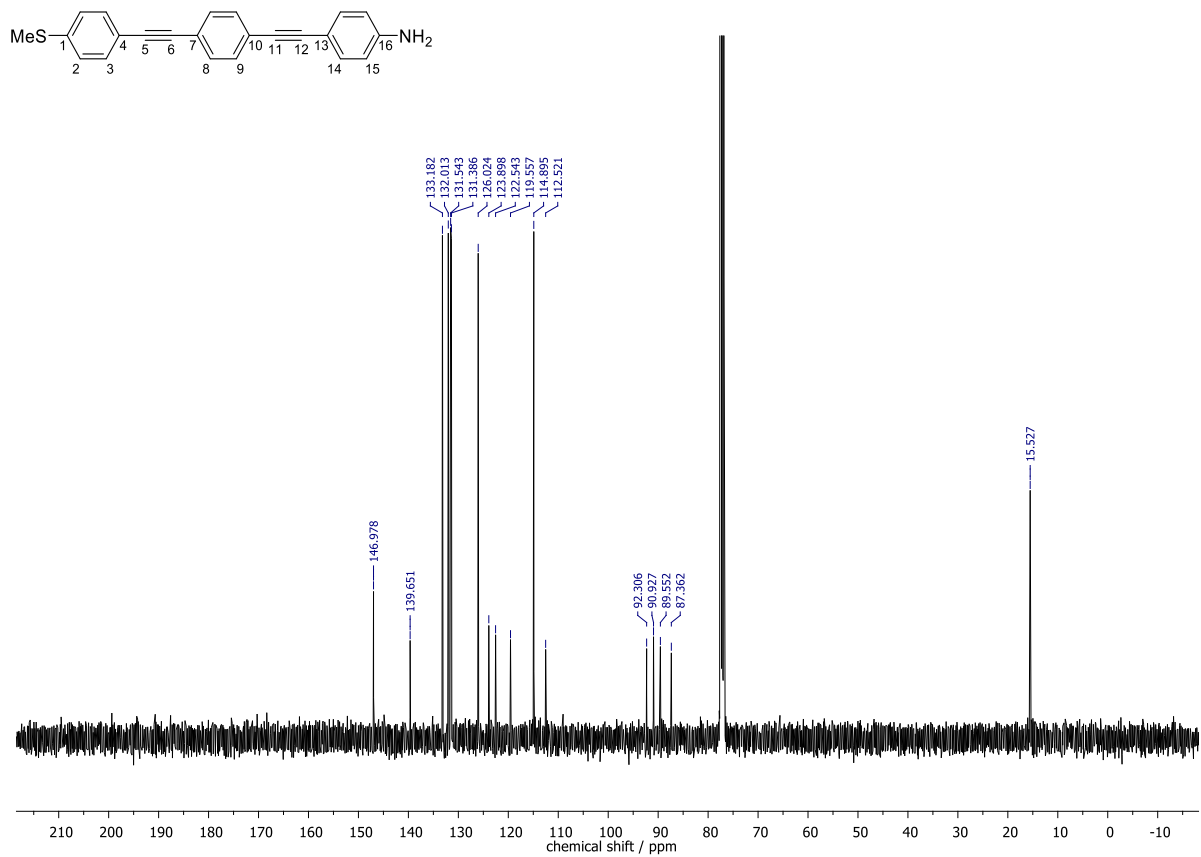


Figure S62: The ¹³C{¹H} NMR spectrum of 6.

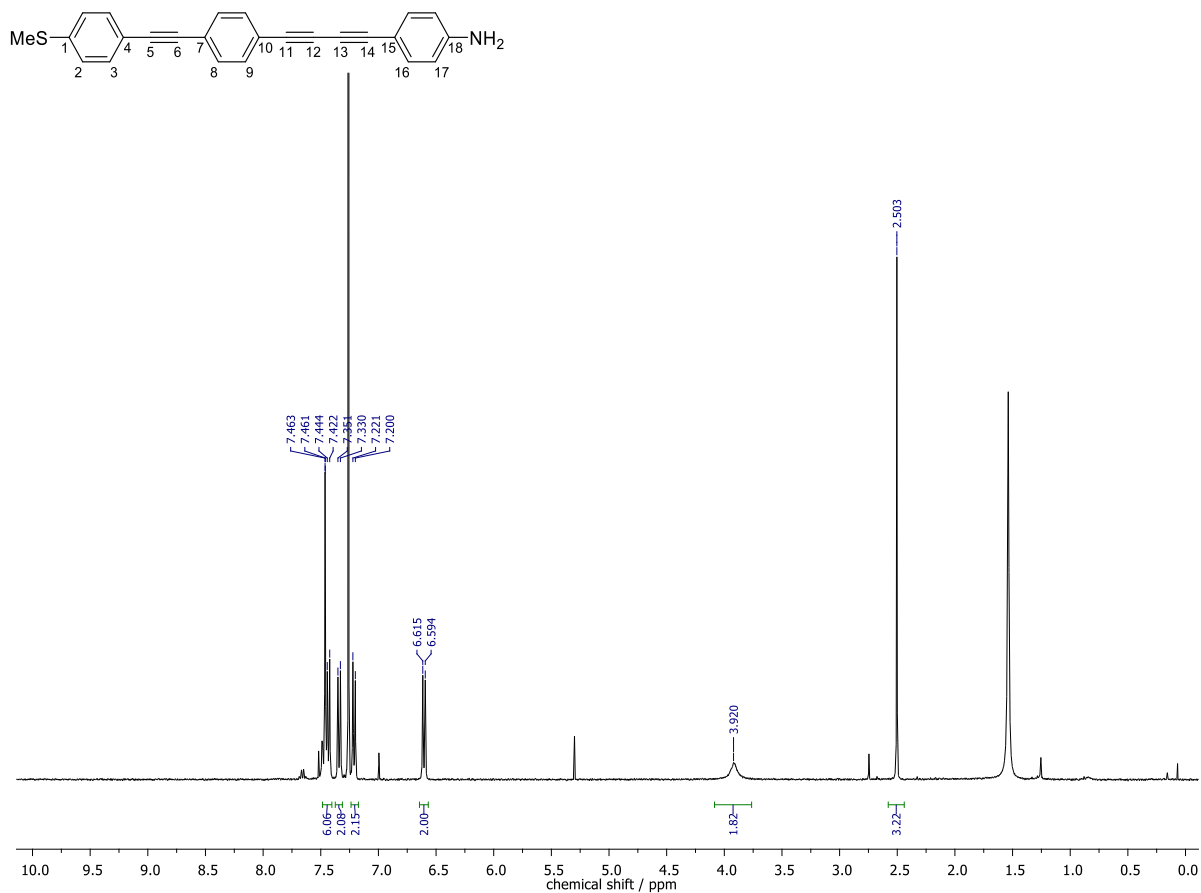


Figure S63: The ¹H NMR spectrum of 7.

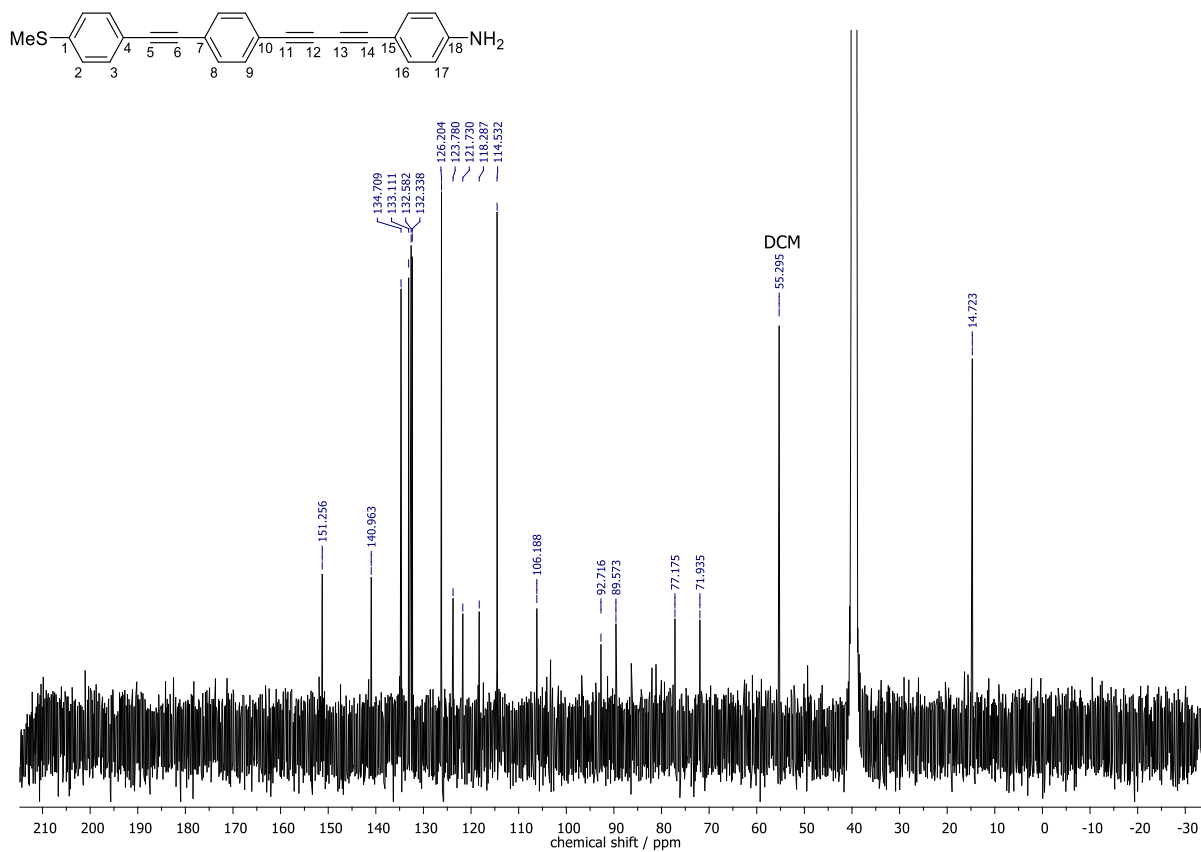


Figure S64: The ¹³C{¹H} NMR spectrum of 7.

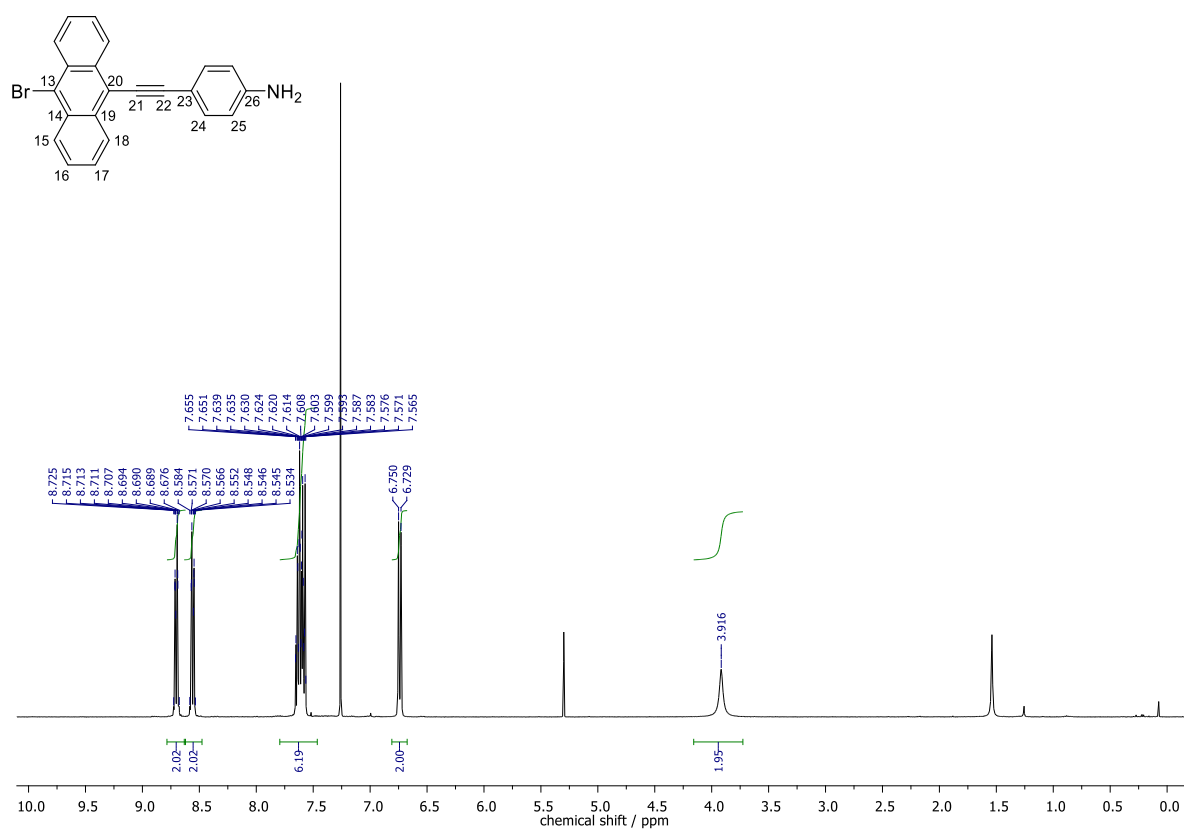


Figure S65: The ^1H NMR spectrum of 9-bromo-10-((4-aminophenyl)ethynyl)anthracene.

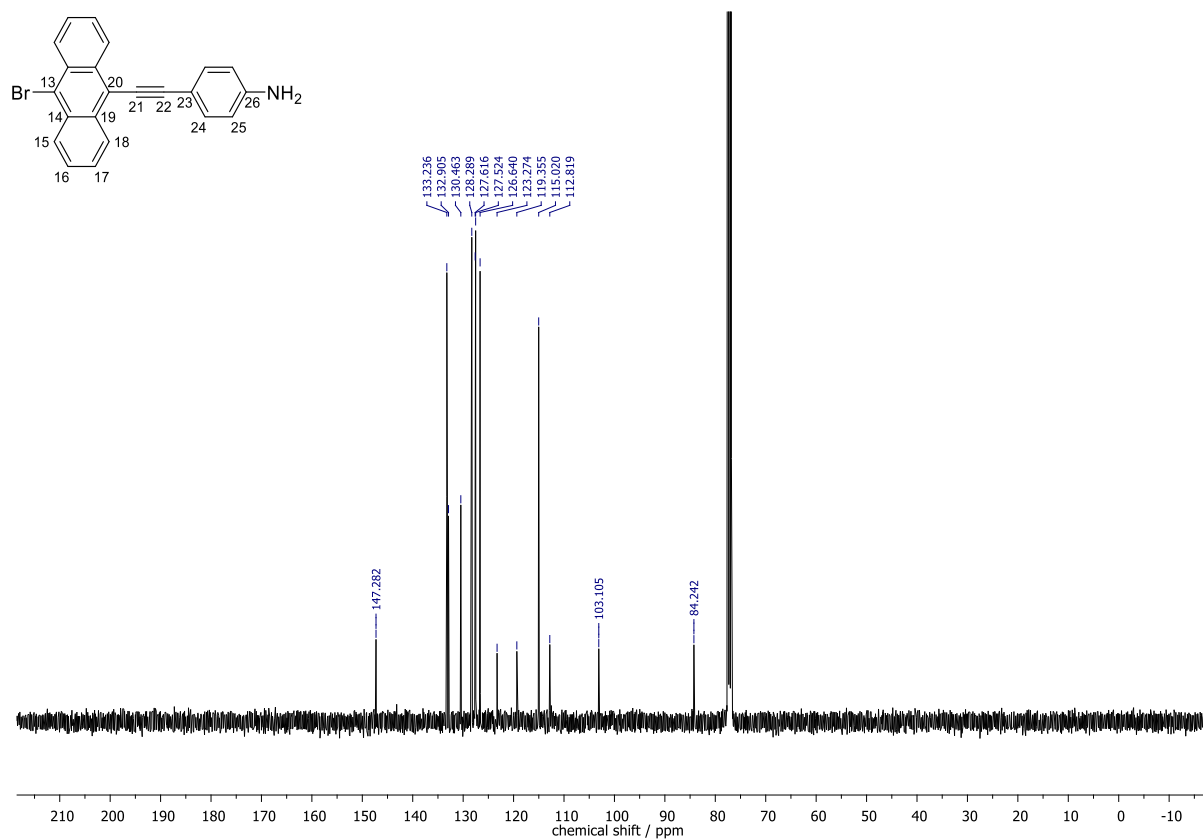


Figure S66: The $^{13}\text{C}\{^1\text{H}\}$ NMR spectrum of 9-bromo-10-((4-aminophenyl)ethynyl)anthracene.

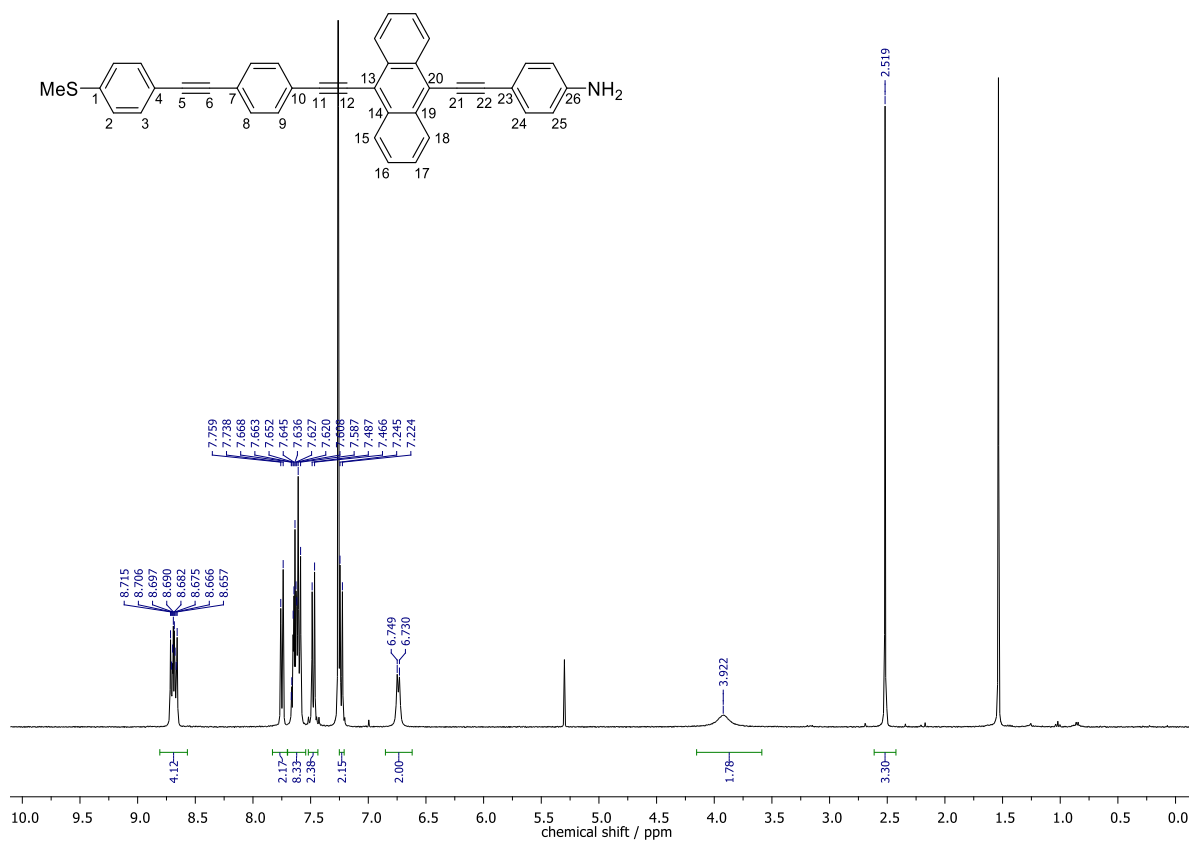


Figure S67: The ^1H NMR spectrum of **8**.

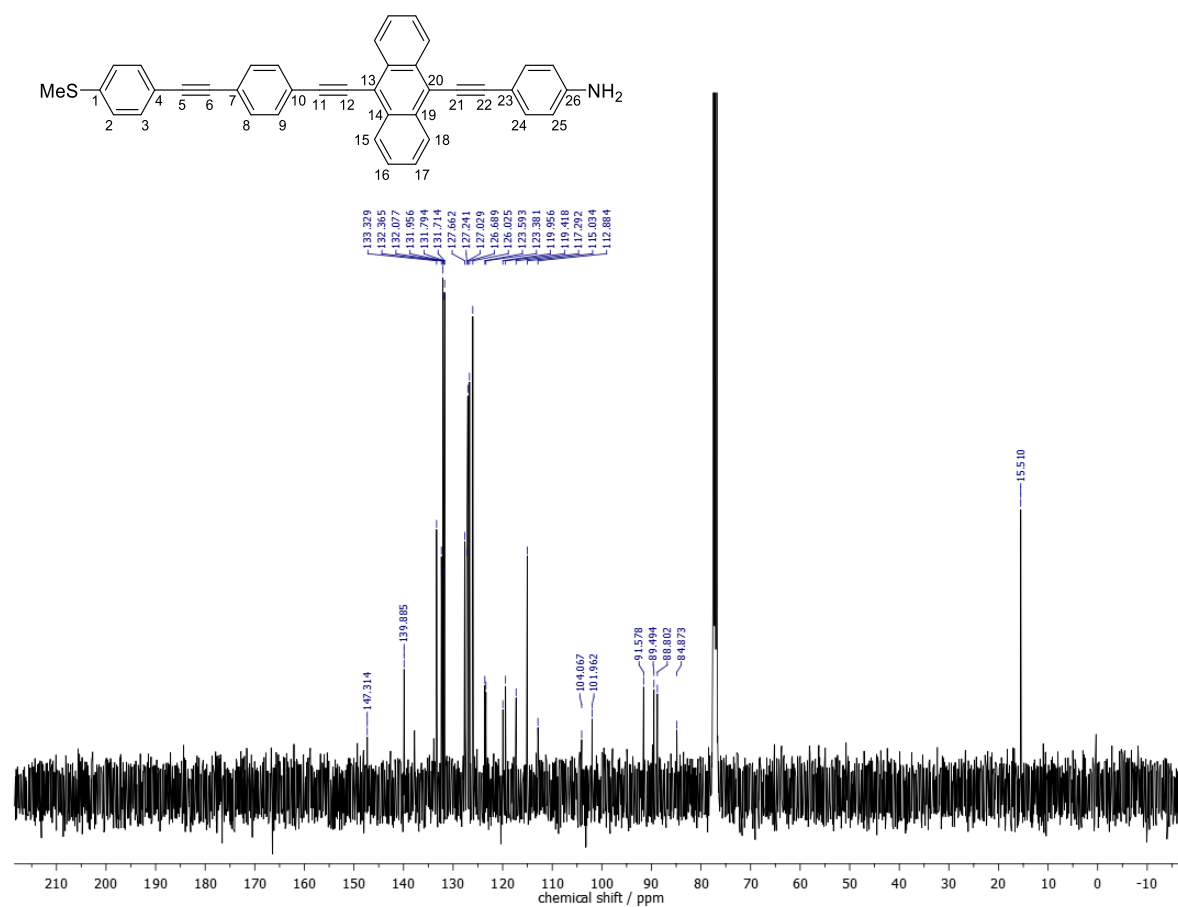


Figure S68: The $^{13}\text{C}\{^1\text{H}\}$ NMR spectrum of **8**.

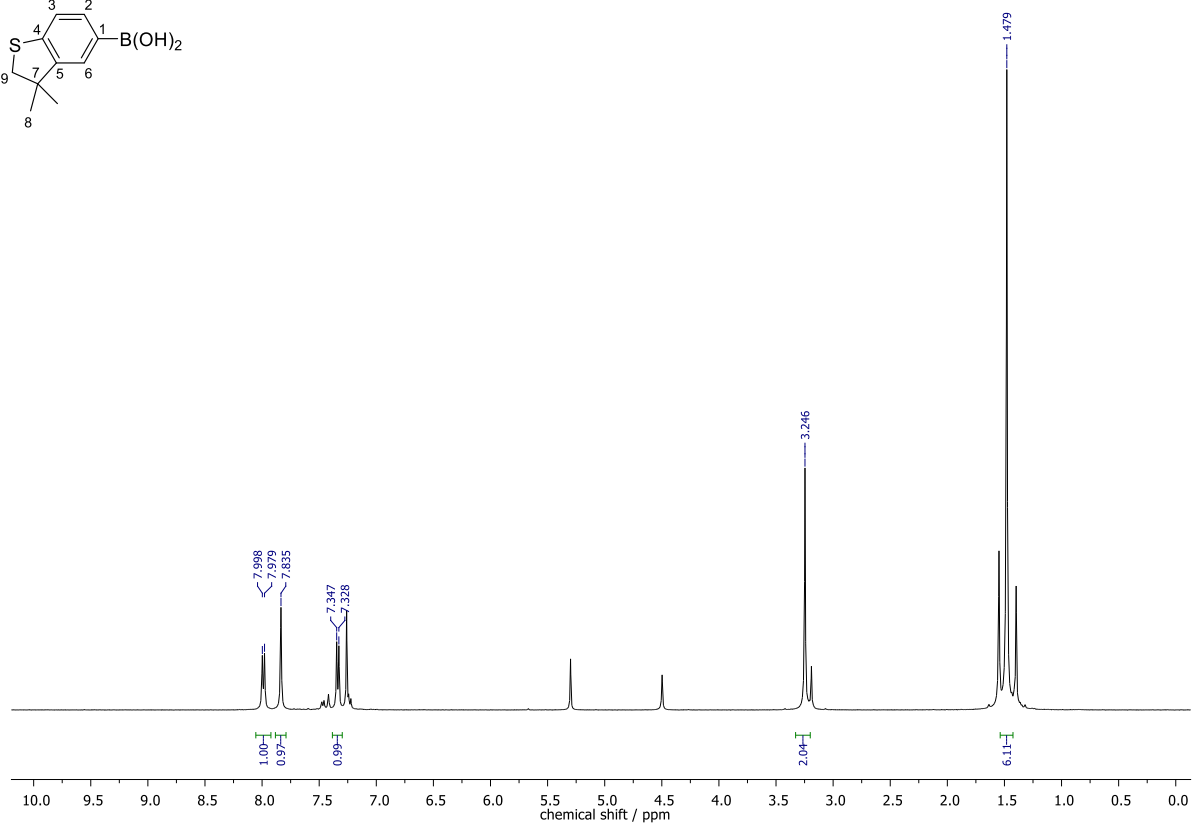
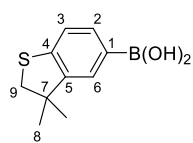


Figure S69: The ^1H NMR spectrum of (3,3-dimethyl-2,3-dihydrobenzo[*b*]thiophen-5-yl)boronic acid.

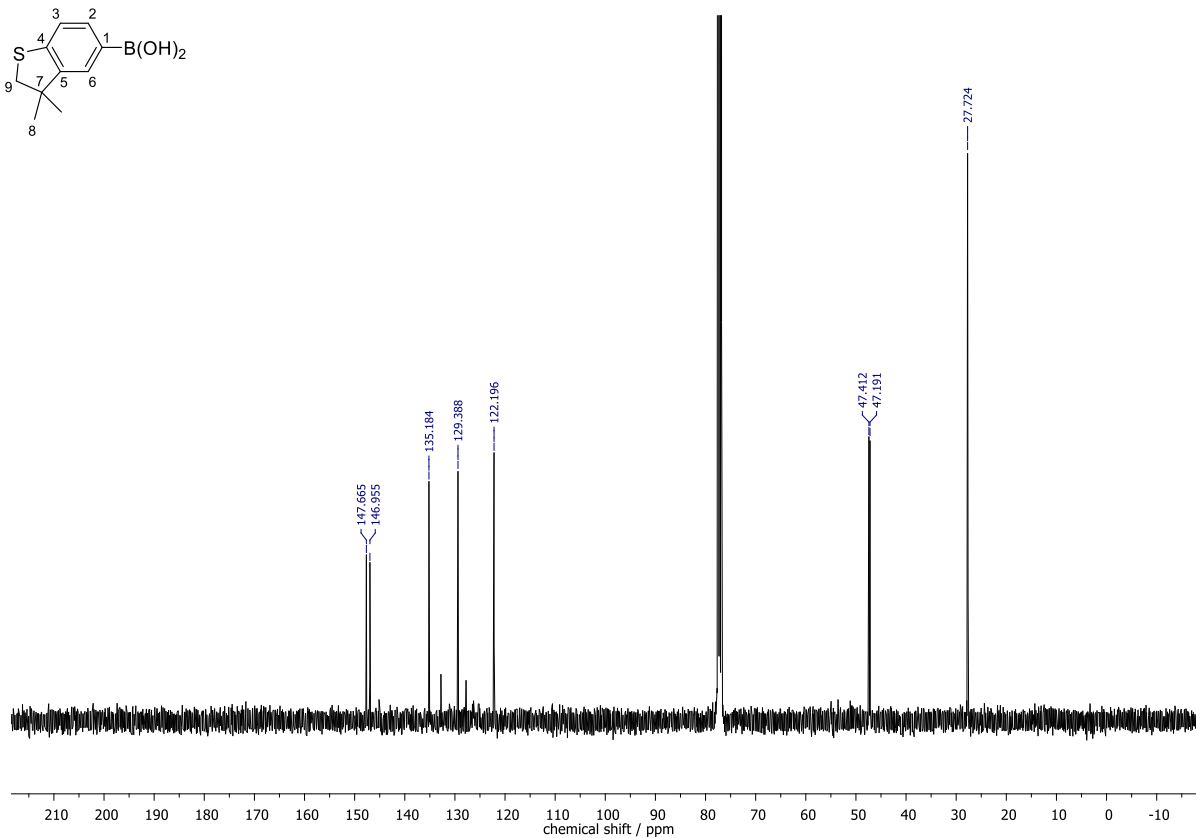
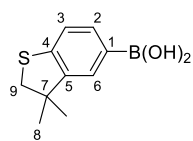


Figure S70: The $^{13}\text{C}\{^1\text{H}\}$ NMR spectrum of (3,3-dimethyl-2,3-dihydrobenzo[*b*]thiophen-5-yl)boronic acid.

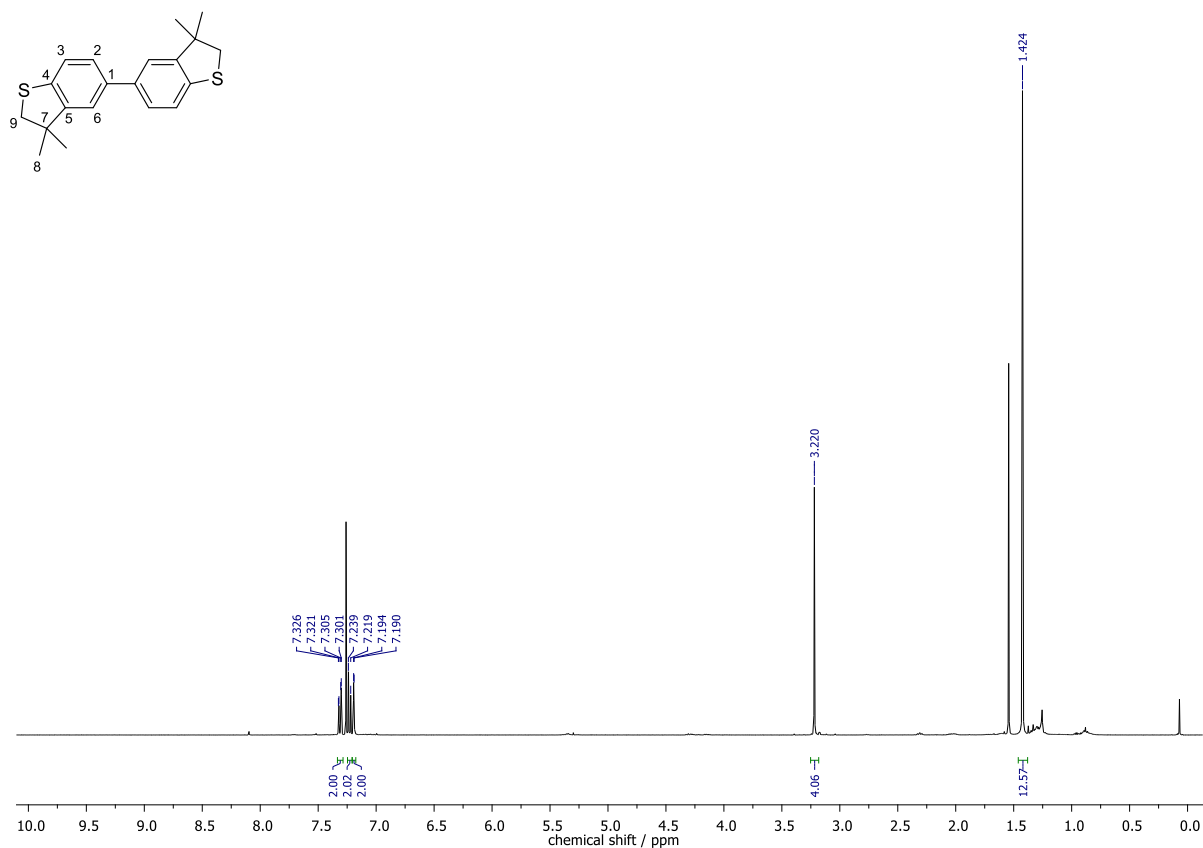


Figure S71: The ^1H NMR spectrum of 3,3,3',3'-tetramethyl-2,2',3,3'-tetrahydro-5,5'-bibenzo[b]thiophene.

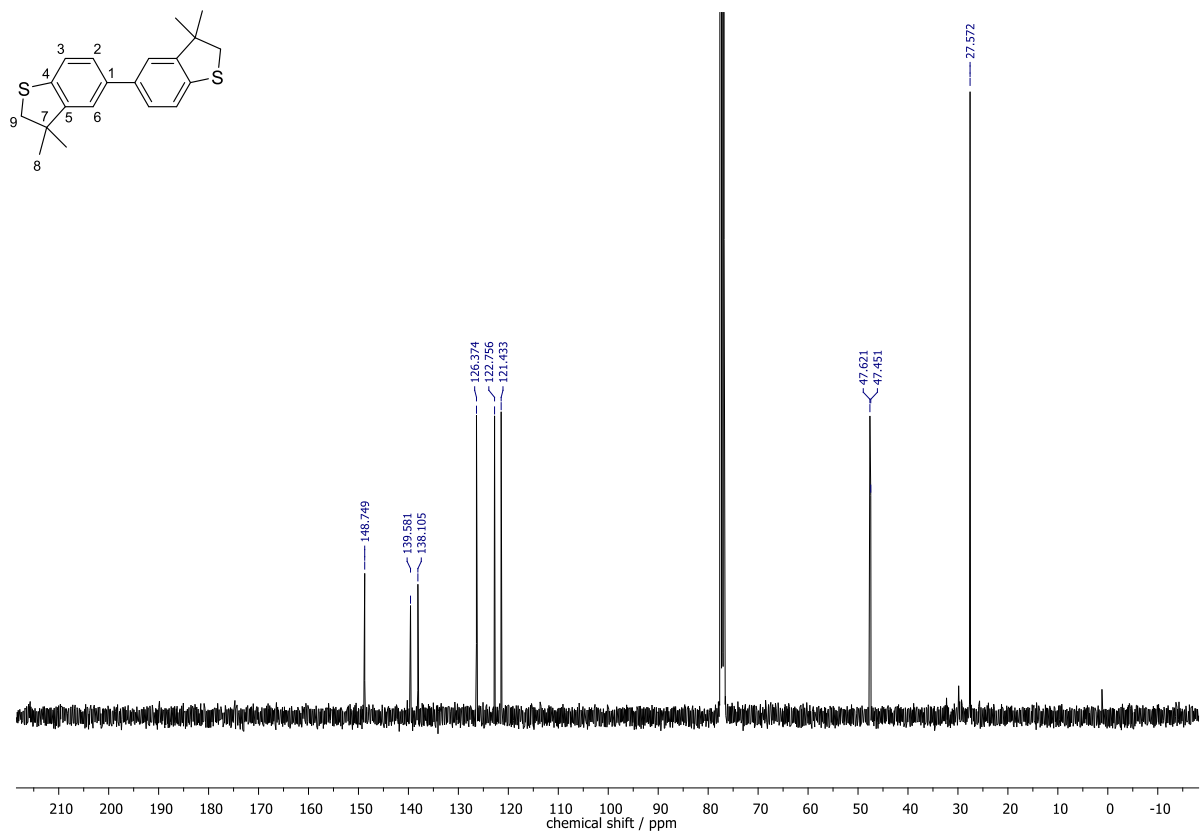


Figure S72: The $^{13}\text{C}\{^1\text{H}\}$ NMR spectrum of 3,3,3',3'-tetramethyl-2,2',3,3'-tetrahydro-5,5'-bibenzo[b]thiophene.

2.6 MS Spectra

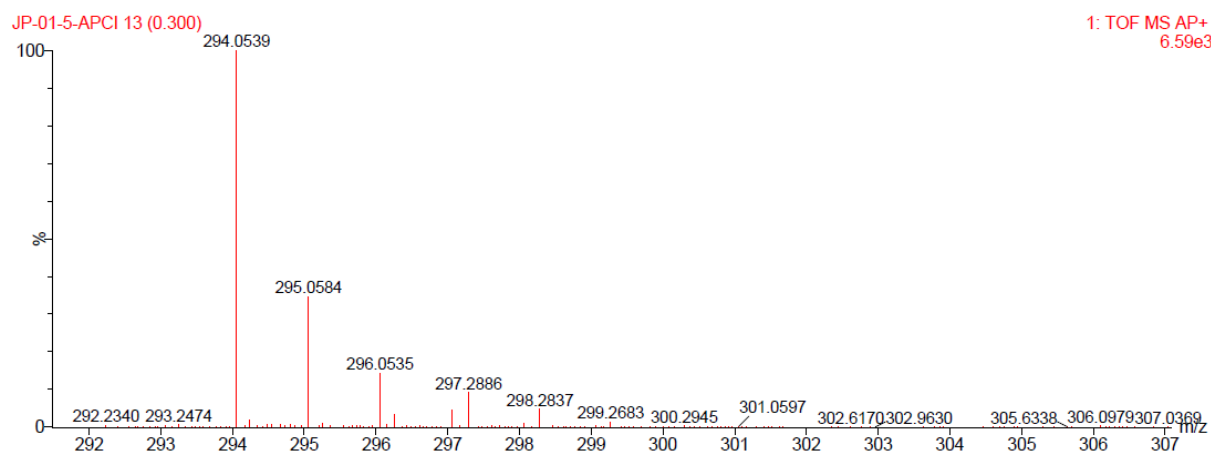


Figure S73: The MS spectrum of **1b**.

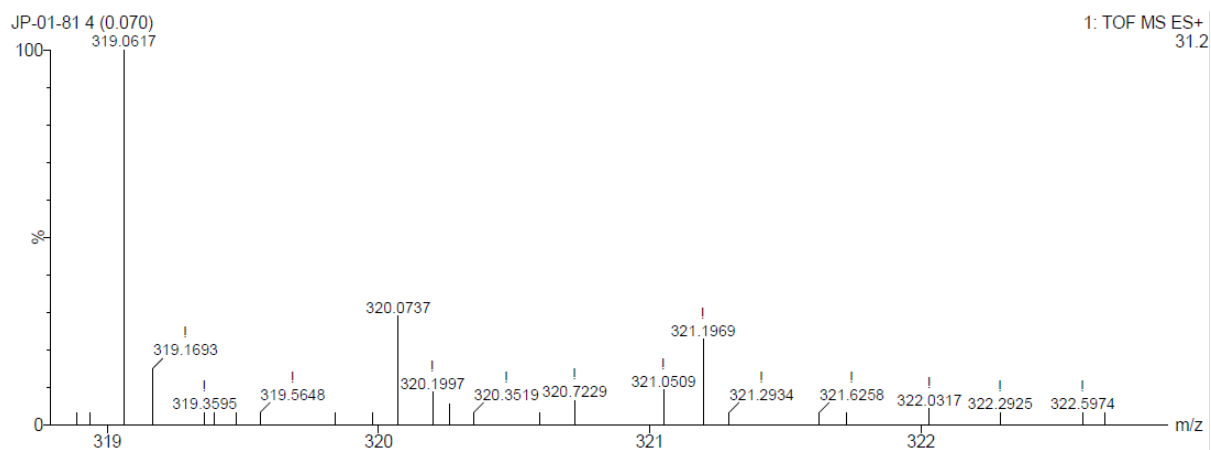


Figure S74: The MS spectrum of **1c**.

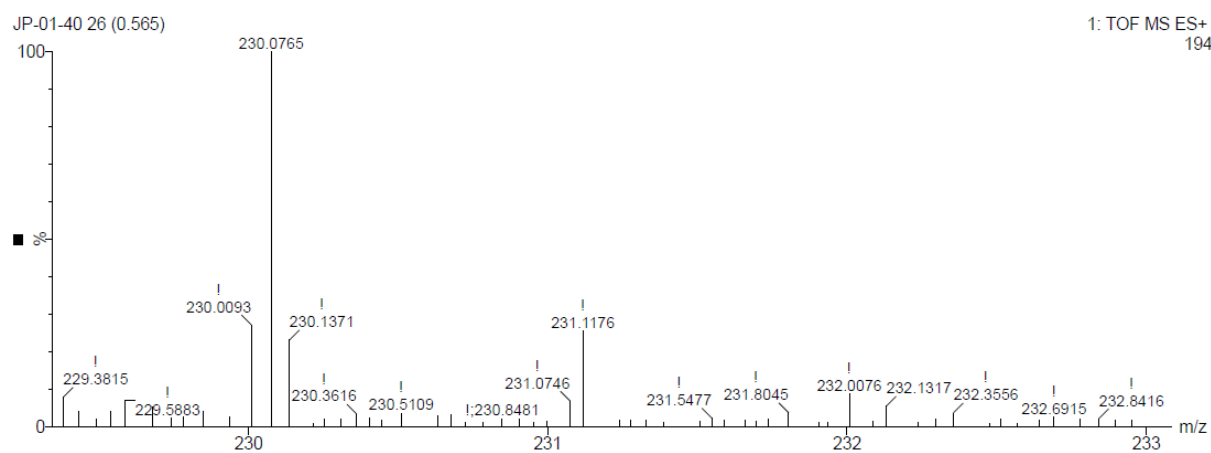


Figure S75: The MS spectrum of **1d-1**.

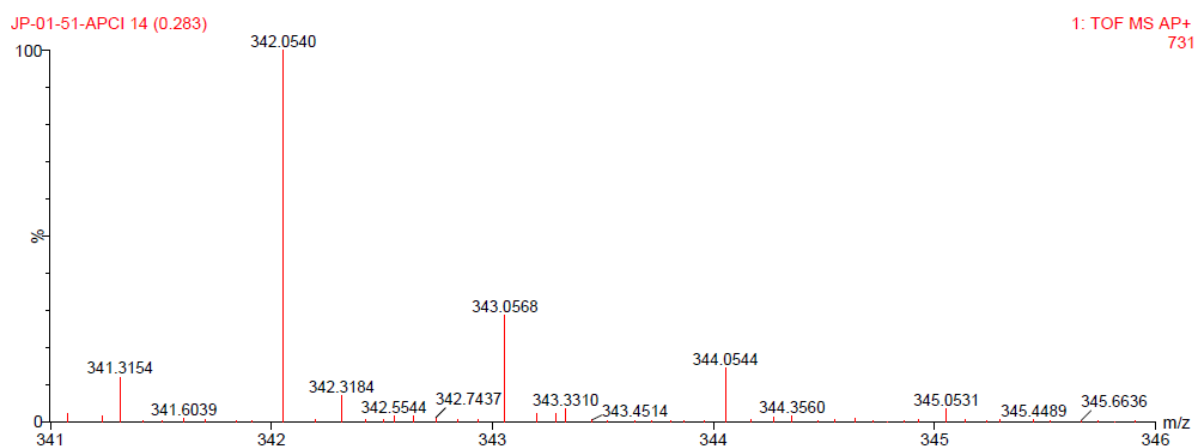


Figure S76: The MS spectrum of **1d**.

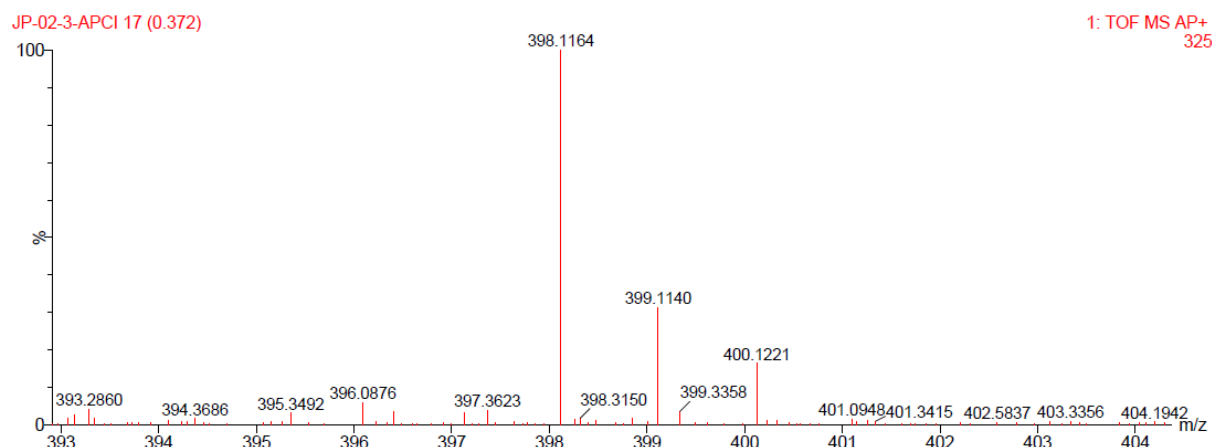


Figure S77: The MS spectrum of **2c**.

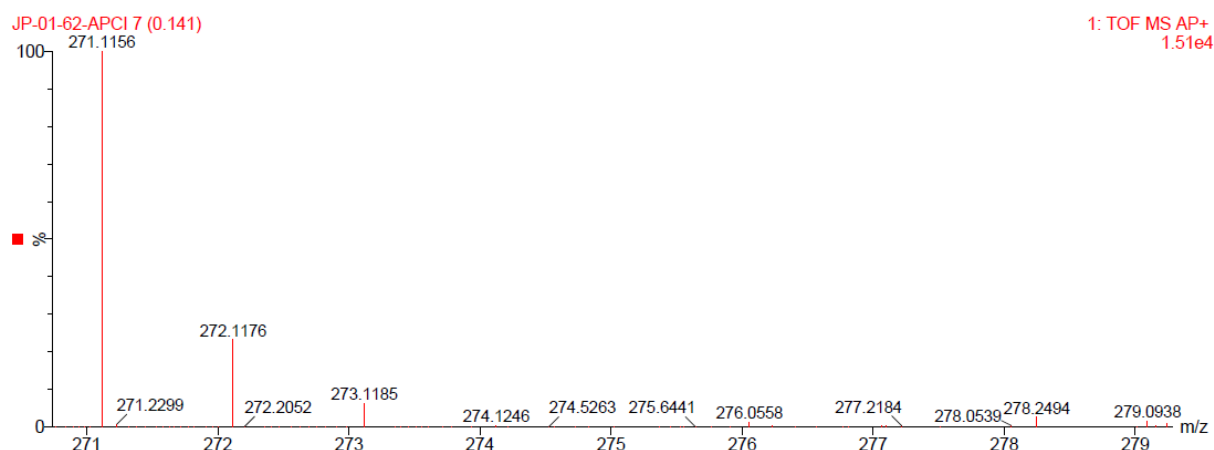


Figure S78: The MS spectrum of **2d-1**.

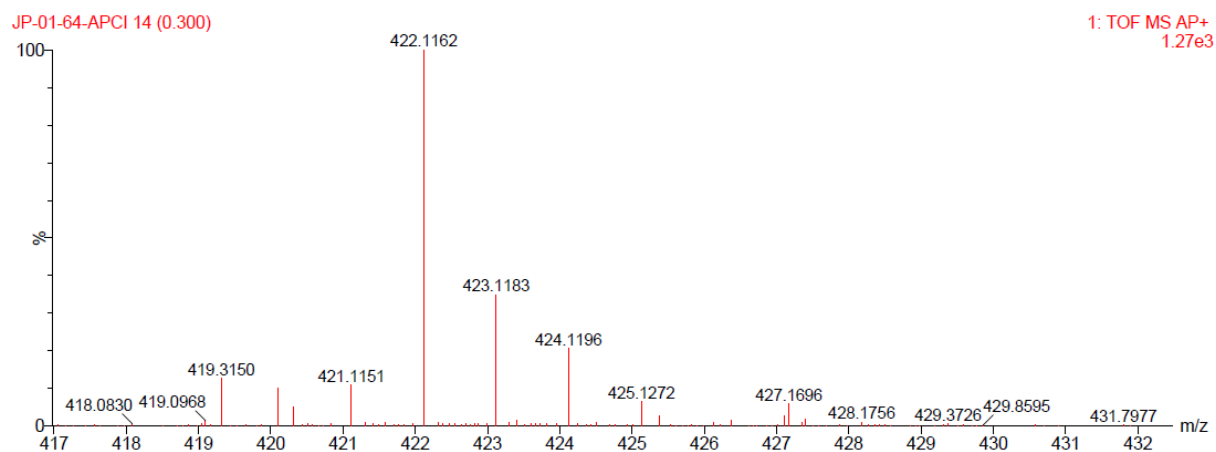


Figure S79: The MS spectrum of **2d**.

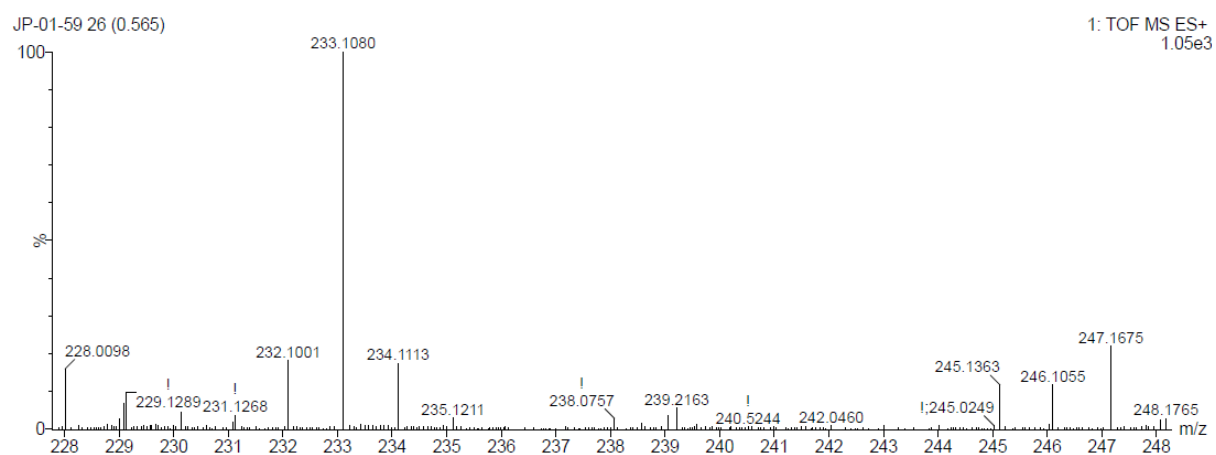


Figure S80: The MS spectrum of **3b**.

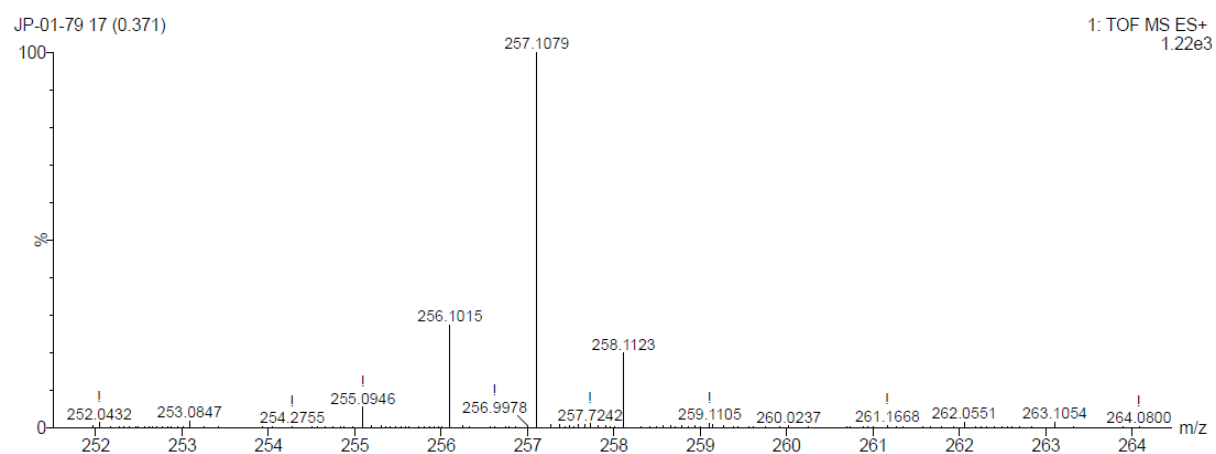


Figure S81: The MS spectrum of **3c**.

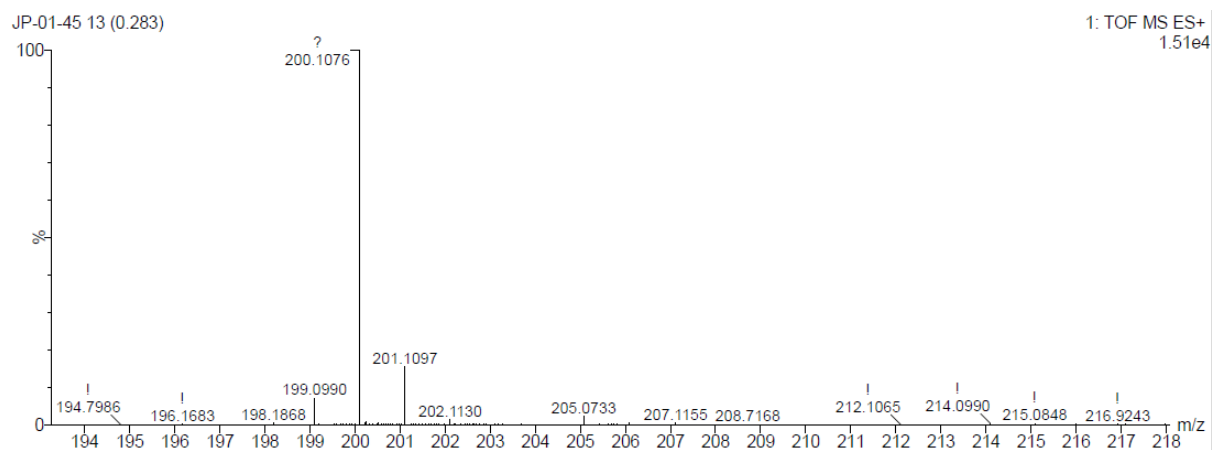


Figure S82: The MS spectrum of **3d-1**.

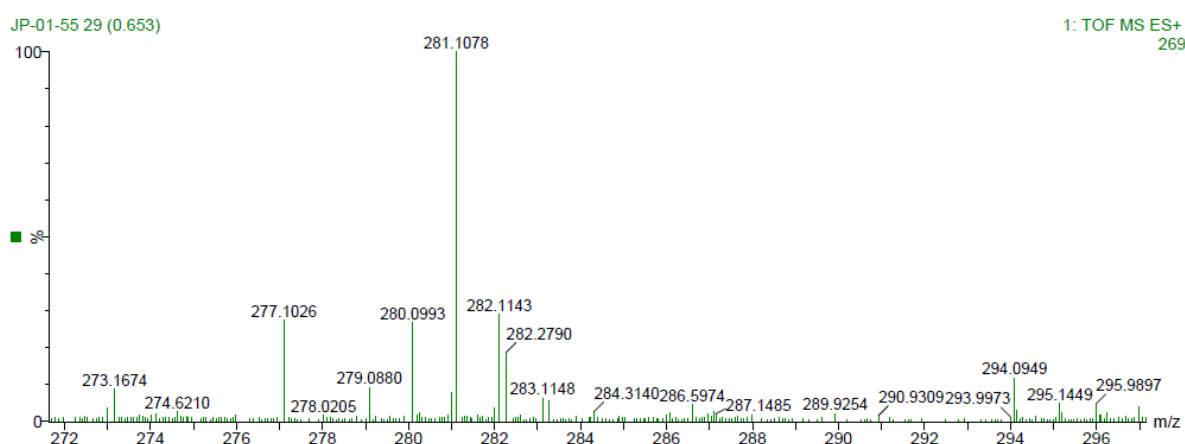


Figure S83: The MS spectrum of **3d**.

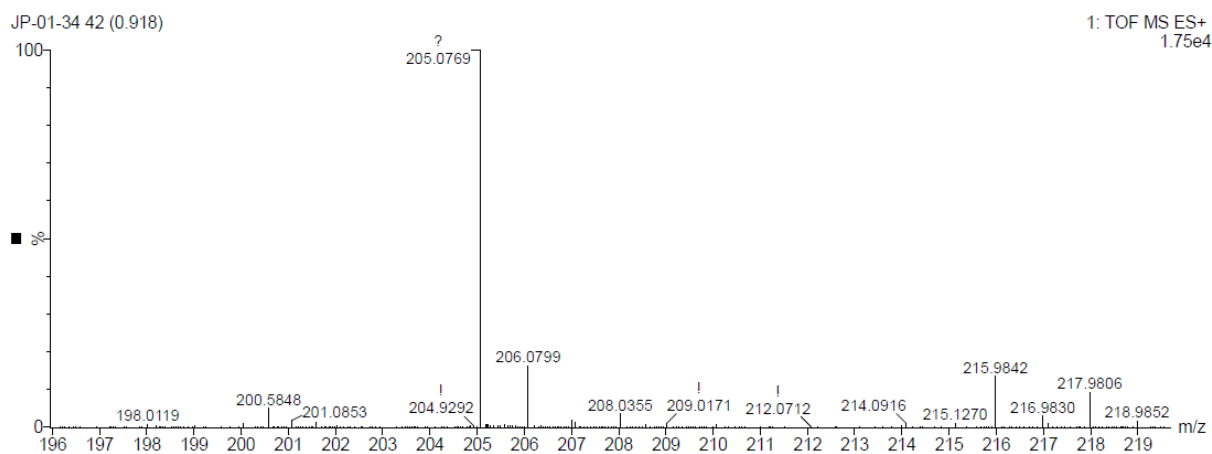


Figure S84: The MS spectrum of **4b**.

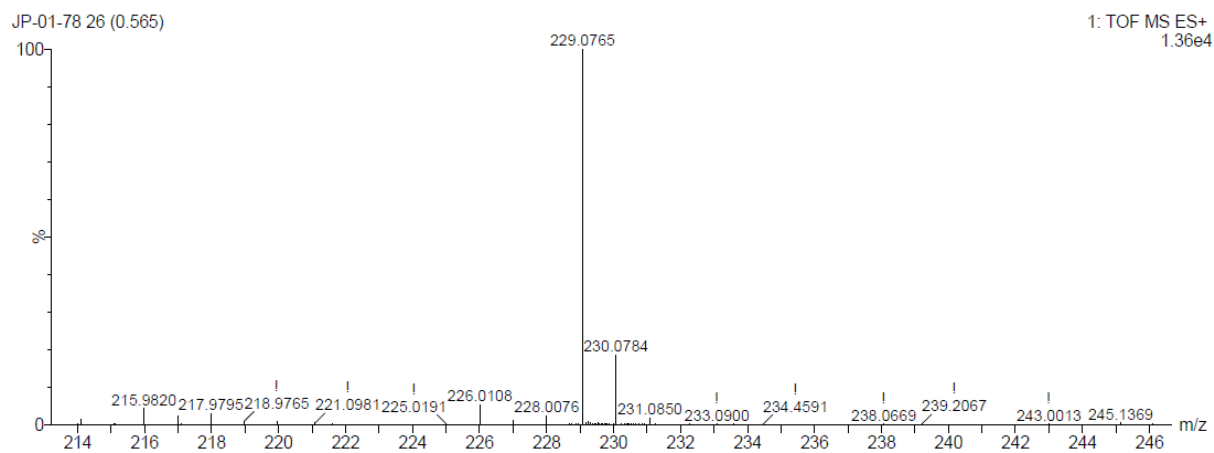


Figure S85: The MS spectrum of **4c**.

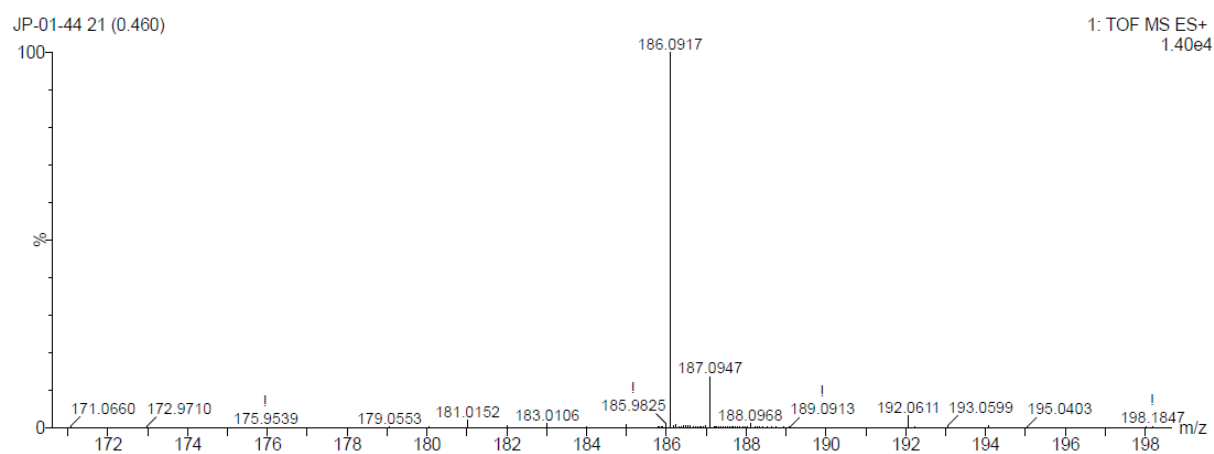


Figure S86: The MS spectrum of **4d-1**.

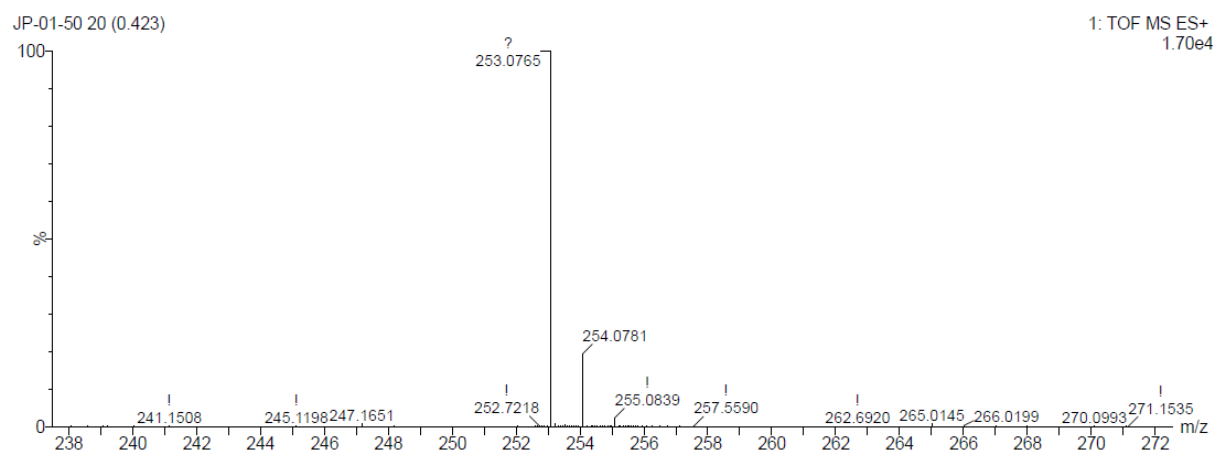


Figure S87: The MS spectrum of **4d**.

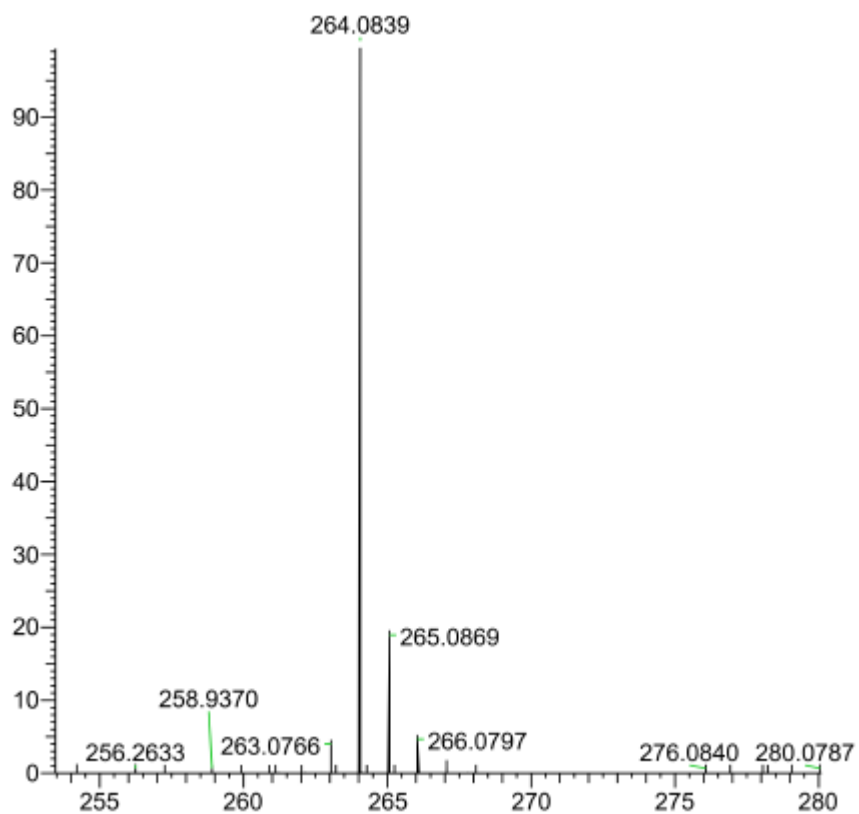


Figure S88: The MS spectrum of **5**.

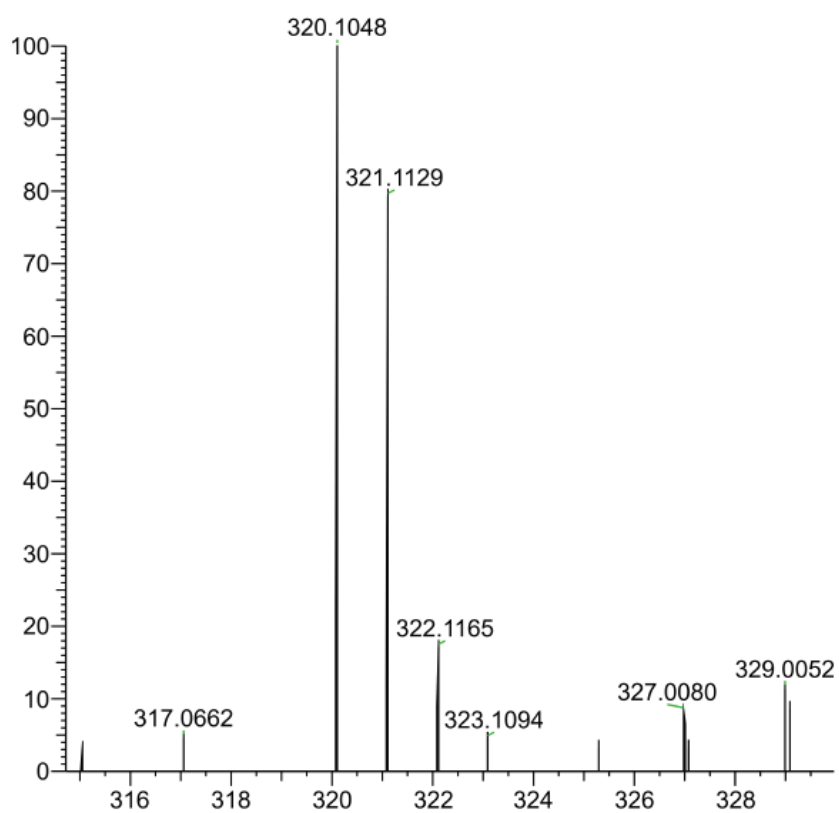


Figure S89: The MS spectrum of 4-((4-(methylthio)phenyl)ethynyl)-1-(trimethylsilylethynyl)benzene.

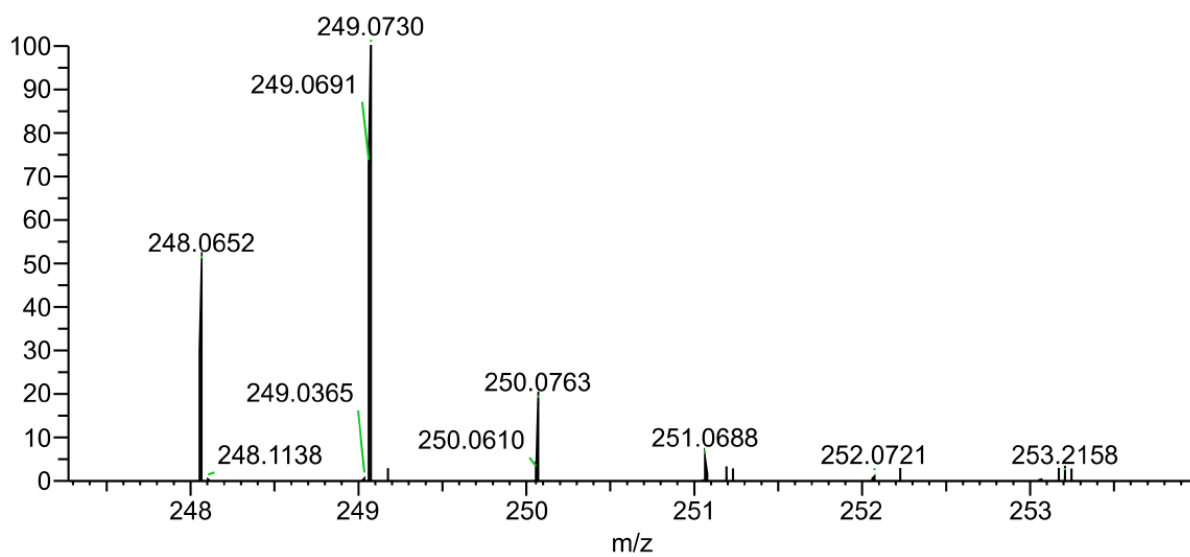


Figure S90: The MS spectrum of 4-((4-(methylthio)phenyl)ethynyl)-1-(ethynyl)benzene.

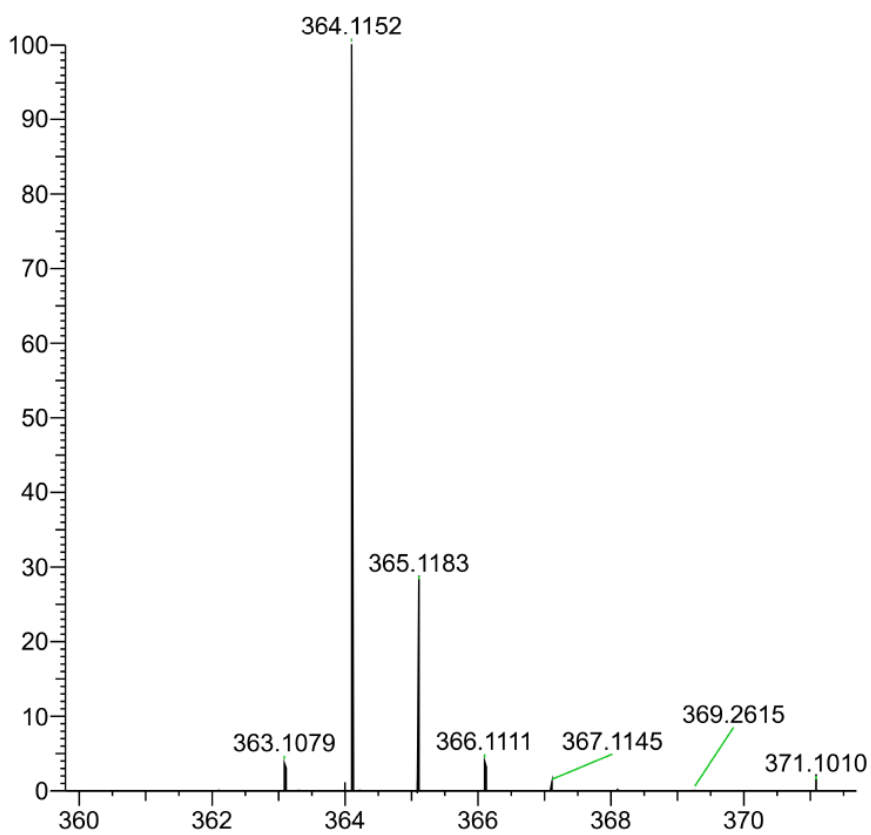


Figure S91: The MS spectrum of 7.

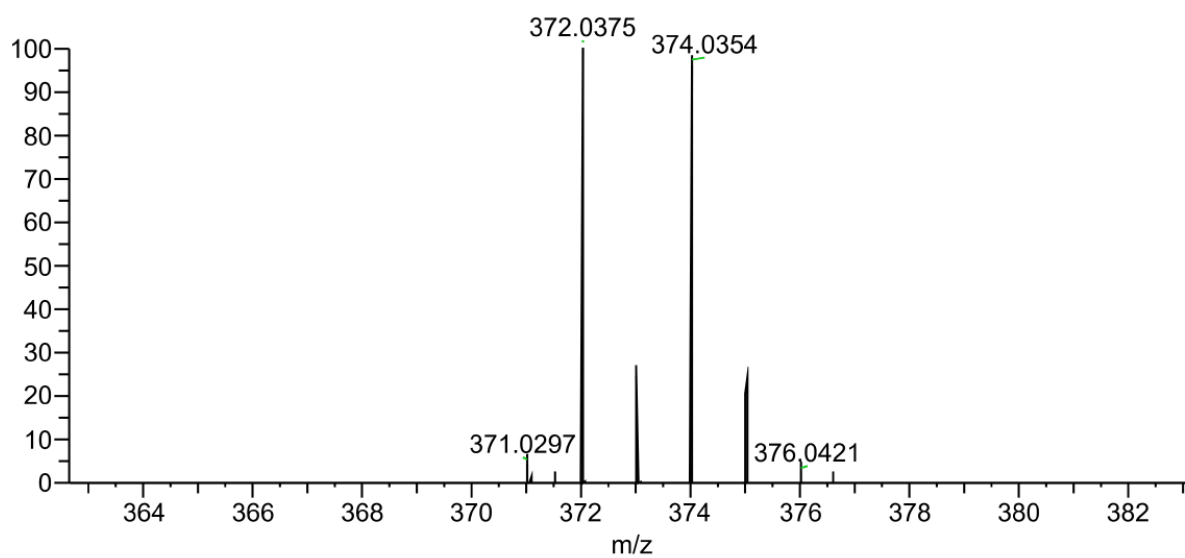


Figure S92: The MS spectrum of 9-bromo-10-((4-aminophenyl)ethynyl)anthracene.

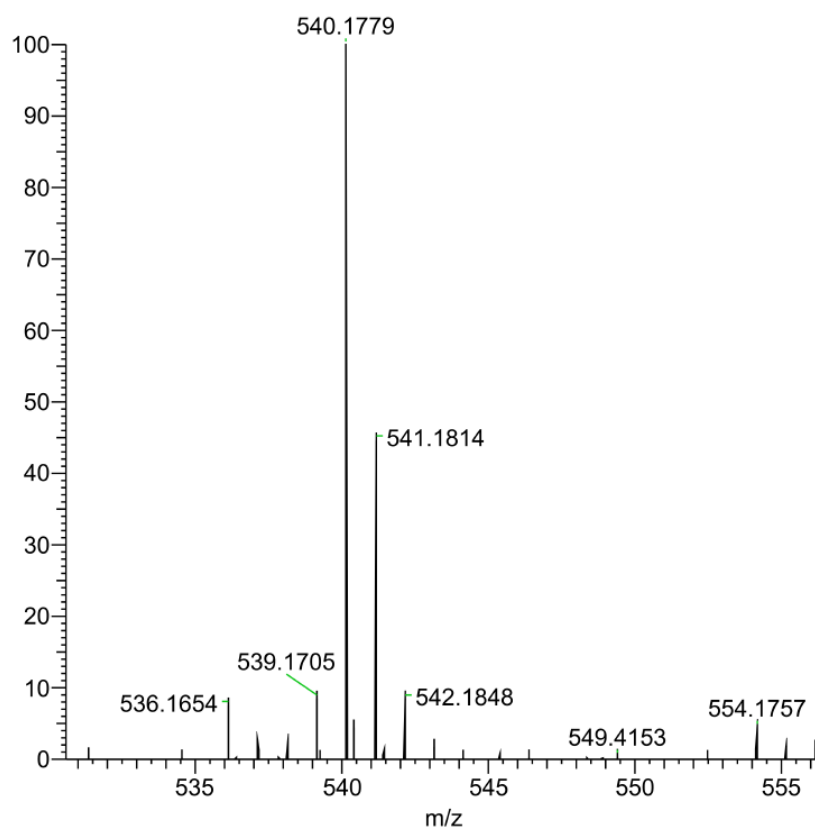


Figure S93: The MS spectrum of **8**.

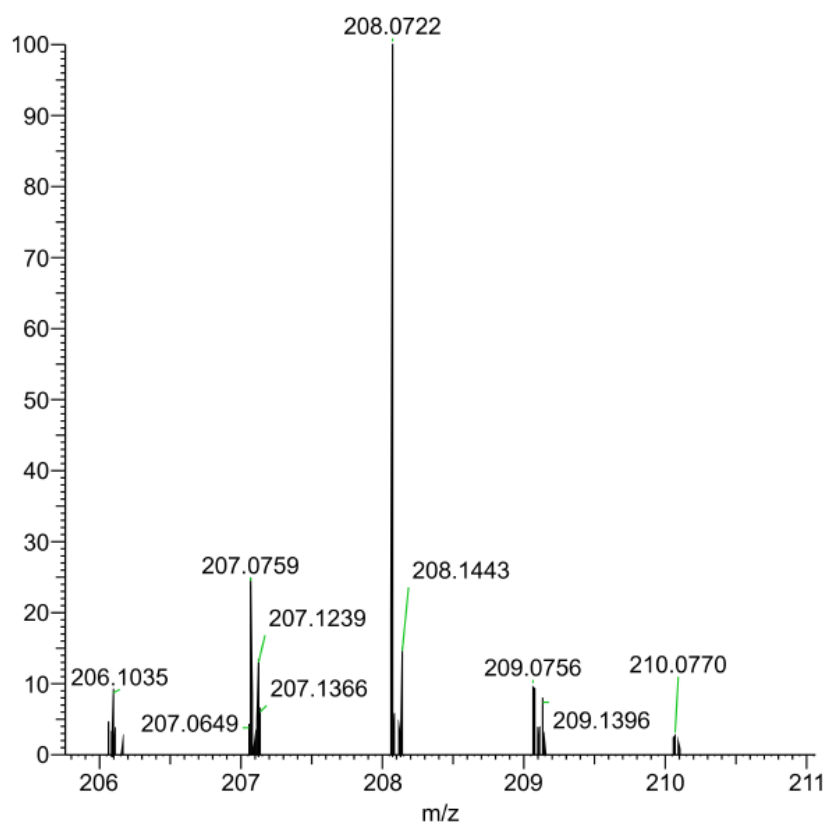


Figure S94: The MS spectrum of (3,3-dimethyl-2,3-dihydrobenzo[b]thiophen-5-yl)boronic acid.

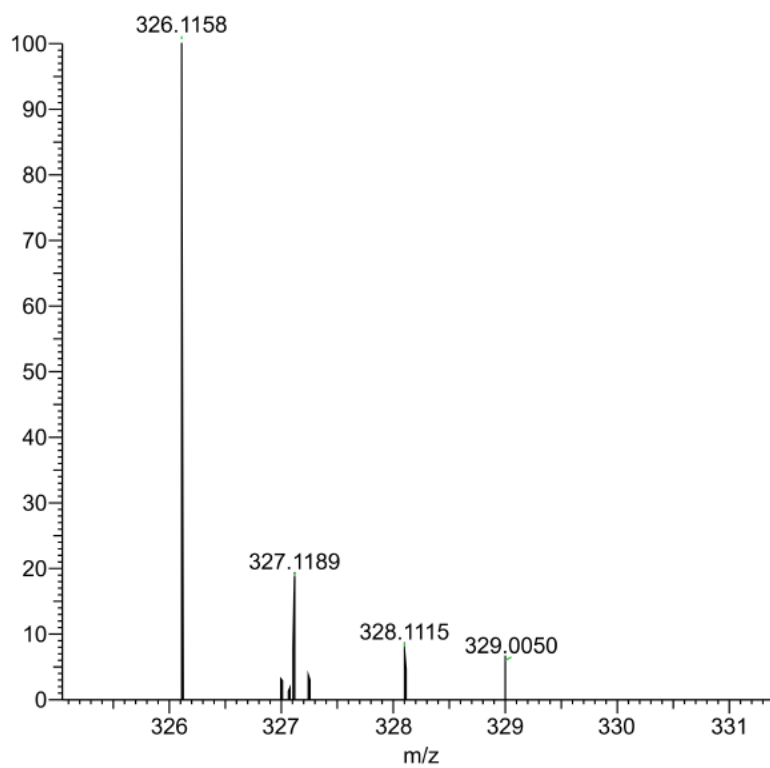


Figure S95: The MS spectrum of 3,3,3',3'-tetramethyl-2,2',3,3'-tetrahydro-5,5'-bibenzo[b]thiophene.

References:

- 1 E. Gorenskaia, M. Naher, L. Daukiya, S. Moggach, D. C. Milan, A. Vezzoli, C. Lambert, R. Nichols, T. Becker and P. Low, *Aust. J. Chem.*, 2021, **74**, 806–818.
- 2 W. Hong, D. Z. Manrique, P. Moreno-García, M. Gulcur, A. Mishchenko, C. J. Lambert, M. R. Bryce and T. Wandlowski, *J. Am. Chem. Soc.*, 2012, **134**, 2292–2304.
- 3 M. Naher, S. Bock, Z. M. Langtry, K. M. O'Malley, A. N. Sobolev, B. W. Skelton, M. Korb and P. J. Low, *Organometallics*, 2020, **39**, 4667–4687.
- 4 S. Marqués-González, D. S. Yufit, J. A. K. Howard, S. Martín, H. M. Osorio, V. M. García-Suárez, R. J. Nichols, S. J. Higgins, P. Cea and P. J. Low, *Dalt. Trans.*, 2013, **42**, 338–341.
- 5 D. C. Milan, A. Vezzoli, I. J. Planje and P. J. Low, *Dalt. Trans.*, 2018, **47**, 14125–14138.
- 6 L. M. Ballesteros, S. Martín, C. Momblona, S. Marqués-González, M. C. López, R. J. Nichols, P. J. Low and P. Cea, *J. Phys. Chem. C*, 2012, **116**, 9142–9150.
- 7 K. West, C. Wang, A. S. Batsanov and M. R. Bryce, *J. Org. Chem.*, 2006, **71**, 8541–8544.
- 8 P. Moreno-García, M. Gulcur, D. Z. Manrique, T. Pope, W. Hong, V. Kaliginedi, C. Huang, A. S. Batsanov, M. R. Bryce, C. Lambert and T. Wandlowski, *J. Am. Chem. Soc.*, 2013, **135**, 12228–12240.
- 9 L. Y. Zhang, P. Duan, J. Y. Wang, Q. C. Zhang and Z. N. Chen, *J. Phys. Chem. C*, 2019, **123**, 5282–5288.
- 10 P. Pachfule, A. Acharjya, J. Roeser, T. Langenhahn, M. Schwarze, R. Schomäcker, A. Thomas and J. Schmidt, *J. Am. Chem. Soc.*, 2018, **140**, 1423–1427.
- 11 L. Su, J. Dong, L. Liu, M. Sun, R. Qiu, Y. Zhou and S. F. Yin, *J. Am. Chem. Soc.*, 2016, **138**, 12348–12351.
- 12 N. R. Champness, A. N. Khlobystov, A. G. Majuga, M. Schröder and N. V. Zyk, *Tetrahedron Lett.*, 1999, **40**, 5413–5416.

- 13 A. G. L. Olive, K. Parkan, C. Givélet and J. Michl, *J. Am. Chem. Soc.*, 2011, **133**, 20108–20111.
- 14 G. M. Sheldrick, *Acta Crystallogr. Sect. A Found. Crystallogr.*, 2015, **71**, 3–8.
- 15 O. V. Dolomanov, L. J. Bourhis, R. J. Gildea, J. A. K. Howard and H. Puschmann, *J. Appl. Crystallogr.*, 2009, **42**, 339–341.
- 16 H. Putz and K. Brandenburg, Diamond - Crystal and Molecular Structure Visualization, <https://www.crystalimpact.de/diamond>.